ICLIAD 64 (4), 437-559, 2023

p-ISSN 0535-5133
e-ISSN 2477-9393

Volumen 64
No. 4
Diciembre 2023

Investigación Clínica

Universidad del Zulia
Facultad de Medicina
Instituto de Investigaciones Clínicas
"Dr. Américo Negrette"
Maracaibo, Venezuela

Investigación Clínica

https://sites.google.com/site/revistainvestigacionesclinicas

Revista arbitrada dedicada a estudios humanos, animales y de laboratorio relacionados con la investigación clínica y asuntos conexos.

La Revista es de Acceso Abierto, publicada trimestralmente por el Instituto de Investigaciones Clínicas "Dr. Américo Negrette", de la Facultad de Medicina, de la Universidad del Zulia, Maracaibo, Venezuela.

Investigación Clínica está indizada en Science Citation Index Expanded (USA), Excerpta Medica/EMBASE y Scopus (Holanda), Tropical Diseases Bulletin y Global Health (UK), Biblioteca Regional de Medicina/BIREME (Brasil), Ulrich's Periodicals, Journal Citation Reports (USA), Index Copernicus (Polonia), SIIEC Data Bases, Sección Iberoamérica (Argentina) e Infobase Index (India), Redalyc y las bases de datos: SciELO (www.Scielo.org.ve), Revencyt, LILACS, LIVECS, PERIODICA y web de LUZ: http://www.produccioncientificaluz.org/revistas

Para cualquier otra información dirigir su correspondencia a:

Dra. Elena Ryder, Editora
Instituto de Investigaciones Clínicas
"Dr. Américo Negrette"
Facultad de Medicina, Universidad del Zulia
Maracaibo, Venezuela.

Teléfono:
+58-0414-6305451

Correos electrónicos:
elenaryder@gmail.com
riclinicas@gmail.com

Páginas web:
https://sites.google.com/site/revistainvestigacionesclinicas

http://www.produccioncientificaluz.org/revistas

For any information please address correspondence to:

Dr. Elena Ryder, Editor
Instituto de Investigaciones Clínicas
"Dr. Américo Negrette"
Facultad de Medicina, Universidad del Zulia
Maracaibo, Venezuela.

Phone:
+58-0414-6305451

E-mails:
elenaryder@gmail.com
riclinicas@gmail.com

Web pages:
https://sites.google.com/site/revistainvestigacionesclinicas

http://www.produccioncientificaluz.org/revistas

Universidad del Zulia
Publicación auspiciada por el
Vicerrectorado Académico
Serbiluz-CONDES

CODEN: ICLIAD
Versión impresa ISSN: 0535-5133
Depósito legal pp 196002ZU37
Versión electrónica ISSN: 2477-9393
Depósito legal ppi 201502ZU4667

Artes finales:
Lisbeny Valencia
lisbenyvalencia@gmail.com

Invest Clin 64(4): 437 - 439, 2023 https://doi.org/10.54817/IC.v64n4a00

EDITORIAL
El Premio Nobel de Medicina o Fisiología 2023.

El 2 de octubre del 2023, la Asamblea Nobel del Instituto Karolinska, en Estocolmo, Suecia, anunció que el Premio Nobel en Fisiología o Medicina fue otorgado conjuntamente a Katalin Karikó y Drew Weissman "por sus descubrimientos concernientes a las modificaciones de bases (nucleosídicas), que permitieron el desarrollo de vacunas efectivas de ARN mensajero (ARNm), contra la COVID-19". Aunque una lectura rápida del veredicto podría sugerir que se premiaba al desarrollo de la vacuna contra la COVID-19, en realidad ese no fue el caso. Por instrucciones de Alfred Nobel, el premio de Medicina se adjudicaría solo por un descubrimiento, no necesariamente por la aplicación práctica de un descubrimiento. Eso explica, por ejemplo, que los científicos que desarrollaron las vacunas contra la poliomielitis no recibieron el Premio Nobel, sino que fue adjudicado en 1954 a John F. Enders, Thomas H Weller y Frederick C Robbins "por su descubrimiento de la capacidad de los virus de la poliomielitis para crecer en cultivos de varios tipos de tejido". Ese descubrimiento permitió la producción en gran escala, de los virus que se utilizaron más tarde en el desarrollo de las vacunas contra la poliomielitis (la inactivada inyectable de Jonas Salk en 1955 y la atenuada oral de Albert Sabin en 1961). De hecho, la única vacuna que ha ameritado un Premio Nobel fue la desarrollada contra la fiebre amarilla, concedido en 1951 a Max Theiler "por sus descubrimientos concernientes a la fiebre amarilla y como combatirla" [1].

El Premio Nobel fue otorgado a Karikó y Weissman, por sus descubrimientos básicos en relación con modificaciones del ARNm, los cuales más tarde llevaron al desarrollo de una vacuna contra la COVID-19 [2]. El contexto de dichos estudios se sitúa dentro del dogma central de la biología molecular, que estipula que la información genética codificada en el ácido desoxirribonucleico (ADN), se transcribe a ácido ribonucleico mensajero (ARNm), el cual lleva esta información genética a los polirribosomas, donde es traducida a proteínas, que cumplen una gran variedad de funciones, entre ellas, el servir como antígenos inductores de una respuesta inmune. Las vacunas generalmente presentan al sistema inmune, las proteínas virales responsables de la inducción de una respuesta inmune protectora, ya sea como virus atenuados, virus inactivados o subunidades protéicas. Desde los años 90, se ha estado investigado el uso de vacunas basadas en ácido desoxirribonucleico (ADN) como vacunas. Sin embargo, la esperanza que en una época se puso en dicha plataforma vacunal, no ha resultado en vacunas prácticas, incluyendo el hecho de que el ADN vacunal debe migrar al núcleo celular donde debe ser transcrito al ARNm correspondiente, que entonces debe migrar al citoplasma para ser traducido a la proteína viral inmunogénica. Es así como se postuló que una plataforma basada directamente en ARNm, podría ser más eficiente, cosa que se facilitó por el desarrollo de métodos eficientes para la producción *in vitro* de ARNm. Sin embargo, la molécula de ARNm es sumamente inestable y se degrada fácilmente. Además, cuando el ARNm se inyecta en las altas concentraciones, necesarias para inducir la producción de la proteína de interés, se inducen respuestas inflamatorias que serían inaceptables para una vacuna o proteína terapéutica.

Katalin Karikó nació en 1955 en Hungría, país donde recibió su PhD en 1982, y donde trabajó hasta 1985, año en el que se mudó a los Estados Unidos. En la Universidad de Pensilvania, comenzó a experimentar con diferentes formas de ARN, con el objetivo de optimizar la expresión de proteínas terapéuticas. A finales de los años 90, inició una colaboración con el norteamericano Drew Weissman, un colega inmunólogo también de la Universidad de Pensilvania, especialista en el uso de células dendríticas como mediadoras de la inducción de respuestas inmunes. En el curso de sus trabajos, Karikó y Weissman, encontraron que las células dendríticas reconocían al ARN sintético como una substancia extraña, que llevaba a su activación y a la liberación de citoquinas inflamatorias. Se encontró que esa respuesta era mediada por un mecanismo del sistema inmune de defensa innato, que incluye los receptores de peaje (Toll-like receptors o TLR) presentes en las células dendríticas, que reconocen formas moleculares extrañas conocidas como "patrones moleculares asociados a patógenos ("pathogen-associated molecular patterns" o PAMS), incluyendo los TLR3 y TLR7/8, que reconocen ARN de doble cadena y ARN de cadena sencilla, respectivamente. Los investigadores galardonados con el Premio Nobel, especularon que las modificaciones postranscripcionales que ocurren en los ARN producidos de manera natural, los protegen de ese reconocimiento por el sistema inmune innato. En un artículo publicado en el 2005, demostraron que la sustitución de nucleósidos comunes usados para la síntesis del ARN, especialmente con el uso de psedouridina (Ψ) en vez de uridina, se abolía la respuesta inflamatoria indeseable [3]. En estudios que se publicaron en los años 2008 y 2010, Karikó y Weissman demostraron que el ARN así modificado, resultaba en un aumento marcado en la producción de proteínas, debido a que el ARNm modificado, evade el reconocimiento por la proteína quinasa R (PKR), una enzima que reconoce el ARN apagando el proceso de traducción [4,5]. Esas observaciones representaron un cambio del paradigma en nuestro entendimiento de cómo como las células responden a diferentes tipos de ARN, produciendo el conocimiento básico que varios años más tarde, se aplicó para el rápido desarrollo de vacunas contra la COVID-19.

Aunque los descubrimientos de Karikó y Weissman fueron de importancia fundamental, se necesitaba desarrollar un método de empaque del ARNm modificado, para evitar su hidrólisis y permitir su transporte al citoplasma celular. El método de transporte que se desarrolló, es el de nanopartículas lipídicas, que se dirigen a células presentadoras de antígenos en los nódulos linfáticos, aumentando la respuesta inmune e induciendo la activación de un tipo particular de células CD4 ayudadoras [6]. Con respecto al desarrollo de la vacuna contra la COVID-19, también debe mencionarse el trabajo de Barney Graham y colaboradores, del Centro para el Desarrollo de Vacunas del Instituto Nacional de Higiene de los Estados Unidos, que por medio de estudios de biología estructural, propusieron que ciertas mutaciones en la proteína de la espícula de los Betacoronavirus, preservaban su conformación en un estado de prefusión, mejorando su expresión y aumentando su inmunogenicidad [7].

Aunque el Comité Nobel decidió premiar a Karikó y a Weissman, el rápido desarrollo de vacunas contra la COVID-19 se debió a muchos años de investigación básica y aplicada, llevada a cabo por muchos investigadores, mucho antes de que se declarara la pandemia de la COVID-19 [8]. Con las vacunas contra la COVID-19, la tecnología de ARNm demostró de una manera espectacular su seguridad y efectividad, y abrió nuevas líneas de investigación y desarrollo para el desarrollo de nuevas vacunas y proteínas terapéuticas.

José Esparza
ORCID 0000-0002-2305-6264

The 2023 Nobel Prize in Medicine or Physiology.

The 2023 Nobel Prize in Medicine or Physiology, awarded to Katalin Karikó and Drew Weissman, recognizes the fundamental discovery that the modification of bases in mRNA synthesized in vitro prevents inflammatory responses and increases protein production when it is introduced into the cell. Although these discoveries received little attention when they were published between 2005 and 2010, ten years later they made possible the rapid development of vaccines against COVID-19.

REFERENCIAS

1. **Norrby E.** Yellow fever and Max Theiler: the only Nobel Prize for a virus Vaccine. J Exp Med 2007. 204(12):2779-2784.
2. **The Nobel Assembly at the Karolinska Institutet**. Press Release. The 2023 Nobel Prize in Medicine or Physiology. https://www.nobelprize.org/prizes/medicine/2023/advanced-information/
3. **Karikó K, Buckstein M, Ni H, Weissman D**. Suppression of RNA recognition by Toll-like receptors: The impact of nucleoside modification and the evolutionary origin of RNA. Immunity 2005. 23:165-175.
4. **Karikó K, Muramatsu H, Welsh FA, Ludwig J, Kato H, Akira S, Weissman D.** Incorporation of pseudouridine into mRNA yields superior nonimmunogenic vector with increased translational capacity and biological stability. Mol Ther 2008. 16:1833-1840.
5. **Anderson BR, Muramatsu H, Nallagatla SR, Bevilacqua PC, Sanding LH, Weissman D, Karikó K**. Incorporation of pseudouridine into mRNA enhances translation by diminishing PKR activation. Nucleic Acid Res 2010. 38:5884-5892.
6. **Stuart LM.** In gratitude for mRNA vaccines. New Eng J Med 2021. 385:1435-1438.
7. **Corbett KS, Edwards DK, Leist SR, Abiona OM, Boyoglu-Barnum S, Gillespie RA, Himansu S, Schäfer A, Ziwawo CT, DiPiazza AT, Dinnon KH, Elbashir SM, Shaw CA, Woods A, Fritch EJ, Martinez DR, Bock KW, Minai M, Nagata BM, Hutchinson GB, Wu K, Henry C, Bahl K, Garcia-Dominguez D, Ma L, Renzi I, Kong WP, Schmidt SD, Wang L, Zhang Y, Phung E, Chang LA, Loomis RJ, Altaras NE, Narayanan E, Metkar M, Presnyak V, Liu C, Louder MK, Shi W, Leung K, Yang ES, West A, Gully KL, Stevens LJ, Wang N, Wrapp D, Doria-Rose NA, Stewart-Jones G, Bennett H, Alvarado GS, Nason MC, Ruckwardt TJ, McLellan JS, Denison MR, Chappell JD, Moore IN, Morabito KM, Mascola JR, Baric RS, Carfi A, Graham BS.** SARS-CoV-2 mRNA vaccine design enabled by prototype pathogen preparedness. Nature 2020. 586:567-571.
8. **Dolgin E**. The tangled history of mRNA vaccines. Nature 2021. 597:318-324.

Invest Clin 64(4): 441 - 450, 2023 https://doi.org/10.54817/IC.v64n4a1

Effects of focused ultrasound on human cervical cancer HeLa cells *in vitro*.

Yanbin Liu[1], Qun Zhao[2], Panpan Liw[3], Yanbin Li[3], Li'an Yi[4] and Haiping Yan[4]

[1]Department of Ultrasound Diagnosis, Affiliated Hospital of Beihua University, Jilin, China.
[2]Department of Cardiovascular Medicine (Group 1, 4th Treatment Area), Affiliated Hospital of Beihua University, Jilin, China.
[3]Department of Ultrasonic Medicine, Qingdao West Coast New Area Traditional Chinese Medicine Hospital (Qingdao Huangdao District Traditional Chinese Medicine Hospital), Qingdao, China.
[4]Department of Health Management Section, Qingdao West Coast New Area Traditional Chinese Medicine Hospital (Qingdao Huangdao District Traditional Chinese Medicine Hospital), Qingdao, China.

Keywords: focused ultrasound; cervical cancer; HeLa cell line; *in vitro* effects.

Abstract. Cervical cancer is the fourth most common malignant tumor in women. Many studies have confirmed that early childbirth, prolificacy, HPV infection, and smoking are some risk factors. This article explored the effects of exposing human cervical cancer HeLa cells to different focused ultrasound intensities *in vitro*. The study employed three groups of cells: 1- a high-intensity treated group, 2- a low-intensity treated group, and 3- a control group. Results showed that after 12 hours of focused ultrasound treatment, the growth inhibition rate of the low-intensity group was 55.6% higher than that of the control group, and the growth inhibition rate of the high-intensity group was 41.2% higher than that of the low-intensity group. Therefore, focused ultrasound had a specific inhibitory effect on the growth of HeLa cells, and the higher the intensity of focused ultrasound, the higher the inhibition rate on cancer cells. In addition, the Cycle Threshold (Ct) values of the three groups of cells before treatment were the same, but the Ct values after treatment had changed. The Ct value of the low-intensity group was 18.1% lower than that of the control group, and the Ct value of the high-intensity group was lower than that of the low-intensity group by 27.8%, showing that focused ultrasound can effectively reduce the activity of HeLa cells *in vitro*.

Correspondence author: Qun Zhao, Department of Cardiovascular Medicine (Group 1, 4th Treatment Area), Affiliated Hospital of Beihua University, Jilin, China. Email: zrx202102bh@163.com

Efectos del ultrasonido focalizado sobre células HeLa de cáncer cervical humano *in vitro*.

Invest Clin 2023; 64 (4): 441 – 450

Palabras clave: ultrasonido focalizado; cáncer de cuello uterino; línea celular HeLa; efectos *in vitro*.

Resumen. El carcinoma de cuello uterino es el cuarto tumor maligno más común en las mujeres. Muchos estudios han verificado que el parto prematuro, la prolificidad, la infección por VPH y fumar son algunos de los factores de riesgo. El propósito de este artículo fue investigar los efectos del tratamiento con diferentes intensidades de ultrasonido focalizado sobre células HeLa de cáncer de cuello uterino humano *in vitro*. Este estudio utilizó tres grupos de células HeLa: 1- un grupo de tratamiento con alta intensidad, 2- un grupo de tratamiento con baja intensidad y 3- un grupo control. Los resultados mostraron que después de 12 horas de tratamiento con ultrasonido focalizado, la tasa de inhibición del crecimiento del grupo de baja intensidad fue 55,6% más elevada que la del grupo control y la tasa de inhibición del crecimiento del grupo de alta intensidad fue 41,2% más elevada que la del grupo de baja intensidad. Por lo tanto, el ultrasonido focalizado tiene un efecto inhibitorio sobre el crecimiento de células HeLa, y cuanto mayor sea la intensidad del ultrasonido focalizado, más elevada será la tasa de inhibición de las células cancerosas. Además, los valores del Umbral de Ciclos [Cycle Threshold (Ct)] de los tres grupos de células eran los mismos antes del tratamiento, pero estos valores tuvieron cambios evidentes después del tratamiento. El valor del Ct del grupo de baja intensidad fue 18,1% inferior al del grupo de control y el valor del Ct del grupo de alta intensidad fue 27,8% más bajo que el del grupo de baja intensidad; lo que demuestra que el ultrasonido focalizado puede reducir la actividad de las células HeLa *in vitro*.

Received: 23-08-2022 Accepted: 01-08-2023

INTRODUCTION

Cervical cancer is the most common malignant tumor of the reproductive organs in women. Based on the statistics, more than 500,000 new cervical cancer cases occur yearly; about 5% of all new cancer patients and more than 80% live in developing countries [1]. Many studies have confirmed that sexual disorders, oral contraceptives, bisphenol A, early sexual life, nutritional factors, premature birth, fertility, human papillomavirus (HPV) infection, and smoking contribute to the pathogenesis [2,3]. Zhang *et al*. investigated the relationship between HPV16 E6 and E7 protein expression and telomerase in cervical cancer carcinogenesis. The results showed that these proteins and telomerase increase gradually with the progression of cervical cancer [4]. Sufficient and improved screening programs to detect this kind of cancer increase the knowledge about its relation with HPV, reducing disease cases in developed countries [5].

Patients may have no apparent symptoms in the early stage of this disease. With

the disease progression, vaginal bleeding and vaginal drainage, and even systemic failure signs like anemia and cachexia in the later stages may appear [6], which seriously threaten the lives and health of most women.

The common symptoms of cervical cancer are vaginal bleeding, vaginal discharge, frequent urination, urgency, constipation, swelling of the lower limbs, and abdominal pain caused by the involvement of adjacent tissues, organs, and nerves. In recent decades, due to the wide application of cervical cytology screening technology, early diagnosis and treatment of cervical cancer and precancerous lesions have become the main reason for reducing morbidity and mortality, thereby improving patient survival. A study investigated the positive effect of using WhatsApp (the internet messaging app) on the health promotion of older women's behavior for early detection of cervical cancer through the visual acetic acid examination [7].

Focused ultrasound technology is a high-tech that has gradually matured and developed in recent years. Its basic principle is to use ultrasound to have good permeability inside the tissue and focus on identification. Through the computer control system, the thermal effect, cavitation effect, and mechanical effect eventually make the target tumor cell degeneration and necrosis to achieve the purpose of treatment[3]tissue disintegration is also possible because of the interaction between the distorted HIFU bursts and either bubble cloud or boiling bubble. Hydrodynamic cavitation is another type of cavitation and has been employed widely in industry, but its role in mechanical erosion to tissue is not clearly known. In this study, the bubble dynamics immediately after the termination of HIFU exposure in the transparent gel phantom was captured by high-speed photography, from which the bubble displacement towards the transducer and the changes of bubble size was quantitatively determined. The characteristics of hydrodynamic cavitation due to the release of the acoustic radiation force and relaxation of compressed surrounding medium were found to associate with the number of pulses delivered and HIFU parameters (i.e. pulse duration and pulse repetition frequency. In recent decades, because focused ultrasound has the advantages of non-invasiveness, quick recovery after surgery, and less pain for patients, it has been increasingly used to treat various solid tumors, such as cervical cancer, uterine fibroids, and pancreatic cancer [8]. Many clinical studies have confirmed that focused ultrasound can play a better role in treating cervical cancer [9,10].

Imankulov *et al*. evaluated the feasibility of using high-intensity focused ultrasound (HIFU) to treat tumors and proved that high-intensity focused ultrasound can effectively inhibit the growth of various tumor cells [11]. Hong *et al*. discussed the effect of HIFU irradiation on the apoptosis-related genes of human pancreatic cancer xenograft tumors. By establishing a nude mouse-human pancreatic cancer YY-1 cell xenograft model and HIFU irradiation, the original TUNEL labeling method was used to detect the apoptosis rate of tumor cells, and it was found that the tumor cell apoptosis rate in the irradiated group was higher [12]. Yuan *et al.* reported that the mechanism by which HIFU enhances anti-tumor immunity has not been well elucidated, and there is emerging evidence that miRNA plays an essential role in the immune response [13].

Focused ultrasound for the treatment of cervical cancer uses the directionality of ultrasound, tissue penetration, and focusing and uses special focusing equipment to focus ultrasound from the outside of the body to the selected treatment area in the body[14]. In some studies, focused ultrasound treatment was recorded, and the average number of treatments was eight times. Most patients completed the follow-up. Among patients who completed follow-up, survival rate statistics were conducted every six months for the 24 months after treatment. The survival rate in the 6th month was 100.00%; the survival rate at the 12th month was 75.93%; the survival rate at the 18th month was 66.67%; the

survival rate at the 24th month was 55.56%. These results show that focused ultrasound can kill cancer tissues in a targeted manner while preserving most normal tissues [15].

This article aimed to analyze the effect of focused ultrasound on human cervical cancer HeLa cells *in vitro*.

MATERIALS AND METHODS

Preparation of Experimental Materials

A medical university's ultrasound engineering institute provided human cervical cancer HeLa cells. The cultured HeLa cells were randomly divided into control, low-intensity, and high-intensity irradiation groups. The control group was treated with conventional interferon in vitro, the low-intensity group was treated with focused ultrasound, and the high-intensity group was treated with an intensity-focused ultrasound instrument (Table 1).

The conventional cell culture method

The cryopreserved human cervical cancer HeLa cells were recovered in a culture bottle containing 10% fetal bovine serum RPM H-1640 nutrient solution, and a single-cell suspension was prepared. Cell growth inhibition was determined by MTT colorimetry (tetrazolium dye colorimetric assay).

The density of human cervical cancer HeLa cells was adjusted to $3x10^3$ cells/mL. The MTT method was used to determine the concentration, and the inhibition rate (R) was calculated as follows:

Inhibition rate (R) = (1-experimental group A value, control group A value) × 100%

The experiment was repeated three times with the same method.

Focused ultrasonic field treatment

Logarithmically grown cells were taken and digested with 0.25% trypsin. They were centrifuged and washed with PBS solution 2~3 times. The cell density was adjusted to 2 x 10^4 cells/mL. The experimental group was divided into low-dose and high-dose groups according to the different intensities of focused ultrasound (0, 1000 and 3000 Watts/cm^2). A volume of 500 μL was taken out of cell suspension from each group and placed in the smallest electric chamber. The fixed electric field intensity was 250 kV/cm, the repetition frequency was 3 Hz, and the pulse width was 800 ps. The control group did not receive focused ultrasound treatment.

Observing the cell morphology under an optical microscope

The cell density was adjusted to $3x10^4$ cells/mL and inoculated into a 24-well culture plate with a preset cover glass. Each well was placed in an incubator for 1ml culture, and the medium changed in the logarithmic growth phase. After 72 hours, the coverslip was removed and stained, and the cell morphology was observed under an optical microscope.

Observing the cell morphology by transmission electron microscopy (TEM)

The cells were inoculated in a culture flask according to the above density. They were collected, fixed before washing through 4% glutaraldehyde, fixed after washing with 1% acid, periodically dehydrated, and then soaked with epoxy resin. They were then embedded to make a fat mass and cut into ultra-thin sections. The cell morphology was observed with TEM.

Table 1
The condition and treatment of Hela cells in different groups.

Serial number	Number of cells	Passages	Treatment
Control group	1.83×10^4	5	Alpha interferon
Low-intensity group	1.75×10^4	5	Low-intensity Focused ultrasound
High-intensity group	1.82×10^4	5	High-intensity focused ultrasound

Detecting cell apoptosis by the TUNEL method

Cell slides were obtained according to the method of observing cell morphology under an optical microscope and cultured in an incubator. After the logarithmic growth phase, the medium was changed, and drugs were added, according to the TUNEL method, which was utilized for detecting apoptotic DNA fragmentation and identifying and quantifying apoptotic cells.

Western blot analysis of BAX and Bcl-2 protein expression

After cell treatment, each group of cells was incubated for 12 hours, suspended in PBS, and counted. The $1x10^6$ cells were pelleted by centrifugation, lysed with 200 mL PMSF cell lysis buffer for one hour, and then centrifuged at 12000 g at 4 °C for 10 minutes. Bcl-2 and BAX primary antibodies were added overnight at 4 °C. The samples were washed three times at room temperature in TBST for 10 minutes each time. Quantity One ® 1-D image analysis software (Bio-Rad) was used to analyze the results. The absorbance of the blot was equal to the average absorbance × area. The ratio of BAX / Bcl-2 was equal to the absorbance of the BAX band/Bcl-2 band.

Immunohistochemical staining (SP method) was performed, and the steps of the SP kit instructions were followed. PBS was used instead of the primary antibody as a negative control, and Fuzhou Maxim Biological Company provided photos of the positive pair.

Real-time Quantitative Polymerase Chain Reaction (rtPCR) and Cycle Threshold (Ct) Determination

Cycle Threshold (Ct) values were determined using the real-time quantitative polymerase chain reaction (rtPCR) method. Total RNA was extracted from the control, low-intensity, and high-intensity HeLa cell samples before and after treatment using the TRIzol reagent. The quality and concentration of the extracted RNA were measured using a NanoDrop spectrophotometer.

The extracted RNA was then reverse-transcribed into cDNA using a reverse transcription kit. The cDNA was used as the template for real-time PCR amplification. The reaction mixture included SYBR Green PCR Master Mix, forward and reverse primers specific to the gene of interest, and the cDNA template.

The cDNA was amplified by real-time PCR using SYBR Green PCR Master Mix on an Applied Biosystems 7500 Fast Real-Time PCR system. The amplification conditions were as follows: initial denaturation at 95 °C for 10 min, followed by 40 cycles of denaturation at 95 °C for 15 sec, annealing at 60 °C for 1 min, and extension at 72 °C for 30 sec.

The Ct value indicates the number of cycles required for the fluorescence signal to surpass the threshold level, which is inversely proportional to the amount of target nucleic acid in the sample. Lower Ct values correspond to higher levels of target nucleic acid.

The Primer Premier software designed PCR primers specific for the reference gene GAPDH, and the target gene was used. Relative expression levels of the gene of interest were calculated using the 2-ΔΔCT method, with GAPDH as the internal control. Fold changes in gene expression were analyzed using the 2-ΔΔCt method, and qRT-PCR was performed in triplicate for each sample. The Ct values of the control, low-intensity, and high-intensity groups before and after treatment were compared to evaluate the effect of various treatments on HeLa cell activity. Lower Ct values were indicative of higher gene expression and cell activity.

Statistical processing

The IBM SPSS 18.0® statistical analysis software was used for statistical processing. All experiments were performed at least three times. MTT results were analyzed for the variance of repeated measurement data, and laser scanning confocal and Western blot detection was performed using the ANOVA test. The difference was statistically significant with $p<0.05$.

RESULTS

Comparison of the mortality of each group of cells after focused ultrasound treatment

The mortality of each group of cells was measured using focused ultrasound treatment of human cervical cancer HeLa cells at three h, six h, 12 h, 24 h, and 48 h. The mortality of cells in each group at 48 h showed an upward trend with time, but the rising speed of each group was different. It can be seen that there is a difference between the death rate of human cervical cancer HeLa cells and the intensity of focused ultrasound have a proportional relationship. In addition, the cell death rate of HeLa cells in the same treatment group reached a peak 12 hours after treatment, which was significantly higher than other time points ($P<0.01$) (Table 2).

Comparison of the growth inhibition rate of focused ultrasound

The growth inhibition of human cervical cancer HeLa cells by focused ultrasound after different times was statistically analyzed. It can be seen from the data in Fig. 1 that focused ultrasound has a specific inhibitory effect on the growth of HeLa cells, and the higher the intensity of focused ultrasound, the higher the inhibition rate on cancer cells. After 12 hours of focused ultrasound treatment, the growth inhibition rate of the low-intensity group was 55.6% higher than that of the control group, the growth inhibition rate of the high-intensity group was 41.2% higher than that of the low-intensity group, and 72 hours after the focused ultrasound treatment, the growth inhibition of the low-intensity group was 55.6% higher than that of the control group. The growth inhibition rate of the high-intensity group was 11.1% higher than that of the low-intensity group.

Western blot detection of BAX and Bcl-2 expression

It can be seen from the data in Fig. 2 that the expression of BAX protein increased significantly after focused ultrasound treatment. The expression of BAX in the low-intensity group was 13.6% higher than that in the control group, and the expression of BAX in the high-intensity group was 2.1 higher than that in the low-intensity group. The expression of Bcl-2 protein decreased after focused ultrasound treatment. The expression of Bcl-2 in the low-intensity group was 15.9% lower than that in the control group, and the expression of Bcl-2 in the high-intensity group was 51.7% lower than that of the low-intensity group.

Changes in Ct values before and after treatment of HeLa cells

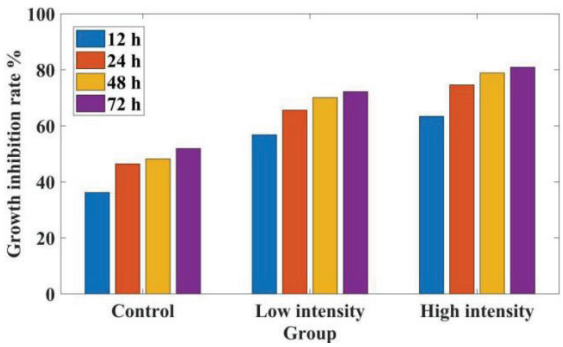

Fig. 1. Comparison of the growth inhibition rate of focused ultrasound on human cervical cancer HeLa cells after different times.

Table 2
The percentage of mortality of different groups of cells at different time points.

Group	3 h	6 h	12 h	24 h	48 h
Control group	1.05±1.25	2.57±0.98	4.67±1.28	5.60±1.22	7.05±3.44
Low-intensity group	35.94±1.68	71.23±0.99	74.22±0.87	57.56±0.99	74.88±1.96
High-intensity group	56.94±3.68	83.24±0.25	85.23±0.45	85.68±2.97	85.88±1.01

Values are mean ± standard deviation.

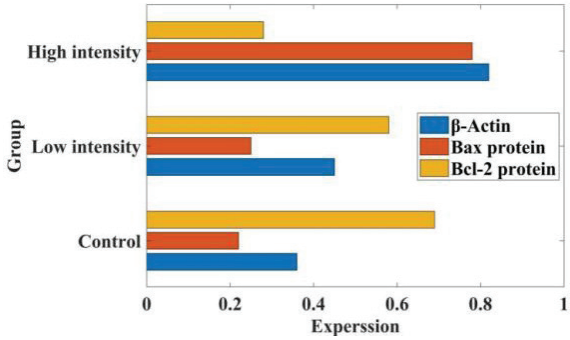

Fig. 2. Comparison of the results of Western blot detection of BAX and Bcl-2 expression.

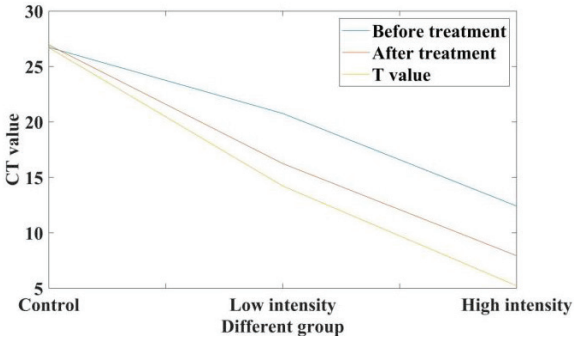

Fig. 3. Changes of Ct values before and after treatment of HeLa cells.

This study recorded the Ct value changes of three groups of human HeLa cells before and after treatment. It can be seen from the data in Fig. 3 that the Ct values of the three groups of HeLa cells before treatment are the same, but the Ct values after treatment have apparent changes. After treatment, the Ct value of the low-intensity group is 18.1% lower than that of the control group. The Ct value of the intensity group is 27.8% lower than that of the low-intensity group, which shows that focused ultrasound can effectively reduce the activity of HeLa cells.

DISCUSSION

This study analyzed the effect of focused ultrasound on human cervical cancer HeLa cells *in vitro,* and it showed that. This study showed that HIFU could be used to treat cervical cancer. Specifically, the following three points: first, this article uses a controlled experiment to compare the *in vitro* effects of low-intensity and high-intensity focused ultrasound. It accurately reflects the inhibitory effect of focused ultrasound on HeLa cells. Secondly, this article uses Western blot to detect the expression of BAX and Bcl-2 proteins, which can accurately reflect the changes in protein expression in HeLa cells and the tumor suppressor effect of focused ultrasound at the protein level. Thirdly, MTT results for repeated measurement data analysis of variance, laser scanning confocal, and Western blot detection using ANOVA test to ensure the experimental results are rigorous and credible.

The research results show that focused ultrasound has a particular inhibitory effect on the growth of human HeLa cells, and the higher the intensity of focused ultrasound, the higher the inhibition rate on cancer cells. After 12 hours of focused ultrasound treatment, the growth inhibition rate of the low-intensity group was 55.6% higher than that of the control group, and the growth inhibition rate of the high-intensity group was 41.2% higher than that of the low-intensity group. A study found that HIFU combined with cisplatin facilitates tumor volume reduction and could be beneficial in treating patients with cervical cancer [16]. In addition, Abel *et al*. reported that HIFU is a potentially safe way to treat cervical cancer [17].

Bcl-2 is a member of the apoptotic gene family. It is known that Bcl-2 is expressed in solid tumors and is mainly located in the cytoplasm and nucleus. Scientists speculate that this may be related to the formation of certain malignant tumors [18]. In the related studies of cervical cancer, although the expression of Bcl-2 has no apparent relationship with tumor histological type, tumor stage, or lymph node metastasis, the five-year survival rate of Bcl-2-positive patients is significantly higher than in BAX-positive patients [19].

In addition, BAX protein expression was significantly increased after focused ultrasound treatment. The expression of BAX in the low-intensity group was 13.6% higher

than that in the control group, and the expression of BAX in the high-intensity group was 2.1 times higher than that in the low-intensity group, while the Bcl-2 protein after focused ultrasound treatment, the expression level decreased. The expression level of BAX in the low-intensity group was 15.9% lower than that of the control group, and the expression level of BAX in the high-intensity group was 51.7% lower than that of the low-intensity group.

According to the study results, the Ct values of the three groups of HeLa cells before treatment were the same, but the Ct values after treatment had changed. After treatment, the Ct values of the low-intensity group were 18.1% lower than those of the control group, and the Ct value of the high-intensity group was 27.8% lower than the low-intensity group, showing that focused ultrasound can effectively reduce the activity of HeLa cells. In addition, focused ultrasound has the highest proportion in treating pancreatic cancer, reaching 51.4%, followed by bone tumors, accounting for 21.1%, while cervical cancer only accounts for 3% (Fig. 4) [20,21]. It can be seen that focused ultrasound has a more favorable prospect for treating cervical cancer.

In summary, this article proposed focused ultrasound as a new treatment method for cervical cancer. This study briefly introduced focused ultrasound as a treatment method, studied the in vitro effects of focused ultrasound on HeLa cells, and analyzed the inhibitory effect of focused ultrasound on cancer cells. The research results show that focused ultrasound has a specific inhibitory effect on the growth of HeLa cells, and the higher the intensity of focused ultrasound, the higher the inhibition rate on cancer cells.

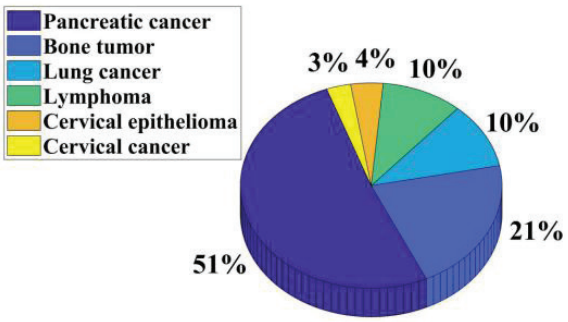

Fig. 4. Application of focused ultrasound in the treatment of solid tumors and its proportion.

ACKNOWLEDGMENTS

We thank Dr. Humberto Martinez for this manuscript's quality enhancement and language-native editing.

Funding

This study was not funded.

Conflict of interests

All of the authors had no personal, financial, commercial, or academic conflicts of interest separately.

Authors' ORCID numbers

- Yanbin Liu (YLiu): 0000-0003-4511-061X
- Qun Zhao (QZ): 0000-0002-1119-503X
- Panpan Liu (PL): 0000-0002-8796-2426
- Yanbin Li (YLi): 0000-0001-5499-8986
- Li'an Yi (LY): 0000-0003-2994-7233
- Haiping Yan (HY): 0000-0001-7449-2616

Authors' Contribution

YLiu: Manuscript editing, revising and final approval of manuscript. QZ: Manuscript editing, revising and final approval of manu-

script. PL: Administrative support. YLi: Conception and design, Collection and assembly of data. LY: Provision of study materials or patients. HY: Data analysis and interpretation.

REFERENCES

1. **Hu B, Luo W, Zhang M, Zhao X, Yang L, Wang Y**. Effects of dexmedetomidine on hemodynamics, stress response, lung compliance, and oxygenation index in laparoscopic patients with cervical cancer. Acta Medica Mediterr 2022; 38(3): 2141-2145. *https://doi.org/10.19193/0393-6384_2022_3_327*.
2. **Mohamed Saleh Omar Korbag S, Mohamed Saleh Omar Korbag I**. A new study biological role of hpv infection, oral contraceptive use, sex hormones and bisphenol A and increase rate cancer of cervical in libya. J Med Chem Sci 2020; 3(4): 354-362. *https://doi.org/10.26655/JMCHEMSCI.2020.4.5*.
3. **Zhou Y, Gao XW**. Effect of hydrodynamic cavitation in the tissue erosion by pulsed high-intensity focused ultrasound (pHIFU). Phys Med Biol 2016; 61(18): 6651-6667. *https://doi.org/10.1088/0031-9155/61/18/6651*.
4. **Zhang Y, Ji X, Gu S, Wu H, Fu B.** The correlation between HPV 16 e6 and e7 proteins and telomerase expression in cervical cancer carcinogenesis. Acta Medica Mediterr 2022; 38(2): 831-836. *https://doi.org/10.19193/*0393-*6384_2022_2_126*.
5. **Jalil AT, Mohammad WT, Karevskiy A, Dilfy SH**. Histological diagnosis and staging of cervical cancer samples collected from women in Dhi-Qar Province. J Med Chem Sci 2023; 6(2): 269-279. *https://doi.org/10.26655/*JMCHEMSCI.*2023.2.9*.
6. **Zhang L, Liu L, Huang Y, Tuo Y, Song J**. Relationship between single nucleotide polymorphism of dna repair genes ercc1 and ercc2 and cervical cancer susceptibility. Acta Medica Mediterr 2021; 37(6): 3013-3017. *https://doi.org/10.19193/0393-6384_2021_6_472*.
7. **Soetrisno S, Ismarwati I, Nurinasari H**. The effectiveness of community development model by using Whatsapp toward old women behavior in early detection of cervical cancer. J Med Chem Sci 2021; 4(4): 341-350. *https://doi.org/10.26655/JMCHEMSCI.2021.4.5*.
8. **Liu NN, Khoo BC, Zhang AM**. Study on the structure and behaviour of cavitation bubbles generated in a high-intensity focused ultrasound (HIFU) field. Eur Phys J E 2019; 42(6): 1-13. *https://doi.org/10.1140/epje/*i2019-*11833-8*.
9. **Mai X, Chang Y, You Y, He L, Chen T**. Designing intelligent nano-bomb with on-demand site-specific drug burst release to synergize with high-intensity focused ultrasound cancer ablation. J Control Release 2021; 331: 270-281. *https://doi.org/10.1016/j.jconrel.2020.09.*051.
10. **Zhu L, Huang Y, Lam D, Gach HM, Zoberi I, Hallahan DE, Grigsby PW, Chen H, Altman MB.** Targetability of cervical cancer by magnetic resonance-guided high-intensity focused ultrasound (MRgHIFU)-mediated hyperthermia (HT) for patients receiving radiation therapy. Int J Hyperth 2021; 38(1): 498-510. *https://doi.org/10.1080/02656736.2021.*1895330.
11. **Imankulov S, Baygenzhin A, Rustemova K, Tashev I, Fedotovskikh G, Shaimardanova G, Zhampeissov N, Erlan M.** The impact of high-intensity focused ultrasound on the hydatid *Echinococcus Cyst* (Experiment in vitro). Int J Adv Res 2016; 4(10): 372-382. *https://doi.org/10.21474/IJAR0 1/1801*.
12. **Hong L, Guo Z, Xing W, Yu H, Liu Ch, Yang X, Wang H.** Effects of high-intensity focused ultrasound on apoptosis-associated gene expression in xenografts with human pancreatic cancer. Natl Med J China 2017; 97(9): 694-697. *https://doi.org/10.3760/cma.j.issn.0376.2491.2017.09.013*.
13. **Yuan SM, Li H, Yang M, Zha H, Sun H, Li XR, Li AF, Gu Y, Duan L, Luo JY, Li CY, Wang Y, Wang ZB, He TC, Zhou L.** High intensity focused ultrasound enhances antitumor immunity by inhibiting the negative regulatory effect of miR-134 on CD86 in a murine melanoma model. Oncotarget 2015; 6(35): 37626-37637. *https://doi.org/10.18632/oncotarget.5285*.

14. **Dosanjh A, Harvey P, Baldwin S, Mintz H, Evison F, Gallier S, Trudgill N, James ND, Sooriakumaran P, Patel P.** High-intensity focused ultrasound for the treatment of prostate cancer: A national cohort study focusing on the development of stricture and fistulae - ScienceDirect. Eur Urol Focus 2021; 7(2): 340-346. *https://doi.org/10.1016/j.euf.2019.11.014*.
15. **Childers C, Edsall C, Gannon J, Whittington AR, Muelenaer AA, Rao J, Vlaisavljevich E.** Focused ultrasound biofilm ablation: investigation of histotripsy for the treatment of catheter-associated urinary tract infections (CAUTIs). IEEE Transactions on Ultrasonics, Ferroelectrics, and Frequency Control, 2021; 68(9): 2965-2980. *https://doi.org/10.1109/TUFFC.2021.3077704*.
16. **Lee YY, Cho YJ, Choi JJ, Choi CHm, Kim TJ, Kim BG, Bae DS, Kim YS, Lee JW.** The effect of high-intensity focused ultrasound in combination with cisplatin using a xenograft model of cervical cancer. Anticancer Res 2012; 32(12): 5285-5289.
17. **Abel M, Ahmed H, Leen E, Park E, Chen M, Wasan H, Price P, Monzon L, Gedroyc W, Abel P.** Ultrasound-guided trans-rectal high-intensity focused ultrasound (HIFU) for advanced cervical cancer ablation is feasible: A case report. J Ther Ultrasound 2015; 3(1): 1-4. *https://doi.org/10.1186/s40349-015-0043-6*.
18. **Frenzel A, Grespi F, Chmelewskij W, Villunger A**. Bcl2 family proteins in carcinogenesis and the treatment of cancer. Apoptosis 2009; 14(4): 584-596. *https://doi.org/10.1007/s10495-008-0300-z*.
19. **Zhao LW, Zhong XH, Yang SY, Zhang YZ, Yang NJ**. Inotodiol inhabits proliferation and induces apoptosis through modulating expression of cyclinE, p27, bcl-2, and bax in human cervical cancer HeLa cells. Asian Pacific J Cancer Prev 2014; 15(7): 3195-3199. *https://doi.org/10.7314/APJCP.2014.15.7.3195*.
20. **Hsiao YH, Kuo SJ, Tsai H Der, Chou MC, Yeh GP**. Clinical application of high-intensity focused ultrasound in cancer therapy. J Cancer 2016; 7(3): 225-231. *https://doi.org/10.7150/jca.13906*.
21. **Tang F, Zhong Q, Ni T, Chen Y, Liu Y, Wu J, Feng Z, Lu X, Tan S, Zhang Yu.** Salvage high-intensity focused ultrasound for residual or recurrent cervical cancer after definitive chemoradiotherapy. J Clin Oncol 2022; 40(16_suppl): e17524-e17524. *https://doi.org/10.1200/jco.2022.40.16_suppl.e17524*.

Invest Clin 64(4): 451 - 459, 2023 https://doi.org/10.54817/IC.v64n4a2

Caracterización de la gravedad del intento de suicidio en adolescentes hospitalizados en un hospital público de Chile.

Lautaro Barriga

Escuela de Psicología, Universidad Bernardo O Higgins, Santiago, Chile.
Escuela de Psicología, Universidad Gabriela Mistral, Santiago, Chile.

Palabras clave: adolescentes; hospitalización; intento de suicidio; trastorno mental; abuso sexual.

Resumen. El suicidio de adolescentes aumentó en las Américas. En Chile, el intento de suicidio de adolescentes es un problema de salud pública que necesita una urgente solución. Se realizó un estudio cuantitativo, comparativo y retrospectivo con el objeto de proporcionar al hospital estrategias de intervención y de articulación con la red territorial de salud mental. Se revisaron, compararon y relacionaron los aspectos sociodemográficos y clínicos de 96 fichas de adolescentes hospitalizados por intento de suicidio entre enero del 2017 a diciembre del 2018. Se conformaron dos grupos de estudio; el grupo I, con 14 adolescentes previamente internados en la Unidad de Tratamientos Intensivos y el grupo II, con 82 adolescentes que no requirió de esta unidad. Se estudió el género, edad, escolaridad, antecedentes de abuso sexual, diagnósticos de trastornos mentales, co-morbilidades, cuidador con trastorno mental y consultas previas en salud mental. Se utilizó estadística descriptiva y odd ratio. En el grupo I, con un 92% de adolescentes hombres, se observó un 57% de depresión grave y el 100% de sus integrantes sufrió abuso sexual; en el grupo II, con un 91% de adolescentes mujeres, se encontró un 79% de depresión moderada, un 85,3% de desarrollo anormal de la personalidad y el 70% de sus integrantes sufrieron abuso sexual. El abuso sexual explicó el mayor porcentaje de la varianza (29%). Se concluye que el hospital debe considerar en sus intervenciones las características distintivas de los grupos de estudio y coordinar con la red territorial de salud mental la continuidad de cuidados.

Autor de correspondencia: Lautaro Bernardo Barriga Carvajal. Escuela de Psicología, Universidad Bernardo O Higgins. Dirección Postal: Avenida Viel 1497. Santiago, Chile. Teléfono: +56 954242914. Correo electrónico: lautaro.barriga@ubo.cl

Characterization of the severity of suicide attempts in adolescents hospitalized in a public hospital in Chile.

Invest Clin 2023; 64 (4): 451 – 459

Keywords: adolescents; hospitalization; suicide attempt; mental disorder; sexual abuse.

Abstract. Adolescent suicide has increased in the Americas. In Chile, attempted suicide in adolescents is a public health problem that needs an urgent solution. A quantitative, comparative and retrospective study was conducted to provide the hospital with intervention strategies and articulation with the territorial mental health network. The sociodemographic and clinical aspects of 96 records of adolescents hospitalized for attempted suicide between January 2017 and December 2018 were reviewed, compared, and related. Two study groups were formed: Group I, 14 adolescents previously hospitalized in the Intensive Treatment Unit and Group II, 82 adolescents who did not require this unit. Gender, age, education, history of sexual abuse, diagnoses of mental disorders, co-morbidities, previous mental health consultations, and caregivers with mental disorders were studied. Descriptive statistics and odds ratios were used. In group I, with 92% male adolescents, severe depression was observed in 57% of cases, and 100% of its members suffered sexual abuse; in group II, with 91% female adolescents, 79% moderate depression was found, 85.3% abnormal personality development and 70% of its members suffered sexual abuse. Sexual abuse explained the highest percentage of the variance (29%). It is concluded that the hospital must consider the distinctive characteristics of the study groups and coordinate with the territorial network of mental health the continuity of care in its interventions.

Recibido: 25-10-2022 Aceptado: 01-08-2023

INTRODUCCIÓN

El suicidio es todo acto intencional por el cual una persona se provoca la muerte; asociado a este concepto se encuentra el intento de suicidio que son los actos auto-lesivos intencionales que no provocan la muerte [1,2]. El suicidio genera más de 800.000 mil muertes anuales en el mundo; esto equivale a un suicidio cada 40 segundos con una proyección de 1,5 millones de suicidios para el término del año 2023, representando uno de los mayores problemas de salud a nivel mundial [3]. En estas últimas décadas, las Américas registraron más de 7 suicidios por hora, con 4,6 casos de mujeres y 15,1 casos de hombres, afectando principalmente a la población de adolescentes [4,5]. Se estima que por cada suicidio de adolescente se realizaron entre 1 a 20 intentos con repercusiones en el entorno familiar, escolar y social [6,7]. En Chile, el suicidio es la segunda causa de muerte de adolescentes, observándose que las mujeres adolescentes lideran los intentos de suicidio, pero son los hombres adolescentes quienes lo consuman tres veces más [8,9]. Con relación

a las tasas de suicidio de adolescentes, estas pasaron de 5,83 casos por 100.000 habitantes en el año 1990, a 9,28 casos en el año 2005 y a 11,8 en el año 2013 [9]. El suicidio no es una enfermedad, sin embargo, padecer de un trastorno mental es un importante factor de riesgo [10]. Los adolescentes chilenos tienen alta prevalencia de trastornos mentales en comparación a los adolescentes de otros países latinoamericanos. Así, Chile tiene un 14,6% de trastornos disruptivos, un 8,3% de trastornos ansiosos y un 5,1% de trastornos afectivos (depresión y bipolaridad) que, por lo general, cursan con desarrollos anormales de la personalidad [11,12]. El diagnóstico más frecuente del adolescente en los centros chilenos especializados de salud mental es el trastorno depresivo con intento de suicidio, diagnóstico que, en la actualidad, constituye un importante problema de salud pública; mientras que adolescentes con trastornos bipolares registran escasas consultas, pero tienen un alto riesgo de suicidio incluso con tratamiento farmacológico [12,13]. Adolescentes con diagnósticos de trastornos afectivos pueden incrementar hasta un 60% la probabilidad de muertes por suicidio; en este grupo etario no existe otra enfermedad que genere tanta interferencia y discapacidad como la mental [14,15]. El plan chileno de salud mental 2017-2025 busca estrategias para la intervención de las Unidades de Cuidados de Hospitalización Intensivos en Psiquiatría (UCHIP) de adolescentes con o sin intento de suicidio y para la articulación de las redes territoriales de salud mental [16,17].

El propósito del estudio fue revisar, en un determinado período de tiempo, los aspectos sociodemográficos y clínicos de adolescentes hospitalizados en una UCHIP por intento de suicidio para proporcionar al hospital estrategias de intervención y de articulación con la red territorial de salud mental.

MATERIAL Y MÉTODO

Se realizó un estudio descriptivo, de tipo comparativo y retrospectivo usando un método cuantitativo. Se conformaron dos grupos de estudio; el grupo I, con 14 adolescentes de mayor gravedad previamente internados en la Unidad de Tratamientos Intensivos (UTI) y el grupo II, con 82 adolescentes que no requirió de esta unidad. El objetivo fue comparar y relacionar a los grupos de estudio; de igual modo, aportar a la UCHIP estrategias de intervención y articulación con los dispositivos de la red territorial de salud mental. Los datos se recogieron de las fichas clínicas de adolescentes entre los 14 años 0 mes a 17 años 11 meses de edad que estuvieron hospitalizados en la UCHIP del hospital público Roberto del Río de la ciudad de Santiago de Chile, entre enero del 2017 a diciembre del 2018. Las variables estudiadas fueron: edad, género, escolaridad, antecedente de abuso sexual, diagnóstico del trastorno mental (eje I) realizado por médico psiquiatra, según la Clasificación Internacional de Enfermedades en su 10ª versión[18] (CIE-10), dado que al momento del estudio el hospital no utilizaba la versión CIE-11. También se estudió el diagnóstico de la co-morbilidad o funcionamiento de la personalidad (eje II) realizado por el psicólogo tratante según la CIE-10, número de días de hospitalización en la UCHIP, consultas en centros de la red territorial de salud mental (se consideraron 10 o más consultas en los 6 meses previos a la hospitalización en la UCHIP) y cuidador responsable con trastorno mental con o sin tratamiento.

Los criterios de inclusión fueron los siguientes: adolescentes entre 14 años 0 mes a 17 años 11 meses de edad hospitalizados en la UCHIP entre enero del 2017 a diciembre del 2018; adolescentes con trastornos mentales e intento de suicidio que, por la gravedad del intento, previamente necesitaron atención en la UTI (grupo I) y adolescentes con trastornos mentales e intento de suicidio que no necesitaron la UTI (grupo II); adolescentes con o sin co-morbilidad, es decir, con o sin diagnóstico de desarrollo anormal de la personalidad; adolescentes escolarizados; adolescentes con o sin ante-

cedentes de abuso sexual; adolescentes con 10 o más consultas en dispositivos de salud mental de la red territorial en los 6 meses previos a la hospitalización en la UCHIP; adolescentes con familiar en el rol de cuidador responsable y adolescentes cuyo cuidador responsable porte un trastorno mental con o sin tratamiento.

Se excluyen: adolescentes hospitalizados en la UCHIP menores de 14 años y mayores de 17 años 11 meses; adolescentes hospitalizados en la UCHIP con altas administrativas; adolescentes hospitalizados en la UCHIP de hogares de menores, residencias u otros lugares cuyo cuidador responsable no es un familiar; adolescentes sin intento de suicidio y, finalmente, adolescentes con menos de 10 consultas en dispositivos de salud mental de la red territorial en los 6 meses previos a la hospitalización en la UCHIP.

Se utilizó un muestreo intencionado. Se revisaron las bases de datos de la UCHIP entre enero del 2017 a diciembre del 2018 y se seleccionaron las fichas clínicas que cumplían con los criterios de inclusión. Se obtuvieron 96 fichas, 14 correspondieron al grupo I y 82 al grupo II. Asimismo, de las 96, 79 eran de adolescentes mujeres y 17 de adolescentes hombres.

Se utilizó un análisis descriptivo y de frecuencia para identificar las características sociodemográficas y clínicas, tanto de la muestra total como separada por grupos. Para obtener la significancia de las variables cuantitativas se utilizó la prueba de U Mann Whitney, para estudiar las asociaciones entre las variables de los grupos se utilizó la prueba de Chi-cuadrado de Pearson (X^2) y la regresión lineal múltiple por pasos sucesivos, donde la variable dependiente fue el intento de suicidio y las variables predictoras la edad, género, escolaridad, abuso sexual, diagnóstico de trastorno mental, co-morbilidad, consultas previas a la hospitalización y cuidador con trastorno mental. El análisis se complementó con el cálculo de Odds Ratio (OR). Para el procesamiento de los datos se utilizó el programa estadístico Statistical Package for Social Sciences (SPSS) versión 15,0. El nivel de significancia en todas las pruebas se estableció en un $p<0,05$.

Estudio aprobado por el comité de ética del Servicio de Salud Metropolitano Norte (SSMN) de la ciudad de Santiago de Chile, acreditado por la Secretaría Regional Ministerial de Salud (SEREMI) y que adscribe a las normativas de los principios éticos internacionales, fundamentalmente de la declaración de Helsinki. Los datos fueron tratados con confidencialidad, custodiados por el investigador responsable y eliminados al termino del estudio.

RESULTADOS

El grupo II tuvo cinco veces más adolescentes que el grupo I. La edad promedio de los adolescentes en las fichas analizadas fue de 16 años 1 mes, y una desviación estándar (DE) de 1,76. Por género, se observó que un 82,3% eran adolescentes mujeres y un 17,7% eran adolescentes hombres. En el grupo I (92,9% de adolescentes hombres y 7,1% de adolescentes mujeres), la edad promedio fue de 15 años 9 meses (DE=1,1); en el grupo II (91,5% de adolescentes mujeres y 8,5% de adolescentes hombres) fue de 16 años 5 meses (DE= 1,8). Inter-grupo no hubo diferencias significativas en las variables edad, escolaridad y duración de la hospitalización; sin embargo, la variable género mostró diferencia significativa ($X^2_{(5)}=9,344$; gl:6; $p<0,05$); es decir, ser adolescente hombre con intento de suicidio y atenciones en la UTI tiene mayor probabilidad de estar hospitalizado en la UCHIP que un adolescente hombre con intento de suicidio sin atenciones en la UTI (OR= 12,5; 95% IC= 2,57-60,7). Otras diferencias significativas se observaron en el cuidador con trastorno mental ($X^2_{(6)}=21,4$; $p<0,05$); en adolescentes con consultas previas a la hospitalización ($X^2_{(9)}=21,54$; $p<0,05$); y en adolescentes víctimas de abuso sexual ($X_{(8)}{}^2=11,32$; $p<0,05$). El 100% de los integrantes del grupo I sufrieron abusos sexuales (Tabla 1).

Tabla 1
Frecuencias porcentuales de las variables por grupos de estudio y nivel de significancia.

Variables	Grupo I N=14	Grupo II N=82	Total N= 96	*p*
Edad (años y meses)				0,687
Media(±desviación estándar)	15, 9 (1,1)	16,5 (1,8)	16,1 (1,7)	
Escolaridad (%)				0,548
Educación básica	7,1	0	1,1	
Educación secundaria	92,9	100	98,9	
Género (%)				0,002*
Hombre	92,9	8,5	20,8	
Mujer	7,1	91,5	79,2	
Cuidador con trastorno mental en tratamiento (%)				0,003*
Sí	57,1	58,5	58,3	
No	42,8	41,5	41,7	
Consultas previas en salud mental (%)				0,001*
Sí	7,1	67,1	58,3	
No	92,9	32,9	41,7	
Víctima de abuso sexual (%)				0,002*
Sí	100	72,7	73,8	
No	0	27,3	26,2	
Duración de la hospitalización				0,780
Media en días (±desviación estándar)	35,0 (8.2)	28,5 (4.7)	31,7	

Test Chi-cuadrado con p significativo*.

Otras diferencias significativas se observaron en el diagnóstico de la conducta alimentaria de anorexia ($X^2_{(10)}$=44,66; p<0,05); en el trastorno bipolar ($X^2_{(9)}$=42,28; p<0,05); en el diagnóstico de la co-morbilidad ($X^2_{(11)}$=76,57; p<0,05) y; en el diagnóstico de depresión ($X^2_{(12)}$=64,47; p<0,05), con mayor probabilidad de encontrar adolescentes con depresión grave en el grupo I (OR= 2,8; 95% IC=1,72-9,19), (Tabla 2).

En la regresión lineal múltiple se evaluaron los supuestos de normalidad, linealidad y homocedasticidad. Su análisis mostró que ser víctima de abuso sexual explica un mayor porcentaje de la varianza (29%) con un β positivo (0,397), antecedente que podría predecir la hospitalización por intento de suicidio. Consultas en dispositivos de salud mental de la red territorial 6 meses antes de la hospitalización explican un 21% de la varianza con un β negativo (-0,301). Cuidador con trastorno psiquiátrico en tratamiento explica un 12% de la varianza con un β negativo (-0,224) y el trastorno depresivo explica muy poco (1%) con un β negativo (-0,056), (Tabla 3).

DISCUSIÓN

El estudio mostró diferencias entre los adolescentes con intento de suicidio hospitalizados en la UCHIP. Los adolescentes que no necesitaron atenciones en la UTI se hospitalizaron cinco veces más que aquellos que necesitaron esta atención. Este resultado podría estar relacionado con el género, ya que quienes necesitaron la UTI fueron adolescentes del grupo I que concentró, principalmente, a hombres. Este hallazgo es concordante con otros estudios [12,13], en los cuales se muestra que adolescentes hombres usan métodos letales y al fracasar su intento

Tabla 2
Frecuencias porcentuales de los diagnósticos por grupos de estudio y nivel de significancia.

Diagnósticos	Grupo I N=14	Grupo II N=82	Total N= 96	*p*
Diagnósticos eje I CIE-10 (%)				
Trastorno depresivo				0,036*
Grave	57,1	2,4	10,4	
Moderado	0	79,2	67,7	
Trastornos de la conducta alimentaria				0,012*
Anorexia	14,4	0	2,1	
Bulimia	0	4,0	3,3	
Trastorno bipolar	21,4	0	3,1	0,001*
Trastorno de ansiedad generalizada	0	8,3	7,2	0,457
Trastorno obsesivo-compulsivo	0	6,1	5,2	0,125
Trastorno psicótico	7,1	0	1,0	0,358
Diagnóstico eje II CIE-10 (%)				
Comorbilidad (%)				0,027*
Sí	28,5	85,3	79,2	
No	71,5	14,7	20,8	

*Test Chi-cuadrado con p significativo.

Tabla 3
Análisis de la regresión lineal múltiple (N=96).

Variables	β	R^2	*p*
- Víctima de abuso sexual	0,397	0,29	0,01
- Consultas de salud mental 6 meses antes de la hospitalización	-0,301	0,21	0,01
-Cuidador con trastorno mental en tratamiento	-0,224	0,12	0,01
- Trastorno depresivo	-0,056	0,01	0,05

Total de la varianza explicada: 63%.

lo repiten con mayor intensidad. Si los adolescentes hombres necesitaron atenderse en la UTI y se caracterizan por realizar intentos más severos, entonces la UCHIP debería diseñar intervenciones psicoterapéuticas específicas que aborde el intento de suicidio por género.

El rol del cuidador es clave en el pronóstico del adolescente. De acuerdo con la literatura, los cuidadores con trastornos mentales sin tratamiento o con tratamiento incompleto son un factor de riesgo para el desarrollo psicológico de niños, niñas y adolescentes, ya que los predisponen a perturbaciones psíquicas e intento de suicidio [19,20]. En virtud de ello, la UCHIP debe identificar la condición de salud mental del cuidador, considerando algunos factores: la forma como realizan los cuidados los cuidadores con trastorno mental sin tratamiento o con tratamiento incompleto; el tipo el tipo de trastorno mental que pueda estar cursando el cuidador que realiza los cuidados; si tiene tratamiento, el tiempo que lleva con el mismo y si sigue las indicaciones que están recibiendo, u otras preguntas que permitan una mayor comprensión del cuidador para implementar intervenciones de apoyo.

Consultas en dispositivos de la red territorial de salud mental 6 meses antes de la hospitalización en la UCHIP es un antecedente a considerar. En el grupo I la consulta fue escasa, esto genera dudas sobre: las razones por las cuales no consultaron; si solicitaron la cita, pero no concurrieron a sus atenciones; quedaron en lista de espera que no avanzó o hubo otra razón. Esta evidencia permite proyectar que los adolescentes del grupo I al alta de la UCHIP concurrirán poco a sus atenciones y terminaran abandonando el tratamiento en los dispositivos de

la red ambulatoria con la posibilidad de nuevos intentos o bien el suicidio. Es conocido que adolescentes hospitalizados por intento de suicidio tienen 8 veces más riesgo de suicidarse comparados con la población general y más del 50% de los suicidios ocurren hasta 16 meses después de intentos frustrados[21,22]. En este sentido, es fundamental que la UCHIP se coordine con los dispositivos de la red territorial para implementar la continuidad de cuidado que beneficia a todos los adolescentes hospitalizados por intento de suicidio. Esto se traduce en una derivación asistida o entrega del paciente de forma personalizada a la red, en seguimiento estrecho, en registros actualizados y planes de rescate de aquellos adolescentes que aborten o asistan de manera irregular. Todo ello implica un enorme desafío de integración y articulación de los saberes del conjunto de la red territorial de salud mental.

Ser víctima de abuso sexual es un evento traumático que afecta principalmente a mujeres y que se caracteriza por alterar el desarrollo emocional, cognitivo, social e instalar ideas suicidias [21]. Si bien en ambos grupos se dieron cifras altas de abuso sexual, es llamativo que el 100% de los integrantes del grupo I fue víctima de abuso; es importante señalar que este grupo concentró a adolescentes hombres con intentos de mayor gravedad. Esto requiere ser profundizado, no obstante se plantea que el abuso sexual en adolescentes hombres es un antecedente que puede predecir intento severo o la muerte por suicidio [25].

Una limitación fue restringir el estudio a 2 años; para ver el movimiento de las variables se debió considerar un mínimo de 5 años. Otra de ellas fue no haber realizado correlaciones entre las variables y no incorporar el número de intentos de suicidio, los tipos de familia, los métodos utilizados en el intento, las formas de abuso sexual, entre otras.

Se concluye que la UCHIP debe considerar en sus intervenciones las características distintivas de los grupos de estudio y coordinarse con los dispositivos de la red territorial de salud mental para implementar la continuidad de cuidados en beneficio de todo adolescente que se hospitaliza por intento de suicidio.

Financiamiento

No se dispuso de financiamiento.

Declaración de conflictos

No existe conflicto de intereses.

Número de ORCID

Lautaro Barriga: 0000-0002-0128-7133.

REFERENCIAS

1. **Pérez-Amezcua B, Rivera-Rivera L, Atienzo E, Castro F, Leyva-López A, Chávez-Ayala R**. Prevalencia y factores asociados a la ideación e intento suicida en adolescentes de educación media superior de la República Mexicana. Salud Pública Méx 2010; 52(4): 324-333. Disponible en: http://www.scielo.org.mx/scielo.php?script=sci_arttext&pid=S0036-36342010000400008&lng=es.
2. **Gonzalez-Forteza C, Ramos L, Vignau L, Ramírez C**. Abuso sexual e intento suicida: asociación con el malestar depresivo y la ideación suicida actuales en adolescentes. Salud Mental 2001 24(4):16-25. Disponible en: http://www.revistasaludmental.mx/index.php/salud_mental/article/view/878/876.
3. **Organización Mundial de la Salud**. Datos y cifras sobre el suicidio: infografía. 2018. Recuperado: abril 2023. Disponible en: https://www.who.int/es/news/item/09-09-2019-suicide-one-person-dies-every-40-seconds
4. **Organización Panamericana de la Salud**. Día Mundial para la Prevención del Suicidio 2017: Tómate un minuto, cambia una vida. Washington D.C.: Pan American Health Organization; 2017. Recuperado: octubre 2022. Disponi-

ble en: https://www.paho.org/hq/index.php?option=com_content&view=article&id=13540%3Aworld-suicide-prevention-day-2017&catid=9347%3 Aworld-suicide-prevention-day&Itemid=42406&lang=es

5. **Dávila C, Luna M**. Intento de suicidio en adolescentes: Factores asociados. Rev Chil Pediatr 2019; 90(6), 606-616. Disponible en: https://www.revistachilenadepediatria.cl/ index.php/rchped/article/view/1012
6. **Department of Health and Human Services. Office of the Surgeon General and National Action Alliance for Suicide Prevention**. National Strategy for Suicide Prevention: Goals and Objectives for Action. Washington: 2012. Recuperado: septiembre 2022. Disponible en: https://www.hhs.gov/surgeongeneral/reports-and-publications/ suicide-prevention/index.html
7. **Department of Health and Human Services. Our priorities.** Youth Mental Health. The U.S. Surgeon General's Advisory: 2021. Recuperado: noviembre 2022. Disponible en: https://www.hhs.gov/surgeongeneral/priorities/youth-mental-health/index.html
8. **Guajardo N, Ojeda F, Achui L, Larraguibel M**. Intervenciones terapéuticas para la conducta suicida en sdolescentes. Rev Chil Psiquiatr Neurol Infanc Adolesc 2015; *26*(2): 145-155. Disponible en: https://www.sopnia.com/wp-content/uploads/2021/05/Revista-SOPNIA_201502.pdf
9. **Ministerio de Salud de Chile**. Plan Nacional de Salud Mental 2017-2025. Departamento de Salud Mental. 2017. Recuperado: octubre 2022. Disponible en https://www.minsal.cl/wp-content/uploads/2017/12/PDF-PLAN-NACIONAL-SALUD-MENTAL-2017-A-2025.-7-dic-2017.pdf
10. **Ministerio de Salud de Chile**. Programa Nacional de prevención del suicidio: orientaciones para su implementación. Departamento de salud mental, División de Prevención y Cntrol de E nfermedades, Subsecretaria de Salud Pública. 2013. Recuperado: septiembre 2022. Disponible en: https://www.minsal.cl/sites/default/files/Programa_Nacional_Prevencion.pdf
11. **De la Barra F, Vicente B, Saldivia S, Melipillan R**. Estudio de epidemiología psiquiátrica en niños y adolescentes en Chile. Estado actual. Rev Med Clin Condes 2012; 23(5): *521-529*. Disponible en: https://www.sciencedirect.com/science/article/pii/S0716864012703462
12. **Vicente B, Saldivia S, Pihán R**. Prevalencias y brechas hoy: salud mental mañana. Acta Bioeth 2016; *22*(1): 51-61. Disponible en: https://www.scielo.cl/scielo.php?script=sci_arttext&pid=S1726-569X2016000100006
13. **Soto-Villaroel P, Véliz A**. Factores que intervienen en riesgo suicida y para suicida en jóvenes chilenos. Propósitos y Representaciones 2020; 8(3), e672. *https://dx.doi.org/10.20511/pyr2020.v8n3.672*.
14. **World Health Organization**. Mental Health: Facing the Challenges, Building Solutions. 2005. Ginebra: WHO.
15. **Unidad de Salud Mental de Chile**. Modelo de Gestión; Centro de Salud Mental Comunitaria. 2018. Recuperado junio 2022. Disponible en: https://www.minsal.cl/wp-content/uploads/2015/09/2018.03.28_MODELO-DE-GESTION-CENTRO-DE-SALUD-MENTAL-COMUNITARIA_DIGITAL.pdf
16. **Araneda N, Sanhueza P, Pacheco G, Sanhueza A**. Suicidio en adolescentes y jóvenes adultos en Chile: Riesgo relativo, tendencias y desigualdades. Rev Panam Salud Pública 2021; 45. Disponible en: https://iris.paho.org/bitstream/handle/10665.2/53353/v45e42021.pdf?sequence=1&isAllowed=y
17. **Gatica-Saavedra M, Vicente B, Rubí P**. Plan Nacional de Salud Mental. Reflexiones en torno a la implementación del modelo de psiquiatría comunitaria en Chile. Rev Méd Chile 2020, 148: 500-505. Disponible en: https://www.scielo.cl/scielo.php?pid=S0034-88720000400500&script=sci_arttext
18. **ICD-10** classification of mental and behavioural disorders: Diagnostic criteria for research, Geneva: World Health Organization, 1993. Disponible en: https://icd.who.int/browse10/2010/en#/V

19. **Ferreira G, Moreira C, Kleinman A, Nader E, Gomes B, Teixeira AMA, Rocca CCA, Nicoletti M, Soares JC, Bussato GF, Lafer B, Caetano SC.** Dysfunctional family environment in affected versus unaffected offspring of parents with bipolar disorder. Aust. N Z J Psychiatry 2013; 47: 1051-1057.
20. **Vivanco B, Grandón P**. Experiencias de haber crecido con un padre/madre con trastorno mental severo (TMS). Rev Chil Neuro-psiquiatr 2016; 54(3): 176-186.
21. **Castro L, Fuertes L, Pacheco O, Muñoz C**. Factores de riesgo relacionados con intento de suicidio como predictores de suicidio, Colombia 2016-2017. Rev Colomb Psiquiat 2021. Disponible en: https://www.sciencedirect.com/science/article/abs/pii/S0034745021000706
22. **Mei-Chih M, I-Chih C, Fu-Chang H**. Inpatient suicide in a general hospital. General Hospital Psychiatry 2009; 31:110-115. Disponible en: https://www.researchgate.net/publication/24185064.
23. **Urrego-Betancourt Y**. El impacto de las experiencias tempranas en la cognición social. Psychologia. Avances de la disciplina 2009; Enero-Junio : 61-80. Recuperado: agosto 2022. Disponible en: https://www.redalyc.org/pdf/2972/297225173004.pdf
24. **Miller A, Eisenlohr-Moul T, Giletta M, Hastings P, Rudolph K, Nock M, Prinstein M**. A within-person approach to risk for suicidal ideation and suicidal behavior: Examining the roles of stress, depression and abuse exposure. J Consult Clin Psychol 2017; 85(7): 712-722. Disponible en: https://www.ncbi.nlm.nih.gov/pmc/articles/PMC5477992/
25. **Lehrer J, Lehrer E, Oyarzún P**. Violencia sexual en hombres y mujeres jóvenes en Chile: Resultados de una encuesta (año 2005) a estudiantes universitarios. Rev M*éd Chile* 2009; 137(5): 599-608.

Invest Clin 64(4): 460 - 470, 2023 https://doi.org/10.54817/IC.v64n4a3

Influencing factors of post-transplantation diabetes mellitus in kidney transplant recipients and establishment of a risk prediction model.

Yuan Dong

First Ward, Department of Kidney Transplantation, The Second People's Hospital of Shanxi Province, Taiyuan, Shanxi Province, China.

Keywords: kidney transplant; diabetes mellitus; influencing factor; prediction model.

Abstract. The aim was to explore the influencing factors of post-transplantation diabetes mellitus (PTDM) in kidney transplant recipients and to establish a risk prediction model. A retrospective analysis was performed on the clinical data of 408 patients subjected to kidney transplantation from May 2015 to March 2022. With the simple random sampling method, they were divided into a training set (n=306) and a test set (n=102) at a ratio of 3:1. According to the occurrence of PTDM, the training set was further classified into PTDM and non-PTDM groups. The influencing factors of PTDM were identified by least absolute shrinkage and selection operator and multivariate logistic regression analysis. A nomogram prediction model was constructed and validated. Non-PTDM and PTDM groups had significantly different preoperative body mass index (BMI), family history of diabetes mellitus, 2-h preoperative and postprandial blood glucose, 2-h preoperative and postprandial peptide index, postoperative hypomagnesemia, whole blood concentration of tacrolimus, triacylglycerol, glycated albumin and fasting blood glucose ($P<0.05$). BMI, family history of diabetes mellitus, 2-h preoperative and postprandial blood glucose, and postoperative whole blood tacrolimus concentration were independent risk factors for PTDM. In contrast, the 2-h preoperative and postprandial peptide index was an independent protective factor ($P<0.05$). The incidence of PTDM in patients receiving kidney transplantation correlates with the family history of diabetes mellitus, preoperative BMI, 2-h postprandial blood glucose, 2-h postprandial peptide index, and postoperative whole blood tacrolimus concentration.

Corresponding author: Yuan Dong. First Ward, Department of Kidney Transplantation, The Second People's Hospital of Shanxi Province, Taiyuan, Shanxi Province, China. Email: dongyuansphsp@sdsch.cn

Factores que influyen en la diabetes mellitus post-trasplante en receptores de trasplante renal y el establecimiento de un modelo de predicción de riesgo.

Invest Clin 2023; 64 (4): 460 – 470

Palabras clave: trasplante renal; diabetes mellitus; factores de influencia; modelo de predicción.

Resumen. El propósito del trabajo fue explorar los factores que influyen en la diabetes mellitus post-trasplante (PTDM) en receptores de trasplante renal y establecer un modelo de predicción. Se realizó un análisis retrospectivo de los datos clínicos de 408 pacientes sometidos A trasplante renal de mayo de 2015 a marzo de 2022. La muestra se obtuvo con el método de generar números aleatorios en una computadora, y fueron divididos en un conjunto de entrenamiento (n=306) y un conjunto de prueba (n=102) en una proporción de 3:1. De acuerdo con la ocurrencia de PTDM, el conjunto de entrenamiento fue clasificado en grupos PTDM y no PTDM. Los factores de influencia de PTDM se identificaron mediante el operador de menor contracción y selección absoluta y el análisis de regresión logística multivari. Se construyó y validó un modelo de predicción de nomograma. Los grupos no PTDM y PTDM presentaron diferencias significativas en el índice de masa corporal (IMC) preoperatorio, antecedentes familiares de diabetes mellitus, glucosa sanguínea preoperatoria y postprandial 2-h, índice de péptido preoperatorio y postprandial 2-h, hipomagnesemia posoperatoria, concentración sanguínea total de tacrolimus, triacilglicerol, albúmina glicosilada sanguínea en ayunos ($p<0,05$). Entre ellos, el IMC, los antecedentes familiares de diabetes mellitus, la glucemia preoperatoria y postprandial de 2-h y la concentración de tacrolimus en sangre total postoperatoria fueron factores de riesgo independientes para PTDM, mientras que el índice de péptido preoperatorio y postprandial de 2-h fue un factor de protección independiente ($p<0,05$). La incidencia de PTDM en pacientes que reciben trasplante renal tiene correlaciones con los antecedentes familiares de diabetes mellitus, IMC preoperatorio, glucosa sanguínea postprandial 2-h, índice de péptido postprandial 2-h y concentración de tacrolimus en sangre total posoperatoria.

Received: 01-12-2022 Accepted: 03-06-2023

INTRODUCTION

Kidney transplantation is currently considered effective in treating end-stage renal disease. The five-year survival rate reaches over 80% among kidney transplant recipients [1], but some still experience different postoperative complications. A common metabolic complication after kidney transplantation is post-transplantation diabetes mellitus (PTDM), increasing the risk of cardiovascular and cerebrovascular diseases and resulting in deaths and seriously affecting the prognosis of patients [2,3]. PTDM, with an incidence of about 4-25%, usually occurs within one year after surgery [4]. It may be triggered

by such factors as the patient's age, family history of diabetes mellitus, high-fat diet, and donor type [5,6]. Thus, exploring the risk factors of PTDM in kidney transplant recipients and constructing a risk prediction model is of great significance in reducing the incidence rate of PTDM and improving the prognosis of patients. This study conducted a retrospective analysis of the clinical data of 312 patients experiencing living-donor kidney transplantation in our hospital from May 2015 to August 2021. On this basis, the influencing factors in the development of PTDM in patients were identified, and a nomogram prediction model was built to provide a clinical reference.

PATIENTS AND METHODS

General data

A retrospective analysis was performed on the clinical data of 408 patients who received kidney transplantation in our hospital (the Second People's Hospital of Shanxi) from May 2015 to March 2022. These patients were assigned to a training set (n=306) and a test set (n=102) at a ratio of 3:1 by generating random numbers on a computer. These two sets were used to construct a risk prediction model and validate the model's prediction performance, respectively. The training set [160 males and 146 females, (34.02 ± 7.71 years old)] and the test set [53 males and 49 females, (34.15±7.32 years old)] did not have significant differences in the general data (P>0.05). The inclusion criteria were: (1) Patients who received allogeneic kidney transplantation for the first time, (2) had a follow-up time ≥ one year, and (3) whose age ≥ 18 years old. Exclusion criteria were patients who (1) had no family history of diabetes before surgery, (2) experienced more than one kidney transplantation, (3) experienced the preoperative use of glucocorticoids for > three months, (4) had incomplete clinical data, or (5) died within one year after transplantation. This study was reviewed and approved by the ethics committee of our hospital, and all enrolled patients were informed and signed the informed consent.

Postoperative immunosuppressive regimen

The postoperative immunosuppressive regimen for patients was orally taking cyclosporine A (3-5 mg·kg^{-1}·d^{-1}) or tacrolimus (0.05-0.10 mg·kg·1·d^{-1}) + mycophenolate mofetil (1.0-1.5 g/d) or sodium mycophenolate (720-1080 mg/d) or mizoribine (3-4 mg·kg^{-1}·d^{-1}). The dose was adjusted based on the plasma concentration of cyclosporine A or tacrolimus. Then methylprednisolone (30 mg/d) was taken orally from the fourth day after surgery, and the dose was reduced to 5 mg on the seventh day after surgery and continually taken.

Clinical data collection

The clinical data of patients collected included (1) preoperative clinical data: age, gender, family history of diabetes mellitus, body mass index (BMI), causes of end-stage renal disease, type of dialysis, dialysis time, type of donor's kidney, warm ischemia time, cold ischemia time, glycated albumin, 2-h postprandial blood glucose, and 2-h postprandial peptide index, and (2) postoperative data: delayed functional recovery of the transplanted kidney, rejection, cytomegalovirus, hypomagnesemia, postoperative immune induction drugs, whole blood concentration of tacrolimus, whole blood concentration of cyclosporine, triglyceride, glycated albumin, total cholesterol, creatinine, urea nitrogen, uric acid and estimated glomerular filtration rate.

Diagnostic criteria

Patients were diagnosed six weeks after kidney transplantation according to the diagnostic criteria issued by the American Diabetes Association (ADA) in 2019 [7] if they had stable immunosuppression, stable renal function, and no acute infection. Those satisfying the diagnostic criteria were included in the PTDM group, while the rest of the patients were included in the non-PTDM group.

Statistical analysis

The statistical analysis of data was performed with the IBM SPSS® 23.0 software. Measurement data were expressed as mean ± standard deviation ($\bar{x} \pm s$), and the *t*-test was applied to compare the two groups. Count data were expressed as a percentage (%), and the χ^2 test was used to compare groups. The independent risk factors of PTDM were analyzed with the least absolute shrinkage and selection operator (LASSO) and multivariate logistic regression. The nomogram prediction model was built by R software, and its predictive value, accuracy, and clinical practicability were evaluated using the receiver operating characteristic (ROC) curve, calibration curve, and decision curve, respectively. A significance level of $\alpha=0.05$ was utilized.

RESULTS

Univariate analysis results of PTDM in patients

Among the 306 patients, the incidence rate of PTDM within one year after surgery was 24.84% (76/306). The non-PTDM group and the PTDM group had statistically significant differences in preoperative BMI, family history of diabetes mellitus, 2-h preoperative and postprandial blood glucose, 2-h preoperative and postprandial peptide, postoperative hypomagnesemia, whole blood concentration of tacrolimus, triglyceride, glycated albumin and fasting blood glucose ($P<0.05$) and no statistically significant differences in other clinical data ($P>0.05$) (Table 1).

Multivariate analysis results of PTDM in patients

The occurrence of PTDM was taken as the dependent variable, and a total of 29 independent variables were included. LASSO reduced the dimensionality of independent variables to avoid model overfitting. The optimal penalty coefficient λ of the model was identified by the 10-fold cross-validation method. When λ kept increasing to one standard error, it was the optimal value of the model. Nine predictors were screened out, including BMI, family history of diabetes mellitus, 2-h preoperative and postprandial blood glucose, 2-h preoperative and postprandial peptide index, postoperative hypomagnesemia, whole blood concentration of tacrolimus, triacylglycerol, glycated albumin and fasting blood glucose (Fig. 1).

With the occurrence of PTDM as the dependent variable (yes =1, no =0), the above nine predictors were included in the multivariate logistic regression model. It was found that BMI, family history of diabetes mellitus, 2-h preoperative and postprandial blood glucose, and postoperative whole blood concentration of tacrolimus were independent risk factors for PTDM. In contrast, the 2-h preoperative and postprandial peptide index was an independent protective factor for PTDM ($P<0.05$) (Table 2).

Model establishment

By means of the "rms" program package, the nomogram prediction model was built based on the five independent influencing factors for predicting the occurrence of PTDM in patients. The results showed that the five independent influencing factors obtained 263 points (56.75 points for the family history of diabetes mellitus, 82.5 points for 2-h preoperative and postprandial blood glucose PG >6.65 mmol/L, 66.25 points for 2-h preoperative and postprandial CPI<5.26, 26 points for BMI >23.85 kg/m^2, and 31.50 points for whole blood concentration of tacrolimus >8.62 C0) in total and the corresponding risk value of PTDM was 0.875, meaning that the probability of PTDM predicted by the model was 87.50% (Fig. 2).

Discrimination evaluation of the nomogram model

Here, the discrimination of the model was evaluated by the ROC curve. The training set obtained the area under the curve (AUC) of 0.758 (95%CI: 0.682-0.834, $p<0.001$) and the C-index of 0.882. The test

Table 1
Clinical data of the two groups of patients.

Preoperative data Item	Non-PTDM group (n=230)	PTDM group (n=76)	t/χ^2 value	*p*
Age (years old)**	34.02±7.71	34.15±7.32	0.892	0.215
Male*	160 (69.57)	53 (69.74)	0.112	0.902
BMI (kg/m²)**	**22.45±1.32**	**24.61±1.45**	**5.943**	**<0.001**
Family history of diabetes mellitus*	**23 (10.00)**	**26 (34.21)**	**6.934**	**<0.001**
Smoking*	57 (24.78)	24 (31.58)	1.082	0.345
Type of dialysis before transplantation			1.023	0.093
Hemodialysis*	187 (81.30)	57 (75.00)		
Peritoneal dialysis*	43 (18.70)	19 (25.00)		
Dialysis time (month)**	25.92±8.12	24.81±7.96	1.009	0.116
Causes of end-stage renal disease			0.863	0.345
Glomerulus nephritis*	171 (74.35)	57 (75.00)		
IgA nephropathy*	29 (12.61)	8 (10.53)		
Polycystic kidney*	18 (7.83)	6 (7.89)		
Others*	12 (5.21)	5 (3.13)		
Type of donor kidney			0.834	0.226
Living body*	34 (14.78)	17 (22.37)		
Corpse*	196 (85.22)	59 (77.63)		
Warm ischemia time (min)**	7.56±5.43	7.67±4.76	0.782	0.324
Cold ischemia time (h)**	5.71±1.24	5.85±1.13	0.343	0.872
Glycated albumin (%)**	13.52±1.12	14.15±1.34	0.345	0.668
2-h postprandial blood glucose (mmol/L)**	**5.33±1.32**	**7.29±1.45**	**4.012**	**0.012**
2-h postprandial peptide index**	**5.42±1.31**	**4.61±1.10**	**3.024**	**0.015**
Delayed functional recovery of transplanted kidney*	22 (9.57)	7 (10.34)	0.283	0.692
Rejection*	6 (2.84)	4 (5.17)	0.091	0.804
Cytomegalovirus*	16 (7.95)	4 (5.17)	0.224	0.782
Hypomagnesemia*	**41 (21.59)**	**27 (41.38)**	**5.9723**	**<0.001**
Postoperative immune induction drugs				
Basiliximab*	46 (20.00)	20 (26.32)	0.852	0.203
Rabbit anti-human thymocyte immunoglobulin*	128 (55.65)	35 (46.05)	0.773	0.334
Antithymocyte immunoglobulin*	132 (57.39)	38 (50.00)	0.765	0.204
Whole blood trough concentration of tacrolimus (C0)**	**7.19±2.21**	**9.34±3.12**	**6.245**	**<0.001**
Whole blood trough concentration of cyclosporine (C0)**	158.23±21.32	161.14±20.34	2.034	0.098
Triacylglycerol (mmol/L)**	**1.96±0.21**	**2.38±0.32**	**7.304**	**<0.001**

Table 1
CONTINUATION

Preoperative data Item	Non-PTDM group (n=230)	PTDM group (n=76)	t/χ^2 value	*p*
Glycated albumin (%)**	**12.78±1.23**	**15.11±1.23**	**5.492**	**<0.001**
Fasting blood glucose (mmol/L)**	**4.32±0.34**	**5.18±0.34**	**7.472**	**<0.001**
Albumin (g/L)**	42.45±1.34	42.45±1.26	0.603	0.402
Total cholesterol (mmol/L)**	3.09±0.34	3.17±0.32	0.282	0.828
Urea nitrogen (mmol/L)**	13.83±1.23	10.45±1.25	0.447	0.548
Creatinine (μmol/L)**	151.31±24.34	151.72±20.23	0.682	0.392
Uric acid (μmol/L)**	309.124±24.23	295.19±20.83	0.332	0.672
Estimated glomerular filtration rate [mL (min·1.73 m^2)]**	60.45±5.72	72.98±5.15	1.114	0.092

Measurement data were expressed as mean ± standard deviation ($\bar{x}$ ± s) and the *t*-test was applied to the comparison between the two groups. Count data were expressed as a percentage (%), and the χ^2 test was applied to the comparison between groups. C0: Whole blood trough concentration. *: n (%); **: ($\bar{x}$ ± s).

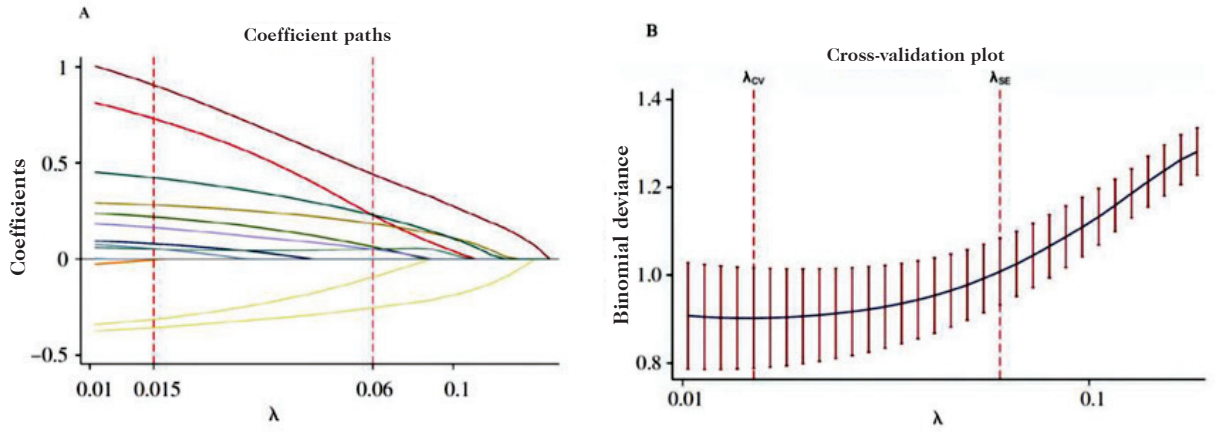

Fig. 1. LASSO regression analysis results for 27 predictors. A: Coefficient curve of 27 variables, B: Optimal clinical features selected by 10-fold cross-validation.

set had an AUC of 0.732 (95% CI: 0.682-0.782, P<0.001) and a C-index of 0.878. The prediction model had a C-index >0.75 in both sets, showing high discrimination (Fig. 3).

Calibration evaluation of the nomogram model

According to the calibration curve of the prediction model plotted, the prediction probability curve of the model well fit the reference probability, and no significant difference was revealed by the Hosmer-Lemeshow test results (P>0.05), indicating high accuracy of the model (Fig. 4).

Efficiency evaluation of the nomogram model

According to the plotted clinical decision curve, the model was far away from the extreme curve in both the training and test sets and obtained high a net benefit, indicating high reliability and practicability of the constructed nomogram model (Fig. 5).

Table 2
Multivariate logistic regression analysis results of related factors affecting PTDM in patients.

Factor	β	SE	Wald	p	OR	95%CI
BMI	1.825	1.538	2.417	0.009	3.474	2.045~4.856
Family history of diabetes mellitus	2.672	2.358	3.983	0.006	4.728	3.049~5.861
2-h preoperative and postprandial blood glucose	0.501	0.146	11.775	0.012	1.156	1.024~1.572
2-h preoperative and postprandial peptide index	-0.342	0.172	0.835	0.003	0.710	0.518~0.849
Postoperative hypomagnesemia	0.794	0.519	7.68	0.066	2.213	0.986~4.733
Whole blood concentration of tacrolimus	2.583	2.067	4.075	0.004	4.369	2.358~5.592
Postoperative triglycerides	0.507	0.179	0.750	0.038	1.661	0.731~2.439
Postoperative glycated albumin	0.502	0.492	0.757	0.024	1.652	0.915~2.903
Postoperative fasting blood glucose	1.578	1.326	2.805	0.091	2.152	0.937~3.498

BMI, family history of diabetes mellitus, 2-h preoperative and postprandial blood glucose, and postoperative whole blood concentration of tacrolimus were independent risk factors for PTDM, while 2-h preoperative and postprandial peptide index was an independent protective factor for PTDM. BMI: Body mass index; CI: confidence interval; OR: odds ratio; PTDM: post-transplantation diabetes mellitus; SE: standard error.

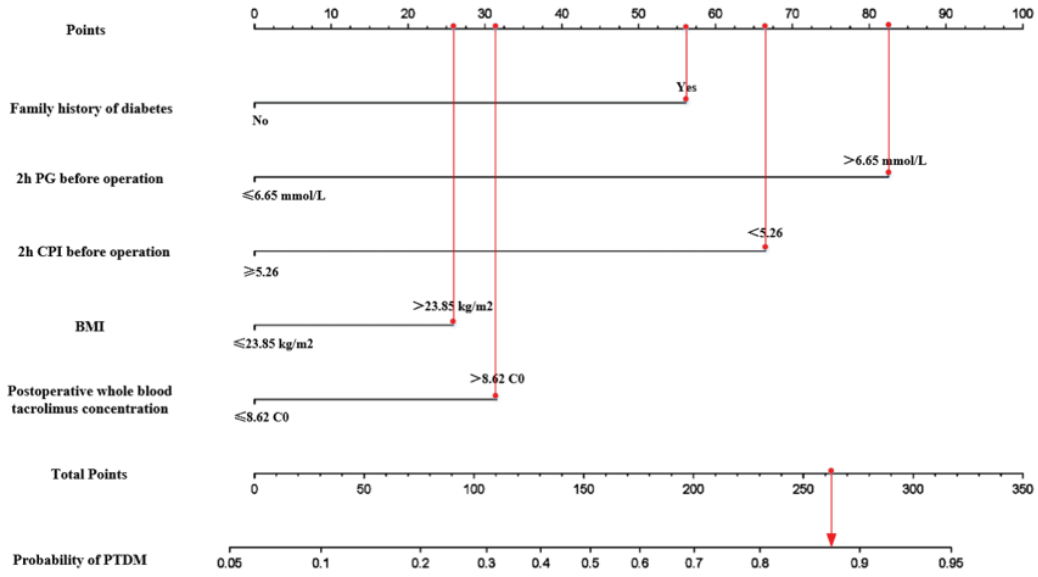

Fig. 2. Nomogram prediction model for predicting PTDM in patients.

DISCUSSION

PTDM is a common complication after kidney transplantation, the pathogenesis of which remains unclear. Its correlation with insulin resistance and insufficient insulin secretion is accepted in most literature [8,9], while hyperglycemia is closely associated with insulin production and target tissue demand. In addition, PTDM is also a high-risk factor inducing cardiovascular and cerebrovascular diseases in kidney transplantation, possibly resulting in the reduction or loss of transplanted kidney function and increased risk of postoperative death in patients [10]. For this reason, exploring the influencing factors of PTDM in kidney transplant recipients is significant in improving patients' prognosis and postoperative survival rate.

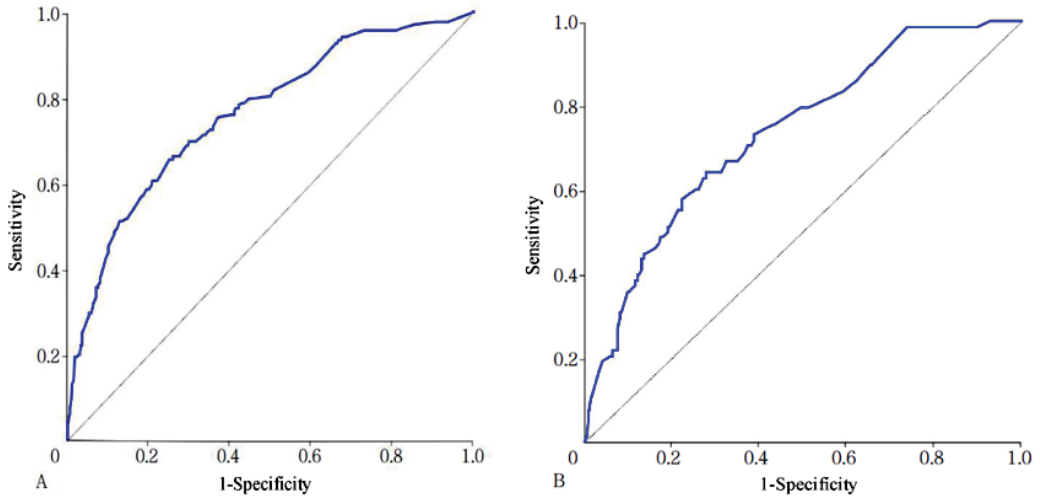

Fig. 3. ROC curves of prediction model in training and test sets. A: Training set, B: test set.

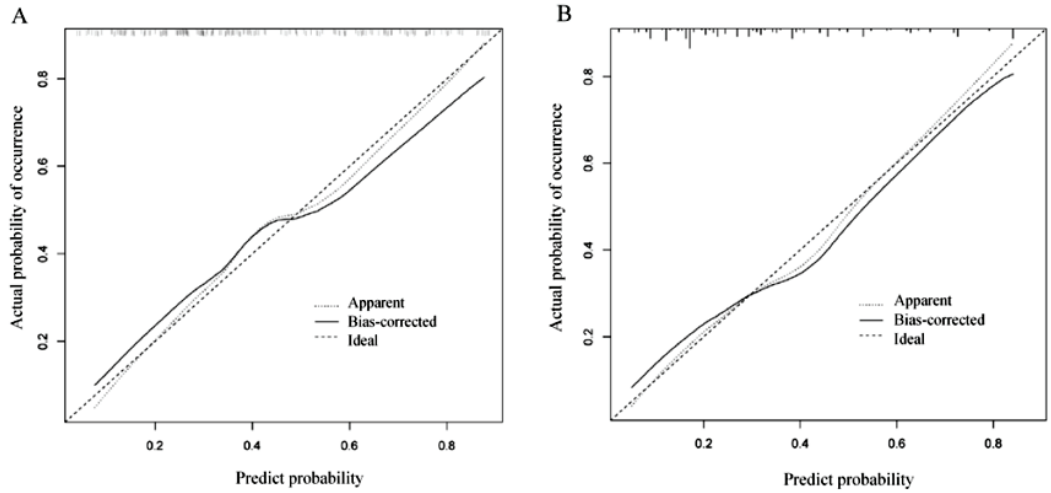

Fig. 4. Calibration curves of nomogram prediction model. A: Training set, B: test set.

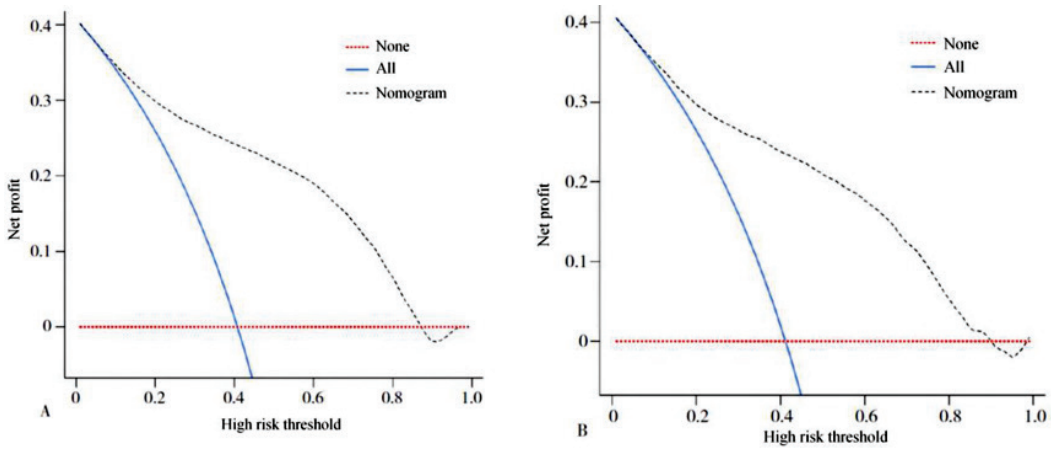

Fig. 5. Clinical decision curve analysis results of prediction model in training and validation sets. A: Training set, B: test set.

A total of 58 patients (24.78%) in this study's test set (n=234) had PTDM within one year after surgery. PTDM is a major cause of postoperative serious infection and even death in patients. Herein, preoperative BMI, family history of diabetes mellitus, 2-h preoperative and postprandial blood glucose, 2-h preoperative and postprandial peptide index, postoperative hypomagnesemia, the whole blood concentration of tacrolimus, triacylglycerol, glycated albumin, and fasting blood glucose were all determined in the univariate analysis to be influencing factors of PTDM in patients. BMI, family history of diabetes mellitus, 2-h preoperative and postprandial blood glucose, and postoperative whole blood concentration of tacrolimus were independent risk factors for PTDM. In contrast, the 2-h preoperative and postprandial peptide index was an independent protective factor for PTDM, as revealed by the multivariate logistic regression analysis result. The close correlation of BMI with the occurrence of PTDM in kidney transplant recipients has been reported in previous literature [11].

According to a study on the Korean population [12], kidney transplant recipients with BMI ≥25 kg/m^2 suffered a 3.64 times higher risk of PTDM than those with BMI< 25 kg/m^2. A possible mechanism is that obesity triggers chronic inflammation and stimulates pancreatic beta cells, thus causing insulin resistance and reduced glucose clearance rate, eventually increasing the risk of PTDM. It was found in a study [13] that a family history of diabetes presented a significant correlation with the risk of PTDM. People with a family history of diabetes may be subjected to abnormal glucose metabolism, which in turn influences the function of pancreatic β-cells and thus causes abnormal changes in postoperative blood glucose levels and even the occurrence of PTDM. Hence, for patients with a family history of diabetes mellitus, measures should be taken to closely monitor their blood glucose and carry out timely interventions to reduce the incidence rate of PTDM. A related study [14] published by the ADA showed that the majority of patients experience an abnormal glucose tolerance stage before diabetes development, and those showing abnormal glucose tolerance possibly become potential diabetic patients. The study of Sato *et al.* [15] unveiled that preoperative glucose tolerance was a risk factor for postoperative diabetes in transplant recipients. The 2-h postprandial peptide index, which reflects the function of pancreatic islet B cells and reduces with the increasing duration of type 2 diabetes mellitus, is related to insulin sensitivity and is considered a protective factor against PTDM in transplant recipients [16]. Moreover, tacrolimus is a typical drug for treating antirejection reactions. Its significantly positive correlation with the occurrence of PTDM and stronger sugar-causing effect than cyclosporine A [17] has been revealed. Additionally, for patients receiving kidney transplantation, the administration of tacrolimus can reduce the synthesis and secretion of insulin in the body, increasing the body's blood glucose level and thus resulting in diabetes [18]. Further, some believe that other important influencing factors on the occurrence of PTDM in transplant recipients include hypomagnesemia and rejection [19]. However, no statistically significant difference in rejection was found between the two groups of patients in this study. In addition, postoperative hypomagnesemia was found in the multivariate analysis not to be an independent influence factor of PTDM, possibly related to the small sample size of this study, which failed to present statistical differences.

Based on the influencing factors on the occurrence of PTDM in kidney transplant recipients, the nomogram model was built in this study, whose predictive performance was evaluated with the ROC curve, calibration curve, and clinical decision curve. The results showed that the predicted value approximated the actual observed value, signifying high discrimination and clinical validity of the model. Compared with a single

influencing factor, the prediction model can better identify patients subjected to high-risk liver metastasis, which boosts the clinical application of the research results.

This study still has some limitations. First, the subjects were collected from a single center, and the types of potential predictive variables collected were limited by clinical practice. Second, the prediction model was built through retrospective analysis, while limited clinical data were collected, and further validation in a prospective cohort was not carried out. Hence, the results may have bias. The research should be further improved by prolonging the follow-up time and increasing the collected data on influencing factors.

In conclusion, the model established in this study showed that BMI, family history of diabetes mellitus, 2-h postprandial blood glucose, postoperative whole blood tacrolimus concentration, and 2-h postprandial peptide index were independent influencing factors for predicting the occurrence of PTDM. Based on this model, attention can be paid to these factors, and early intervention can be taken to reduce the incidence rate of PTDM. Thus, this model is potentially applicable to clinical practice.

Funding

This study was financially supported by the Project No. 2020014.

Conflicts of interest

The author reported no potential conflict of interest.

Author ORCID number

- Yuan Dong: 0000-0001-9630-3281

REFERENCES

1. **Lopes RP, Junior JER, Taromaru E, Campagnari JC, Araújo MRT, Abensur H.** Wünderlich Syndrome in ienal transplant recipients: a case report and literature review. Transplant Proc 2021;53(8):2517-2520. *doi: 10.1016/j.transproceed.2021.08.025*
2. **Jenssen T, Hartmann A.** Post-transplant diabetes mellitus in patients with solid organ transplants. Nat Rev Endocrinol 2019;15(3):172-188. *doi: 10.1038/s41574-018-0137-7*
3. **Hecking M, Sharif A, Eller K, Jenssen T.** Management of post-transplant diabetes: immunosuppression, early prevention, and novel antidiabetics. Transpl Int 2021;34(1):27-48. *doi: 10.1111/tri.13783*
4. **Grundman JB, Wolfsdorf JI, Marks BE.** Post-transplantation diabetes mellitus in pediatric patients. Horm Res Paediatr 2020;93(9-10):510-518. *doi: 10.1159/000514988*
5. **Shivaswamy V, Boerner B, Larsen J.** Post-transplant diabetes mellitus: causes, treatment, and impact on outcomes. Endocr Rev 2016;37(1):37-61. *doi: 10.1210/er.2015-1084*
6. **Conte C, Secchi A.** Post-transplantation diabetes in kidney transplant recipients: an update on management and prevention. Acta Diabetol 2018;55(8):763-779. *doi: 10.1007/s00592-018-1137-8*
7. **American Diabetes Association. 2**. Classification and Diagnosis of Diabetes: Standards of Medical Care in Diabetes-2019. Diabetes Care 2019;42(Suppl 1):S13-S28. *doi: 10.2337/dc19-S002*
8. **Kgosidialwa O, Blake K, O'Connell O, Egan J, O'Neill J, Hatunic M.** Post-transplant diabetes mellitus associated with heart and lung transplant. Ir J Med Sci 2020;189(1):185-189. *doi: 10.1007/s11845-019-02068-7*
9. **Lieber SR, Lee RA, Jiang Y, Reuter C, Watkins R, Szempruch K, Gerber DA, Desai CS, DeCherney GS, Barritt AS.** The impact of post-transplant diabetes mellitus on liver transplant outcomes. Clin Transplant 2019;33(6):e13554. *doi: 10.1111/ctr.13554.*
10. **Boerner BP, Shivaswamy V, Wolatz E, Larsen J.** Post-transplant diabetes: diagnosis and management. Minerva Endocrinol 2018;43(2):198-211. *doi: 10.23736/S0391-1977.17.02753-5.*

11. **Munshi VN, Saghafian S, Cook CB, Werner KT, Chakkera HA.** Comparison of post-transplantation diabetes mellitus incidence and risk factors between kidney and liver transplantation patients. PLoS One 2020;15(1):e0226873. *doi: 10.1371/journal.pone.0226873.*
12. **Yu H, Kim H, Baek CH, Baek SD, Jeung S, Han DJ, Park SK.** Risk factors for new-onset diabetes mellitus after living donor kidney transplantation in Korea - a retrospective single center study. BMC Nephrol 2016;17(1):106. *doi: 10.1186/s12882-016-0321-8.*
13. **Pimentel AL, Hernandez MK, Freitas PAC, Chume FC, Camargo JL.** The usefulness of glycated albumin for post-transplantation diabetes mellitus after kidney transplantation: A diagnostic accuracy study. Clin Chim Acta 2020;510:330-336. *doi: 10.1016/j.cca.2020.07.045*
14. **American Diabetes Association. 1.** Improving Care and Promoting Health in Populations: Standards of Medical Care in Diabetes-2020. Diabetes Care 2020;43(Suppl 1):S7-S13. *doi: 10.2337/dc20-S001.*
15. **Sato T, Inagaki A, Uchida K, Ueki T, Goto N, Matsuoka S, Katayama A, Haba T, Tominaga Y, Okajima Y, Ohta K, Suga H, Taguchi S, Kakiya S, Itatsu T, Kobayashi T, Nakao A.** Diabetes mellitus after transplant: relationship to pretransplant glucose metabolism and tacrolimus or cyclosporine A-based therapy. Transplantation 2003;76(9):1320-1326. *doi: 10.1097/01.TP.0000084295.67371.11.*
16. **Sang YM, Wang LJ, Mao HX, Lou XY, Zhu YJ, Zhu YH.** Correlation of lower 2 h C-peptide and elevated evening cortisol with high levels of depression in type 2 diabetes mellitus. BMC Psychiatry 2020;20(1):490. *doi: 10.1186/s12888-020-02901-9.*
17. **Tong L, Li W, Zhang Y, Zhou F, Zhao Y, Zhao L, Liu J, Song Z, Yu M, Zhou C, Yu A.** Tacrolimus inhibits insulin release and promotes apoptosis of Min6 cells through the inhibition of the PI3K/Akt/mTOR pathway. Mol Med Rep 2021(3):658. *doi: 10.3892/mmr.2021.12297.*
18. **Cheng F, Li Q, Wang J, Hu M, Zeng F, Wang Z, Zhang Y.** Genetic polymorphisms affecting tacrolimus metabolism and the relationship to post-transplant outcomes in kidney transplant recipients. Pharmgenomics Pers Med 2021;14:1463-74. *doi: 10.2147/PGPM.S337947.*
19. **Garnier AS, Duveau A, Planchais M, Subra JF, Sayegh J, Augusto JF.** Serum magnesium after kidney transplantation: a systematic review. Nutrients 2018;10(6):729. *doi: 10.3390/nu10060729.*

Invest Clin 64(4): 471 - 481, 2023 https://doi.org/10.54817/IC.v64n4a4

Antifungal susceptibility of *Aspergillus* genus determined by the Etest® method: eleven years of experience at the Instituto Médico La Floresta. Caracas, Venezuela.

Xiomara Moreno Calderón[1,2], Carolina Macero Estévez[1] and Débora Oliveira Oliveira[1]

[1]Microbiology Department. Instituto Médico La Floresta. Caracas, Venezuela.
[2]Microbiology Department. Bacteriology. Facultad de Medicina, Escuela de Bioanálisis. Universidad Central de Venezuela. Caracas, Venezuela.

Keywords: susceptibility; *Aspergillus* spp; cryptic species; antifungals; Etest diffusion method; minimal inhibitory concentration.

Abstract. This research aimed to determine the susceptibility of *Aspergillus* spp. to four antifungal agents using the Etest® method in several clinical samples (respiratory samples, soft tissue, otic tissue, and ocular tissue, among others) from a private health center in Venezuela. Thirty-three strains were evaluated: 11 *Aspergillus* section *Flavi*, eight *Aspergillus* section *Fumigati,* six *Aspergillus* section *Nigri*, four *Aspergillus* section *Terrei*, and four *Aspergillus* spp. A 0.5 McFarland standard suspension of a 5-day culture of each *Aspergillus* strain was prepared on Potato Dextrose agar and then inoculated on Sabouraud agar plates with 2% glucose. Voriconazole (VCZ), amphotericin B (AMB), caspofungin (CAS), and posaconazole (PCZ) were tested. Minimal inhibitory concentrations (MIC) in μg/mL were determined after 24 and 48 hours of incubation at 35 °C and th range (R), geometric mean (GM), $MIC_{50,}$ and MIC_{90} were calculated. The results for the 33 *Aspergillus* spp. tested after 24 h were the following: VCZ (R = 0.031- 16; GM = 0.145; MIC_{50} = 0.125 and MIC_{90} = 0.5), AMB (R = 0.031-16; GM = 0.644; MIC_{50} = 0.5 and MIC_{90} = 8), CAS (R = 0.031-16; GM = 0.1076; MIC_{50} = 0.063 and MIC_{90} = 1), PCZ (R =0.031 - 0.5; GM = 0.0755; MIC_{50} = 0.063 and MIC_{90} = 0.25). This investigation allowed assessing the antifungal susceptibility profiles of *Aspergillus* spp. isolated from clinical samples by the Etest® method, which is practical, reproducible and easy to perform in microbiology laboratories.

Corresponding author: Xiomara Moreno Calderón. Microbiology Department, Bacteriology Facultad de Medicina, Escuela de Bioanálisis. Universidad Central de Venezuela. Instituto Médico La Floresta. Caracas, Venezuela. Tel.: +584143722227. Email: xmorenoc1356@gmail.com

Susceptibilidad a los antifúngicos del género *Aspergillus* determinada por el método Etest®: once años de experiencia en el Instituto Médico La Floresta. Caracas, Venezuela.

Invest Clin 2023; 64 (4): 471 – 481

Palabras clave: susceptibilidad; *Aspergillus* spp.; especies crípticas; antifúngicos; método de difusión Etest; concentración mínima inhibitoria.

Resumen. El objetivo de esta investigación fue determinar la susceptibilidad de *Aspergillus* spp., a cuatro antifúngicos mediante el método de Etest®, en aislados clínicos (muestras respiratorias, partes blandas, óticas, y oculares, entre otras) provenientes de un centro de salud privado en Venezuela. Se evaluaron 33 cepas: 11 *Aspergillus* sección *Flavi*, ocho *Aspergillus* sección *Fumigati*, seis *Aspergillus* sección *Nigri*, cuatro *Aspergillus* sección *Terrei* y cuatro *Aspergillus* spp. Se preparó una suspensión al 0,5 MacFarland a partir de cultivos de 5 días de incubación de cada cepa de *Aspergillus* en agar Papa Dextrosa, que se inocularon posteriormente en placas de agar Sabouraud con glucosa al 2%. Los antifúngicos ensayados fueron: voriconazol (VCZ), anfotericina B (AMB), caspofungina (CAS) y posaconazol (PCZ). Posterior a la incubación a 35 °C, se determinó la Concentración Mínima Inhibitoria en μg/mL (CMI) para cada antifúngico a las 24 y 48 h. Se calculó el rango (R), media geométrica (MG), CMI_{50} y CMI_{90}. Los resultados a las 24 h para las 33 cepas de *Aspergillus* fueron: VO (R = 0,031- 16; MG = 0,145; CMI_{50} = 0,125 y CMI_{90} = 0,5), AB (R = 0,031-16; MG = 0,644; MIC_{50} = 0,5 y MIC_{90} = 8), CS (R = 0,031-16; MG = 0,1076; MIC_{50} = 0,063 y MIC_{90} = 1), PO (R =0,031 - 0,5; MG = 0,0755; MIC_{50} = 0,063 y MIC_{90} = 0,25). Esta investigación permitió valorar los perfiles de susceptibilidad antifúngica en aislamientos clínicos de *Aspergillus* spp., mediante el método de Etest®, el cual es práctico, reproducible y fácil de realizar en los laboratorios de microbiología.

Received: 15-01-2023 Accepted: 18-05-2023

INTRODUCTION

There has been a recent increase in epidemiological changes in filamentous fungi that cause diseases related to cryptic *Aspergillus* species. These species comprised 10 to 15% of *Aspergillus* isolates in epidemiological inquiries from Spain and the United States, particularly as the cause of invasive aspergillosis (IA) [1-3]. They are referred to as "cryptic" due to being sister species whose morphological distinction is rather complex, as they exhibit different phenotypic and genotypic characteristics[1].

Molecular studies have shown how the conventional identification method, based on morphological characteristics, is limited when it comes to differentiating *Aspergillus* species, as evidenced by the fact that such methodologies could only use one species or section (such as *Fumigati, Flavi, Nidulantes, Usti,* and *Terrei*) to identify morphologically identical species that could be separated through molecular methods [4].

The *Aspergillus* species most frequently isolated in a clinical context are *A. fumigatus*, *A. flavus*, *A. niger*, and *A. terreus*. The members of the *Fumigati* section, consisting of *A. fumigatus sensu stricto* and its cryptic species, are the most commonly isolated from clinical specimens and often from environmental sources. Furthermore, resistance to azoles has increased among clinical samples of the *Fumigati* section [5].

The prophylaxis and treatment of invasive aspergillosis are controversial due to its increasing morbidity and mortality [6]. While voriconazole (VCZ) is the drug of choice, isavuconazole (ISZ) can be used against *Aspergillus* spp., and is considered the most effective by European guidelines [7,8]. Posaconazole (PCZ) is recommended for primary antifungal prophylaxis during induction chemotherapy, immunosuppressive therapy for graft-versus-host disease after hematopoietic stem cell transplantation (HSCT), and salvage therapy for refractory IA [1–5]. Lipid formulations of amphotericin B (AMB) and echinocandins are an alternative to azoles in aspergillosis treatment [9]. However, epidemiological changes, including cryptic *Aspergillus* species' resistance to azoles, are of growing concern [4].

This study evaluated the levels of azoles (VCZ, PCZ), echinocandins (CAS), and amphotericin B susceptibility in *Aspergillus* species found in human samples using the Etest® gradient diffusion method.

MATERIAL AND METHODS

Aspergillus isolates

Clinical isolates of *Aspergillus* spp. were collected during 11 years (2011-2021) from patient samples processed in the Instituto Médico La Floresta microbiology laboratory in Caracas, Venezuela. Each clinical sample came from a different patient. The age, gender, and underlying disease of each patient were recorded. The isolates were preserved in distilled water with glycerol until the moment of the study. The different *Aspergillus* species' identification was based on the criteria by De Hoog *et al.* [10] and Klich *et al.* [11], assessing macro and microscopic aspects from subcultures on Sabouraud Dextrose Agar (SDA-Oxoid, USA), Mycosel Agar (Oxoid, USA), and Potato Dextrose Agar (PDA-Oxoid, USA), incubated in a temperature range between 20-30 °C.

In vitro susceptibility using the gradient diffusion method Etest®

A subculture on PDA agar of each *Aspergillus* spp. isolates were made and incubated for five days to prepare a conidia suspension in 0.85% sterile saline solution. The conidia concentration was determined by a Neubauer counting chamber (Hausser Scientific, Horsham, PA, USA) and standardized at 1 – 5 x 10^6 CFU/mL (Densimat™ bioMérieux, France) at 530 nm [12-14]. Plates containing Müeller-Hinton Agar, 2% glucose with Methylene blue, were inoculated, streaked in three directions, and left to dry for 15 minutes. Etest® strips of each antifungal (AB bioMérieux, France); VCZ, PCZ (0.002-32 μg/ mL), AMB, and caspofungin (CAS=0.016-256 μg/ mL) were placed according to the manufacturer's instructions. Each plate was incubated at 35 °C. MIC was measured at 24 h, with a maximum time of 48 h, in case the lecture was not possible at the stipulated time.

Criteria for interpreting the minimum inhibitory concentration

The MIC was defined as the lowest drug concentration at which the border of the elliptical inhibition zone intercepted the scale on the antifungal strip. To compare the MICs obtained during this study with the epidemiological cut-off values (ECVs) established by the Clinical and Laboratory Standards Institute (CLSI, M61 document, 2017), they were placed between two sequential dilutions taken to the subsequent higher dilution from the reference method. The values on the strip's upper end were taken to the highest concentration allowed, while those on the lower end were left unchanged. Ac-

cording to de CLSI, ECVs in wild and non-wild isolates are classified based on the following MICs: VCZ: *A. fumigatus*=1 μg/mL; *A. flavus, A. niger*, and *A. terrreus*=2 μg/mL. PCZ: *A. flavus*=0.5 μg/mL; *A. niger*=2 μg/mL, *A. terreus*=1 μg/mL. AMB: *A, flavus* and *A. terreus*=4 μg/mL; *A. fumigatus*, *A. niger*, and *A. versicolor*=2 μg/mL. CAS: *A. flavus* and *A. fumigatus*=0.5 μg/mL; *A. niger*=0.25 μg/mL, and *A. terreus*=0.12 μg/mL[15].

Statistical analysis

A database was created in Excel® 2010. The data was analyzed through percentages and central tendency measures: ranges, geometric mean (GM), mode (Mo), and median (Mdn) for each antifungal. The MIC values that inhibited 50% (MIC_{50}) and 90% (MIC_{90}) of the isolates were also calculated.

Quality control

American Type Culture Collection (ATCC®) control strains were used in order to evaluate the susceptibility tests: *A. fumigatus* ATCC® 204305, *Candida krusei* ATCC® 6258, and *Candida parapsilosis* ATCC® 22019.

RESULTS

The strains analyzed came from 33 patients, 18 female and 15 male, aged between 2-76 years and an average of 56 years. Thirty-three *Aspergillus* spp. isolates were identified, mostly from lower respiratory tract samples (17;51.5%), followed by isolates obtained from soft tissue (6;18.2%), ear discharge (4;12.12%), corneal ulcer scraping (2;6.06%), and one of each one from nasal septum, peritoneal fluid, bone marrow, and nail (1;3.03%). Table 1 shows *Aspergillus* species identified through phenotypic tests, isolation place, underlying disease, and MICs for each tested antifungal.

According to the ECV of CLSI, the results showed that 97% of *Aspergillus* isolates tested against VCZ were categorized as wild strains, while for PCZ, all the isolates were categorized as 100% wild strains. However, for AMB, 18.2% of isolates were wild strains.

Fig. 1 (A, B, C, D) shows the graphical distribution of each *Aspergillus* spp. against antifungals with their respective MICs. Table 2 describes the *in vitro* activity according to MICs, CMI_{50} and CIM_{90}.

DISCUSSION

Although it was found that the resistance of *Aspergillus* spp. tested in this study was low, without involving *Aspergillus* species with intrinsic resistance to some antifungals; it is necessary to be cautious when discussing susceptibility patterns in these species of filamentous fungi. The aim is to highlight the importance of monitoring resistance at local, national and international levels while investigating emerging resistance mechanisms [6].

Aspergillus flavus was the most frequent *Aspergillus* species isolated in this study, followed by *A. fumigatus*. This result is not comparable to that reported in the international literature, according to which *A. fumigatus* is the most identified species [1,4,14,16,17]. Susceptibility tests showed that 94% of *Aspergillus* species tested against VCZ had MICs lower than 1 μg/mL compared to the ECVs reported by CLSI, where these species were categorized as wild strains. However, one of the isolates MIC showed ≥16 μg/mL, which could be attributed to the fact that the *Fumigati* section contains *A. lentulus*, which has been observed to be intrinsically resistant to VCZ [18]. The molecular techniques corroborating this description were not feasible for this study. These results were similar to those reported by Castanheira *et al.*[17], who also obtained $MICs_{90}$ of 0.5 μg/mL in *A. fumigatus*, *A. terreus*, and *A. niger* against VCZ, as well as to those obtained by Espinell-Ingroff *et al.* [12]. As is the case for most azoles, VCZ acts on 14-α-sterol demethylase, and on 24-methylene dihydrolanosterol demethylase, another enzyme from the ergosterol biosynthetic pathway.

Table 1
Epidemiological, clinical characteristics and *in vitro* susceptibility to antifungal agents tested in *Aspergillus* spp. Isolates.

Nº	Type of sample	*Aspergillus*	Age	Gender	Diagnosis	VCZ (ug/mL)	AMB (ug/mL)	CAS (ug/mL)	PCZ (ug/mL)
1	Sputum	*A. fumigatus*	68	M	Lung cancer	0.064	0.5	0.125	0.031
2	Sputum	*A. niger*	62	F	Bile duct cancer	0.031	0.063	0.015	0.031
3	Sputum	*A. terreus*	62	M	Bile duct cancer	0.031	8	0.015	0.015
4	Nasal septum	*A. versicolor*	59	M	Lung cancer	0.5	0.5	1	0.250
5	Sputum	*A. terreus*	63	M	Lung cancer	0.25	4	0.125	0.500
6	Sputum	*A. fumigatus*	59	F	COPD	0.125	0.5	0.250	0.064
7	Sputum	*A. fumigatus*	70	F	Pneumonía	0.060	0.125	0.015	0.064
8	Ear discharge canal	*A. flavus*	45	F	Otitis media	0.064	0.5	0.064	0.125
9	Sputum	*A. fumigatus*	66	F	COPD	0.250	0.064	0.015	0.064
10	Foot discharge	*A. terreus*	69	F	Breast cancer	0.125	8	0.031	0.031
11	Bronchoalveolar lavage	*A. fumigatus*	57	F	Aspergilloma	≥16	≥16	0.064	0.5
12	Ear discharge canal	*A. flavus*	2	M	Otitis media	0.125	1	0.015	0.064
13	Jaw discharge	*A. fumigatus*	76	F	Reconstructive surgery	0.250	0.5	0.031	0.250
14	Ear discharge canal	*A. niger*	68	M	Otitis media	0.064	≥16	0.064	0.031
15	Thigh discharge	*A. penicellioides*	52	M	Trauma	0.250	2	0.031	0.063
16	Sputum	*A. flavus*	68	F	COPD	0.250	2	≥16	0.250
17	Sputum	*A. nidulans*	68	F	COPD	0.064	0.125	≥16	0.031
18	Sputum	*A. niger*	68	F	Breast cancer	0.031	1	0.125	0.031
19	Corneal ulcer	*A. flavus*	39	M	Keratitis	0.125	2	0.015	0.063
20	Ear discharge canal	*A. niger*	37	M	Otitis media	0.125	1	0.063	0.031
21	Peritoneal fluid	*A. penicellioides*	49	F	Renal insufficiency	0.250	1	0.5	0.031
22	Bronchoalveolar lavage	*A. flavus*	58	M	COPD	0.25	1	0.015	0.031
23	Sputum	*A. flavus*	57	F	Colon cancer	0.015	0.250	0.015	0.063
24	Endotracheal discharge	*A. flavus*	63	M	Lung cancer	0.015	0.125	0.031	0.063
25	Bronchial discharge	*A. flavus*	53	M	Pneumonia	0.063	0.5	0.015	0.125
26	Bone marrow	*A. fumigatus*	58	F	Lymphoid leukemia	0.5	0.5	0.015	0.125

Table 1
CONTINUATION

Nº	Type of sample	*Aspergillus*	Age	Gender	Diagnosis	VCZ (ug/mL)	AMB (ug/mL)	CAS (ug/mL)	PCZ (ug/mL)
27	Finger discharge	*A. niger*	61	F	Diabetes	0.063	0.125	0.015	0.031
28	Ankle tissue	*A. terreus*	42	F	Trauma	0.250	16	0.250	0.063
29	Nail	*A. flavus*	72	F	Diabetes	0.5	1	1	0.250
30	Sputum	*A. flavus*	68	M	Lung cancer/ COVID	0.5	1	0.063	0.250
31	Leg ulcer	*A. flavus*	81	F	Colon cancer	0.250	0.015	1	0.015
32	Sputum	*A. fumigatus*	18	M	Idiopathic hepatitis	1	0.5	0.25	0.063
33	Corneal ulcer	*A. niger*	35	M	Keratitis	0.031	2	0.063	0.250

VCZ: voriconazole; AMB: amphotericin B; CAS: caspofungin; PCZ: posaconazole, COPD: chronic obstructive pulmonary disease.

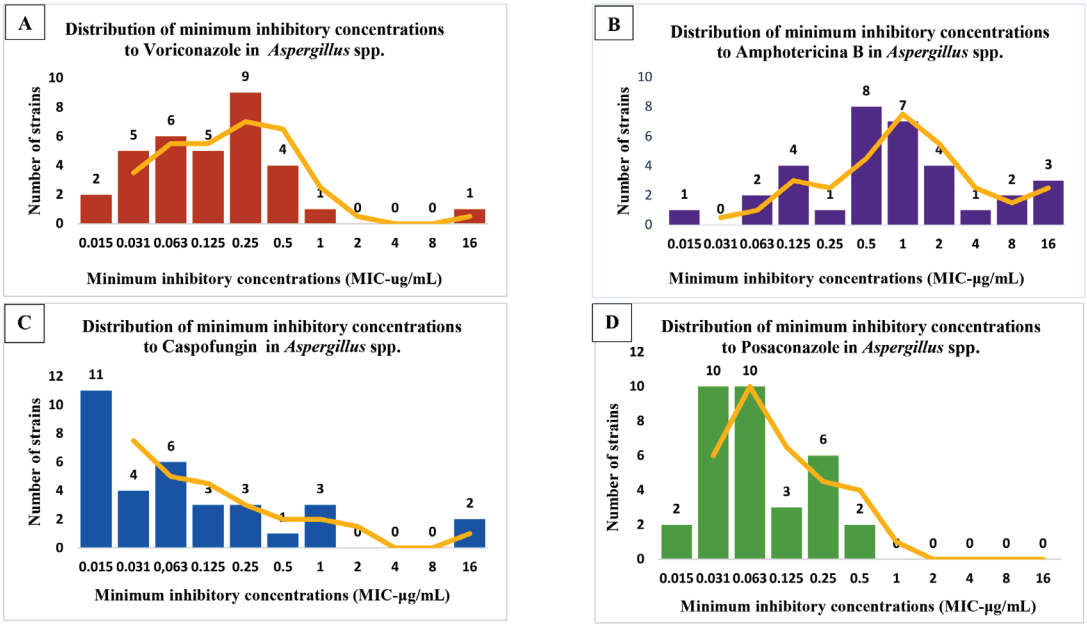

Fig. 1. Distribution of the different minimum inhibitory concentrations (MIC) obtained for *Aspergillus* spp. isolates (n=33), compared by antifungal agents tested. A) voriconazole; B) amphotericin B; C) caspofungin; and D) posaconazole.

This mechanism of action could explain the effectiveness of this antifungal compared to other azoles [19]. These drugs, VCZ in particular, are the first line of prophylaxis and treatment for fungal infections, although fluconazole is inactive against filamentous fungi [20].

PCZ is one of the last triazoles effective against various filamentous fungi, even Mucorales. Therefore, it has become the antifungal of choice in primary and salvage prophylaxis, especially for oncohematology patients [21]. The mean of the MIC (0.063 µg/mL), the MIC_{50} (0.063 µg/mL), and the

Table 2
Activity of antifungal agents tested by the E-Test® gradient diffusion method against *Aspergillus* spp. (n=33)

Antifúngicos	Range	Mean	Mode	Median	MIC_{50}	MIC_{90}
Voriconazole	0.015-16	0.015	0.25	0.125	0.125	0.5
Anphotericin B	0.015-16	0.1732	0.5	1	0.5	8
Caspofungin	0.015-16	0.0848	0.015	0.063	0.063	1
Posaconazole	0.015-0.5	0.0723	0.031	0.063	0.063	0.25

MIC_{50}: minimal inhibitory concentration that inhibited the growth of 50% of the isolates; MIC_{90}: minimal inhibitory concentration that inhibited the growth of 90% of the isolates. MIC: μg/mL.

MIC_{90} (0.25 μg/mL) obtained through this research shows the excellent *in vitro* activity of this triazole when compared to the ECVs reported by CLSI. The most frequently obtained MICs were 0.031 μg/mL and 0.063 μg/mL, although MICs for PCZ were relatively low. These results are similar to those obtained by Build *et al.* [22], confirming this drug's effectiveness in the tested isolates. However, that study suggests that high doses of PCZ could be used to treat azole-resistant *Aspergillus* spp. isolates.

Several studies have reported about the resistance of *A. fumigatus* to azoles. This is probably due to cross-resistance between triazoles used in agriculture [14,17,23,24]. These resistances are transmitted to humans through food and water consumption [9]. Most of them are mediated by the *cyp51A* gene. Depending on the specific mutation, one or even all triazoles can be resistant [4]. Resistance rates vary widely among medical centers worldwide, reporting high rates or rates of 1% or less [23-25]. MICs varied between Aspergillus species against AMB. Fortunately, resistance to this antifungal is very rare. Even so, the MIC was above the ECV reported by the CLSI in six of the Aspergillus species isolates. Four *A. terreus* isolates showed MICs ≥ 4 μg/mL, while MICs of both one *A. niger* isolate and one *A. fumigatus* were ≥ 2 μg/mL

The *Fumigati* section susceptibility profile is not consistent because this section contains *A. lentulus* and A. *fumigatiaffinis*, which have high MICs for azoles and AMB [26]. Despite this, it should be noted that data obtained from the *Fumigati* section regarding MICs were two dilutions lower than those reported by Denardi *et al.*[9] (Brazil) and Castanheira *et al.* [17] (global study).

Aspergillus terreus is known to be intrinsically resistant to AMB, but this depends on the cryptic species within the *Terrei* section [16]. Despite testing a few isolates, this study's A. terreus MICs results are comparable to those reported in the literature. *Aspergillus terreus* has emerged as an opportunistic pathogen, capable of causing pulmonary aspergillosis, onychomycosis, and fungal keratitis, among other diseases; it has also garnered attention due to its natural *in vitro* and *in vivo* resistance [19].

Amphotericin B is the antifungal of choice to treat severe fungal infections. Most hospitals or healthcare services commonly use it. The selective pressure in these environments could contribute to the emergence of resistant phenotypes. Resistance to AMB is most likely associated with low levels of ergosterol in the cell membrane, which reduces the effectiveness of the drug because of mutations in the *Erg3* gene that inactivate 5,6 sterol desaturase, an enzyme that functions as a step in the sterol biosynthetic pathway, creating dysfunctional sterols. There are also Aspergillus species capable of producing enzymes with reducing activity, decreasing the oxidative stress of AMB in fungal metabolism [28,29].

In this study, other isolates, such as A. niger and A. nidulans, were categorized as non-wild-type or AMB-resistant strains. In any case, although other studies have reported similar results, the number of isolates tested from these species was not significant enough to obtain sufficient data to draw more informed conclusions [7-29].

Echinocandins are one of the new antifungals used for aspergillosis treatment. These molecules inhibit the synthesis of β-(1,3)-d-glucan synthase, indirectly affecting β-(1,3)-d-glucan incorporation into fungal cell walls. Caspofungin is used successfully in salvage therapy against IA. During this study, 94% of *Aspergillus* species were resistant against CAS, and showed mean, MIC_{50}, and MIC_{90} values of 0.063 μg/mL, 0.063 μg/mL, and 1 μg/mL, respectively, when compared to the ECVs reported by CLSI. The GM of the *Aspergillus* spp. against CAS (0.063 μg/mL) is a lower dilution than that of Denardi *et al*. [9] (0.078 μg/mL) regardless of the methodology used. In the treatment of aspergillosis, echinocandins are focused mainly on the wall of the apical region of the *Aspergillus* hyphae, ignoring the rest of the fungal structures. The activity of this group of antifungals thus affects the growth rate of the fungus but leaves other physiological aspects intact [30]. Two other isolates, *A. flavus* and *A. nidulans*, showed MIC ≥ 16 μg/mL, categorizing them as non-wild. Resistance to echinocandins is not common among *Aspergillus* species; however, some recent reports of resistance to CAS [30,31] are consistent with our findings.

These cryptic species are significant mainly because they can display intrinsic resistance with an *in vitro* rate of around 40% against at least one antifungal [6, 13]. The resistance rate against azoles, polyenes, and echinocandins varies by region, hence the importance of getting global epidemiological data. Furthermore, MICs from environmental and clinical samples of azole-resistant *Aspergillus* species should be compared to understand this antifungal resistance phenomenon. In order to determine a precise ECV that could improve the use of clinical cut-off points for *Aspergillus* species, it seems imperative to obtain both more epidemiological and more semiotic data (clinical and molecular), which includes the treatment of IA caused by resistant strains to different antifungal drugs [1,17,23].

We ratify the need to identify the different species in each section using molecular techniques and include susceptibility tests. In this study, the Etest® agar strip diffusion method proved to help obtain ECV-guided MICs established by CLSI. These MICs provided clinical guidelines for treating infections caused by *Aspergillus* species isolated in Venezuela.

Conflict of interest

The authors declare they have no conflicts of interest.

Funding

The Instituto Médico La Floresta Microbiology Department entirely financed the study.

ORCID number of authors

- Xiomara Moreno Calderón (XM): 0000-0002-5924-615
- Carolina Macero Estévez (CM) 0000-0002-7620-7580
- Débora Oliveira Oliveira (DO): 0000-0003-3279-1591

Authors Contribution

XM study conceptualization and design; research; analysis and interpretation of results; preparation, writing, review and editing of the final manuscript. CM and DO research; analysis, interpretation of results and final manuscript editing.

REFERENCES

1. **Cho S-Y, Lee D-G, Kim W-B, Chun H-S, Park C, Myong J-P, Park Y-J, Choi JK, Lee HJ, Kim SH, Park SH, Choi SM, Choi HJ, Yoo JH.** Epidemiology and antifungal susceptibility profile of *Aspergillus* species: comparison between environmental and clinical isolates from patients with hematologic malignancies. J Clin Microbiol 2019; 57: e02023 18. *https://doi.org/10.1128/JCM.02023-18.*
2. **Alastruey-Izquierdo A, Mellado E, Peláez T, Pemán J, Zapico S, Alvarez M, Rodriguez-Tudela JL, Cuenca-Estrella M, FILPOP Study Group**. Population-based survey of filamentous fungi and antifungal resistance in Spain (FILPOP Study). Antimicrob Agents Chemother 2013; 57(7):3380 –3387. *https://doi.org/10.1128/AAC.00383-13.*
3. **Balajee SA, Kano R, Baddley JW, Moser SA, Marr KA, Alexander BD, Andes D, Kontoyiannes DP, Perrone G, Peterson S, Brandt ME, Pappas PG, Chiller T.** Molecular identification of *Aspergillus* species collected for the Transplant-Associated Infection Surveillance Network. J Clin Microbiol 2009; 47:3138 –3141. *https://doi.org/10.1128/JCM.01070-09.*
4. **Sabino R, Gonçalves P, Melo A, Simões D, Oliveira M, Francisco M, Viegas C, Carvalho D, Martins C, Ferreira T, Toscano C, Simões H, Veríssimo C.** Trends on *Aspergillus* epidemiology—Perspectives from a National Reference Laboratory Surveillance Program. J Fungi 2021; 7, 28. *https://doi.org/10.3390/ jof7010028.*
5. **Snelders E, Van Der Lee HAL, Kuijpers J, Rijs AJ M.M, Varga J, Samson RA, Mellado E, Donders ART, Melchers WJG, Verweij PE.** Emergence of azole resistance in *Aspergillus fumigatus* and spread of a single resistance mechanism. PLOS Medicine 2008; 5(11): 1629-1637. [e219]. *https://doi.org/10.1371/journal.pmed.0050219.*
6. **Cantón E, Córdoba S, Melhem M, Pemán J, Rivas P**. Estudio de la sensibilidad a los antifúngicos en los pacientes con Enfermedad Fúngica Invasora. En: Aproximación Clínica Diagnóstica de la Enfermedad Fúngica Invasora. Capítulo 7. Micellium 2017.
7. **Bassetti M, Bouza E**. Invasive mould infections in the ICU setting: complexities and solutions. J Antimicrob Chemother 2017;72(1): i39-i47. *https://doi.org/10.1093/jac/dkx032.*
8. **Cornely OA, Hoenigl M, Lass-Flörl C, Chen SC, Kontoyiannis DP, Morrissey CO, Thompson III GR, for the Mycoses Study Group Education and Research Consortium (MSG -ERC) and the European Confederation of Medical Mycology (ECMM).** Defining breakthrough invasive fungal infection-Position paper of the mycoses study group education and research consortium and the European Confederation of Medical Mycology. Mycoses 2019;62(9):716-729. *https://doi.org/10.1111/myc.12960.*
9. **Bedin Denardi, L, Hoch Dalla-Lana B, Pantella Kunz de Jesus F, Bittencourt Severo C, Morais Santurio J, Zanette RA, Alves SH.** In vitro antifungal susceptibility of clinical and environmental isolates of *Aspergillus fumigatus* and *Aspergillus flavus* in Brazil. The Braz J Infect Dis 2018; 22(1), 30–36. *https://doi.org/10.1016/j.bjid.2017.10.005.*
10. **De Hoog GS, Guarro J, Gené J, Figueras MJ**. Atlas of Clinical Fungi. Segunda edición. Central bureau voor Schimmel cultures, Utrecht: Universitat Rovira i Virgili, Reus; 2000. p. 442-519.
11. **Klich MA, Pitt JI**. A laboratory guide to the common *Aspergillus* species and their 19 teleomorphs. Canberra: CSIRO - Division of Food Processing. 2da. Edition. 1998. p. 116.
12. **Espinel-Ingroff A, Rezusta A**. E-test method for testing susceptibilities of *Aspergillus* spp. to the new triazoles voriconazole and posaconazole and to established antifungal agents: comparison with NCCLS broth microdilution method. J Clin Microbiol 2002; 40(6):2101-2107. *https://doi.org/10.1128/JCM.40.6.2101-2107.2002.*
13. **Guinea J, Peláez T, Alcalá L, Bouza E**. Correlation between the E-Test and the CLSI M38-A microdilution method to determine the activity of amphotericin B, voricona-

zole, and itraconazole against clinical isolates of *Aspergillus fumigatus*. Diagn Micr Infec Dis 2007; 57:273-276. *https://doi.org/10.1016/j.diagmicrobio.2006.09.003.*

14. **Imbert S, Normand AC, Ranque S, Costa JM, Guitard J, Accoceberry I, Bonnal C, Fekkar A, Bourgeois N, Houzé S, Hennequin C, Piarroux R, Dannaoui E, Botterel F.** Species identification and in vitro antifunagal susceptibility of *Aspergillus terreus* species complex clinical isolates from a French Multicenter Study. Antimicrob Agents Chemother 2018; 62: e02315-02317. *https//doi.org/10.1128/AAC.02315-17.*
15. **Clinical and Laboratory Standards Institute (CLSI).** Performance Standards for Antifungal Susceptibility Testing of Filamnetous Fungi, Approved Guideline. CLSI document M61. Wayne, PA; Clinical and Laboratory Standards Institute; 2017.
16. **Guinea J.** Updated EUCAST clinical breakpoints against *Aspergillus*, implications for the clinical. J Fungi 2020; 6: 343. *https://doi.org/10.3390/jof6040343.*
17. **Castanheira M, Deshpande LM, Davis AP, Rhomberg PR, Pfaller MA.** Monitoring antifungal resistance in a global collection of invasive yeasts and molds: application of CLSI epidemiological cut-off values and whole-genome sequencing analysis for detection of azole resistance in *Candida albicans*. Antimicrob Agents Chemother 2017; 22;61(10): e00906-17. *https://doi.org/10.1128/AAC.00906-17.*
18. **Balajee SA, Gribskov JL, Hanley E, Nickle D, Marr KA.** *Aspergillus lentulus* sp. nov., a new sibling species of *A. fumigatus*. Eukaryot Cell 2005; 4:625– 632. *https://doi.org/10.1128/EC.4.3.625-632.2005.*
19. **Pérez-Cantero A, López-Fernández L, Guarro J, Capilla J.** Azole resistance mechanisms in *Aspergillus*: update and recent advances. Int J Antimicrob Agents 2020;55(1):105807. *https://doi.org/10.1016/j.ijantimicag.2019.09.011.*
20. **Ruiz-Camps I, Cuenca-Estrella M.** Antifúngicos para uso sistémico. Enferm Infecc Microbiol Clin 2009; 27(6):353-362. *https://doi.org/10.1016/j.eimc.2009.04.001.*
21. **Cornely OA, Mertens J, Winston DJ, Perfect J, Ullmann AJ, Wals TJ, Helfgott D, Holowiecki J, Stockelberg D, Goh YT, Petrini M, Hardalo C, Suresh R, Angulo-Gonzalez D**. Posaconazole vs. fluconazole or itraconazole prophylaxis in patients with neutropenia. N Engl J Med 2007; 356: 348-359. *https://doi.org/ 10.1056/NEJMoa061094.*
22. **Buil JB, Hagen F, Chowdhary A, Verweij PE, Meis JF.** Itraconazole, voriconazole, and posaconazole CLSI MIC distributions for wild-type and azole-resistant *Aspergillus fumigatus* isolates. J Fungi (Basel, Switzerland). 2018; 4(3): e103. *https://doi.org/10.3390/jof4030103.*
23. **Fuhren J, Voskuil WS, Boel CH, Haas PJA, Hagen F, Meis JF, Kusters JG.** High prevalence of azole resistance in *Aspergillus fumigatus* isolates from high-risk patients. J Antimicrob Chemother 2015; 70:2894–2898. *https://doi.org/ 10.1093/jac/dkv177.*
24. **Pfaller MA, Messer SA, Boyken L, Rice C, Tendolkar S, Hollis R, Diekema DJ.** *In vitro* survey of triazole cross-resistance among more than 700 clinical isolates of *Aspergillus* species. J Clin Microbiol 2008; 46:2568–2572. *https://doi.org/ 10.1128/JCM.00535-08.*
25. **Pham CD, Reiss E, Hagen F, Meis JF, Lockhart SR.** Passive surveillance for azole resistant *Aspergillus fumigatus*, United States, 2011–2013. Emerg Infect Dis 2014; 20:1498–1503. *https://doi.org/ 10.3201/eid2009.140142.*
26. **Alcazar-Fuoli L, Mellado E, Alastruey-Izquierdo A, Cuenca-Estrella M, Rodriguez-Tudela JL.** *Aspergillus* Section *Fumigati*: antifungal susceptibility patterns and sequence-based identification. Antimicrob Agents Chemother 2008;52(4):1244–1251. *https://doi.org/10.1128/AAC.00942-07.*
27. **San Juan JL, Fernández CM, Almaguer M, Perurena MR, Martínez GF, Velar RE, IInait MT.** Sensibilidad in vitro de cepas cubanas de *Aspergillus* spp. de origen clínico y ambiental. Biomédica 2017; 37:452-459. *https://doi.org/10.7705/biomedica.v34i2.3447.*

28. Cavassin FB, Bau´-Carneiro JL, Vilas-Boas RR, Queiroz-Telles F. Sixty years of amphotericin B: an overview of the main antifungal agent used to treat invasive fungal infections. Infect Dis Ther 2021; 10(1):115-147. *https://doi.org/10.1007/s40121-020-00382-7.*

29. Seo K, Akiyoshi H, Ohnishi Y. Alteration of cell wall composition leads to amphotericin B resistance in *Aspergillus flavus*. Microbiol Immunol 1999; 43:1017-1025. *https://doi.org/10.1111/j.1348-0421.1999.tb01231. x.*

30. Mayr A, Aigner M, Lass-Flörl C. Caspofungin: ¿When and how? The microbiologist's view. Mycoses 2011; 55:27-35. *https://doi.org/10.1111/j.1439-0507.2011.02039.x.*

31. Pfaller MA, Boyken L, Hollis RJ, Kroeger J, Messer SA, Tendolkar S, Diekema DJ. Wild-type minimum effective concentration distributions and epidemiologic cut-off values for caspofungin and *Aspergillus* spp. as determined by Clinical and Laboratory Standards Institute broth microdilution methods. Diagn Microbiol Infect Dis 2010; 67(1):56-60. *https://doi.org/10.1016/j.diagmicrobio.2010.01.001.*

Invest Clin 64(4): 482 - 494, 2023 https://doi.org/10.54817/IC.v64n4a5

Effects of SU5416 on angiogenesis and the ERK-VEGF/MMP-9 pathway in rat endometriosis.

Danyang Zhao[1], Qiufang Bao[1], Lihong Chen[1,2,3] and Lie Zheng[1,2]

[1]Department of Obstetrics and Gynecology, the First Affiliated Hospital, Fujian Medical University, China.
[2]Department of Gynecology, National Regional Medical Center, Binhai Campus of the First Affiliated Hospital, Fujian Medical University, China.
[3]Fujian Key Laboratory of Precision Medicine for Cancer, the First Affiliated Hospital, Fujian Medical University, China.

Keywords: angiogenesis; endometriosis; ERK-VEGF/MMP-9 pathway; SU5416.

Abstract. SU5416 is a small molecule vascular endothelial growth factor (VEGF) receptor signal transduction inhibitor, which can block the VEGF receptor autophosphorylation and inhibit receptor tyrosine kinase signal transduction, thereby reducing VEGF activity. However, there are few reports about the correlation of SU5416 to the occurrence and angiogenesis in endometriosis. In this study, we observed the effects of VEGF receptor inhibitor SU5416 on angiogenesis in endometriosis in rats. Thirty female specific-pathogen-free Sprague-Dawley rats were randomly divided into sham operation group (SOG), model group (MG), and SU5416 group (n=10 for each group). In the SOG, only the uterus was cut and sutured, and endometriosis models were established in the MG and SU5416 group by autologous transplantation. The SU5416 group was injected with 15 mg/kg SU5416 intraperitoneally, and the SOG and MG were intraperitoneally injected with an equal volume of normal saline for 6 weeks. The volume of ectopic lesions was lower in the SU5416 group at 42 d postoperatively than in the MG ($p<0.05$). The proportion of CD31-positive cells in the endometrial tissue of the SU5416 group was lower than that of the MG ($p<0.05$); angiopoietin-1 (Ang-1), angiopoietin-2 (Ang-2), laminin-5γ2 (LN-5γ2) and phosphorylation of ERK (P-ERK), VEGF, matrix metalloproteinase (MMP)-2, and MMP-9 protein expressions were lower in the SU5416 group than in the MG ($p<0.05$). VEGF receptor inhibitor SU5416 can inhibit endometriosis angiogenesis and reduce inflammatory response in rats, and its mechanism of action may be related to the down-regulation of the ERK-VEGF/MMP-9 pathway expression.

Corresponding author: Lihong Chen. No. 20, Chazhong Road, Fuzhou, Fujian 350005, China. Phone: +86-13506986776. E-mail: whcelh@163.com. Lie Zheng. No. 20, Chazhong Road, Fuzhou, Fujian 350005, China. Phone: +86–13905918829. E-mail: zelie@sina.com

Efecto del SU5416 sobre la angiogenesis y la via ERK-VEGF/ MMP-9 en la endometriosis de ratas.

Invest Clin 2023; 64 (4): 482 – 494

Palabras clave: angiogénesis; endometriosis; vía ERK-VEGF/MMP-9; SU5416.

Resumen. SU5416 es un inhibidor de la transducción de señales del receptor del factor de crecimiento endotelial vascular (VEGF), una molécula pequeña, capaz de bloquear la autofosforilación del receptor VEGF e inhibir la transducción de señales de la tirosina quinasa del receptor, reduciendo así la actividad del VEGF. Sin embargo, existen escasos informes acerca de la correlación entre SU5416 y la aparición y angiogénesis de la endometriosis. En este estudio, hemos observado los efectos del inhibidor del receptor del VEGF, SU5416, sobre la angiogénesis en la endometriosis en ratas. Treinta ratas Sprague-Dawley hembra, libres de patógenos específicos, fueron divididas aleatoriamente en un grupo de operación simulada (SOG), un grupo de modelo (MG) y un grupo de SU5416 (n=10 en cada grupo). En el SOG, solo se realizó una incisión en el útero y se suturó, mientras que en los grupos MG y SU5416 se establecieron modelos de endometriosis mediante trasplante autólogo. Al grupo SU5416 se le inyectaron 15 mg/kg de SU5416 por vía intraperitoneal, y tanto el SOG como el MG recibieron una inyección intraperitoneal de un volumen igual de solución salina normal durante 6 semanas. El volumen de lesiones ectópicas fue menor en el grupo SU5416 a los 42 días después de la operación en comparación con el MG ($p<0,05$); la proporción de células CD31 positivas en el tejido endometrial del grupo SU5416 fue inferior a la del MG ($p<0,05$); las expresiones de las proteínas angiopoyetina-1 (Ang-1), angiopoyetina-2 (Ang-2), laminina-5γ2 (LN-5γ2) y la fosforilación de ERK (P-ERK), VEGF, metaloproteinasa de matriz (MMP)-2 y MMP-9 fueron menores en el grupo SU5416 que en el MG ($p<0,05$). El inhibidor del receptor del VEGF, SU5416, puede inhibir la angiogénesis de la endometriosis y reducir la respuesta inflamatoria en ratas, y su mecanismo de acción puede estar relacionado con la regulación a la baja de la expresión de la vía ERK-VEGF/MMP-9.

Received: 22-02-2023 Accepted: 08-09-2023

INTRODUCTION

Endometriosis (EMs) is a benign morphological manifestation, but the biological behaviors such as implantation invasion, aggressive growth and distant metastasis are similar to those of malignant tumors, which can induce painful intercourse, dysmenorrhea, chronic pelvic pain, and infertility up to 25%-35% [1,2]. The specific etiology of this disease has not been elucidated, and it is mostly thought to be related to genetic factors, endometrial implantation, retrograde menstruation, implantation, and immune regulation [3,4]. However, both endometrial implantation and menstrual reflux implantation depend on adequate blood supply, so angiogenesis plays a key role in the occurrence and development of EMs.

Vascular endothelial growth factor (VEGF) is an autocrine and paracrine growth factor that can improve vascular permeability, damage the tight junctions of vascular endothelial cells, induce endothelial cell proliferation, and promote extracellular fluid accumulation, vascular leakage, and neovascularization [5,6]. Matrix metalloproteinase-9 (MMP-9), one of the important protein hydrolases in the family of MMPs, disrupts basement membrane integrity and promotes neovascularization and vascular endothelial cell outgrowth, thus playing an important role in the ectopic implantation, adhesion, and growth of endometrial cells [7]. Therefore, downregulation of VEGF and MMP-9 expression is particularly critical in inhibiting angiogenesis and blocking signaling in vascular endothelial cells. SU5416 is a small molecule VEGF receptor signaling inhibitor, which can block VEGF receptor autophosphorylation, inhibit receptor tyrosine kinase signaling, and reduce VEGF activity [8]. It was found that SU5416 in a rat pulmonary hypertension model reduced pulmonary inflammatory response, inhibited intimal proliferation of small pulmonary arteries, and promoted pulmonary vascular remodeling [9]. However, there are few reports on the relevance of SU5416 on the development of EMs and angiogenesis worldwide. The objective of this study was to analyze the effects of SU5416, a VEGF receptor inhibitor, on angiogenesis and ERK-VEGF/MMP-9 signaling pathway in EMs in rats.

MATERIAL AND METHODS

Experimental animals

The experiment procedures conformed to the relevant requirements of the Regulations of the People's Republic of China on the Administration of Laboratory Animals; 30 female specific-pathogen-free (SPF) Sprague-Dawley (SD) rats weighting 180-200 g were purchased from (purchased from Beijing Viton Lihua Laboratory Animal Technology Co., Ltd; animal Use License), Animal Use License No.: SYXK (Beijing) 2018-0015, Laboratory Animal Production License No.: SCXK (Beijing) 2018-0022. Rats were housed at a temperature of (24±1) °C, relative humidity of 50%, and noise<80 db. The researcher changed the bedding, and cleaned and disinfected the rat cages regularly.

Drugs, reagents and instruments

VEGF receptor inhibitor SU5416 (Shanghai Hengfei Biotechnology Co., Ltd., China), Two-steps IHC detection kits for rat tissues (Shanghai Qi Ming Biotechnology Co., Ltd., China), Western blot electrophoresis instrument (Bio-Rad Inc., USA), BCA protein concentration assay kit (Beijing Solaibao Technology Co. Ltd., China), Hematoxylin Eosin Staining Kit (Wuhan PhD Bioengineering Co., Ltd., China), angiopoietin (Ang)-1, Ang-2, laminin-5γ2 (LN-5γ2), phosphorylation of ERK (P-ERK), VEGF, MMP-2, MMP-9, GAPDH antibodies (CST Biotechnology Co., Ltd., USA), Horseradish Peroxidase (HRP)-Labeled Goat Anti-Rabbit Immunoglobulin (Ig) G (Solepow Technology Co., Ltd., China), VEGF, MMP-9, and GAPDH primers (synthesized by Sangon Biotech (Shanghai) Co., Ltd.), fluorescent quantitative PCR kit (Lot. No. 639519, Takara Bio Inc., Japan), Trizol kit (Thermo Fisher Science, USA), RNA extraction kit (Nanjing Novozymes Biotechnology Co., Ltd., China), reverse transcription kit (Genecopoeia, Inc., USA), 5415D high-speed centrifuge (Eppendorf, Germany), and CX21 optical microscope (Olympus, Japan), Light Cycler 2.0 Real-time PCR instrument (Roche Equipment Ltd., Switzerland), -80℃ ultra-low temperature refrigerator (SANYO, Japan), enzyme immunoassay analyzer (Shanghai Kunke Instruments Co., Ltd., China), surgical instruments (Beijing Youcheng Jiaye Biotechnology Ltd., China), VEGF, MMP-9, GAPDH primers (Shanghai Bioengineering Co., Ltd., China), vernier calipers (Shanghai YuYan Scientific Instruments Co., Ltd., China), etc.

METHODS

Model establishment and grouping

Thirty female SPF SD rats were randomly divided into sham operation group (SOG), model group (MG), and SU5416 group (n=10 for each group). In the SOG, only the uterus was cut and sutured. The EMs models were established in the MG and SU5416 group by autologous transplantation, that is, the rats were anesthetized by intraperitoneal injection of 10% chloral hydrate at a dose of 300 mg/kg, and the rats were placed in the supine position and fixed on the operating table, disinfected. A 2 cm incision was made in the middle of the lower abdomen, the uterus and endometrium were separated, and two 5mm × 5mm fragments were taken from the left uterine horn, which were quickly transplanted into the rat mesenteric artery with abundant blood vessels. The abdominal cavity was washed and sutured layer by layer, and the postoperative anti-infection was performed for 3 days. The success criteria for model establishment: the graft was opened 14 d postoperatively, and the volume of the graft was observed visually to be increased, with a light red, round or oval vesicle with internal fluid accumulation, and the surface was covered with a large number of blood vessels and closely adhered to the surrounding tissues. The SU5416 group was injected intraperitoneally with 15 mg/kg SU5416 twice a week, and the sham operation and MGs were injected intraperitoneally with equal volume of saline for 6 weeks. Every procedure was approved by the Animal Care and Use Committee of the First Affiliated Hospital of Fujian Medical University.

Morphology of normal and ectopic endometrial tissue and volume of ectopic lesions in rats

At 42 d after surgery, morphological changes of endometrial tissue in rats were observed under optical microscope; at 14 d and 42 d after surgery, the width and length of ectopic lesions were measured using vernier calipers, and the volume of lesions was calculated = length×width^2×0.5.

Specimen collection

After 24h after the last administration, 3mL of tail vein blood was collected from rats, left for 15min, centrifuged at 2000×g for 15min, and the supernatant was stored in an ultra-low temperature refrigerator at -80℃. After anesthesia, the rats were executed and dissected. In the MG and SU5416 group, ectopic endometrium was removed, and in the SOG, normal endometrium was removed. Each specimen was immediately cut into three parts and rinsed with saline, and 1g of tissue was cut off and stored in an ultra-low temperature refrigerator at -80℃, which were used for real-time quantitative PCR and western blot assay. The remaining endometrium tissue was fixed with 4% paraformaldehyde, dehydrated in gradient alcohol, transparent in xylene, embedded in paraffin, and routinely pathologically sectioned.

Immunohistochemical staining method

CD31 is a platelet endothelial cell adhesion molecule expressed at the tight junctions between endothelial cells, which regulates the process of angiogenesis and reflects the microvessel density (MVD), and can therefore be used as a marker for the measurement of microangiogenesis. In this study, the number of CD31 positive cells in endometrial tissues was mainly detected by immunohistochemical detection. Paraffin sections were dewaxed, soaked in alcohol from high to low gradient, rinsed with distilled water, incubated with 0.3% H_2O_2 for 30 min, blocked with 5% serum for 2 h, incubated with CD31 primary antibody at 4℃ overnight, rinsed with TBST, immunohistochemical staining, rinsed with distilled water, dehydrated in gradient alcohol, transparent in xylene, and sealed. The staining was observed using light microscopy, and any five fields of view of each section were photographed. The number of CD31 positive cells and the total number of cells were counted,

and the proportion of CD31 positive cells was calculated. Proportion of CD31 positive cells = number of CD31 positive cells/total number of cells × 100%.

Enzyme-linked immunosorbent assay (ELISA)

The spare serum was taken, and the levels of serum VEGF, MMP-9, interleukin (IL)-1, IL-2, IL-6 and tumor necrosis factor (TNF)-α were determined according to the instructions of the ELISA kit. Blank wells (no sample and enzyme reagents were added to the blank control wells, the rest of the procedure was the same), standard wells and test sample wells were set respectively. Standard (50 μL) was accurately added on the ELISA coated plate. Sample diluent (40 μL) was added to the test sample wells, and then 10 μL of test sample was added (the final sample dilution was five times). The sample was added to the bottom of the well of ELISA plate without touching the wall of the well, and was gently shaken and mixed. After sealing the plate with sealing film, the sample was incubated at 37 °C for 30 min. The 30 times concentrated washing solution was diluted with 30 times distilled water for further use. After carefully removing the sealing film, the solution was discarded, and the sample was shaken dry. Each well was filled with washing solution, and after leaving for 30 s, the solution was discarded, repeating this for 5 times and patting dry. Enzyme reagent (50 μL) was added to each well, except blank wells. The plate was the sealed with sealing film, and the sample was incubated at 37° C for 30 min. After washing the plate as the above method, Chromogen solution A (50 μL) was added to each well first, and then Chromogen solution B (50 μL) was added to each well, and the mixture was gently shaken and mixed for chromogenic reaction at 37 °C for 15 min. The stop solution (50 μL) was added to each well to stop the reaction (at this time, the blue immediately turned to the yellow). The blank well was set to zero, and the optical density (OD) of each well at 450 nm wavelength was measured.

Quantitative real-time fluorescence (qRT-PCR)

Spare uterine tissue was taken and total RNA from uterine tisuue extracted according to the instructions of Trizol kit and total RNA extraction kit, and use reverse transcription kit to reverse-transcribe the total RNA into cDNA. Using the reverse transcribed cDNA as a template, the expression of VEGF and MMP-9 was detected by Real-time PCR instrument. The total reaction volume was 20 μL, GAPDH was used as the internal reference, and the relative expression of genes in each group was calculated by the 2-ΔΔCt method.

Western blot

The spare remaining uterine tissue was taken, followed by the BCA method for protein quantification, 12% SDS-polypropylene gel electrophoresis, wet transfer to PVDF membrane, treatment with a closure solution for two h at room temperature in a shaker, primary antibody (1:500 dilution) (Ang-1, Ang-2, LN-5γ2, P-ERK, VEGF, MMP-2, MMP-9, GAPDH) was added, incubated overnight at 4 °C, and the membrane was washed three times with TBST for 15 minutes each time. HRP-labeled Goat Anti-Rabbit IgG secondary antibody (1:2000 dilution) was added, incubated for two hours at room temperature, and the membrane was washed three times with TBST for 15 minutes each time. Enhanced chemiluminescence (ECL) reagents were used to develope the color and quantitative analysis was performed using Image J software. GAPDH (1:1000 dilution) was used as the internal reference, and the ratio result indicated the relative concentration of the target protein.

Statistical analysis

Statistical Package for the Social Sciences (SPSS) 24.0 statistical analysis software was used, and the measurement data conforming to normal distribution were ex-

pressed as $\bar{x} \pm s$ and compared using one-way analysis of variance (ANOVA) while least significant difference (LSD)-t test was used for two-way comparison, $p<0.05$ was considered statistically significant difference.

RESULTS

Volume of ectopic lesions

The volume of ectopic lesions in the MG and SU5416 group at 42 days after operation was higher than that at 14 days after operation ($p<0.05$), but there was no significant difference in the volume of ectopic lesions between the MG and SU5416 group at 14 days after operation ($p>0.05$); the volume of ectopic lesions in the SU5416 group was lower than that in the MG at 42 days after operation ($p<0.05$), indicating that SU5416 could effectively inhibit the increase in the volume of ectopic lesions in rats (Fig. 1).

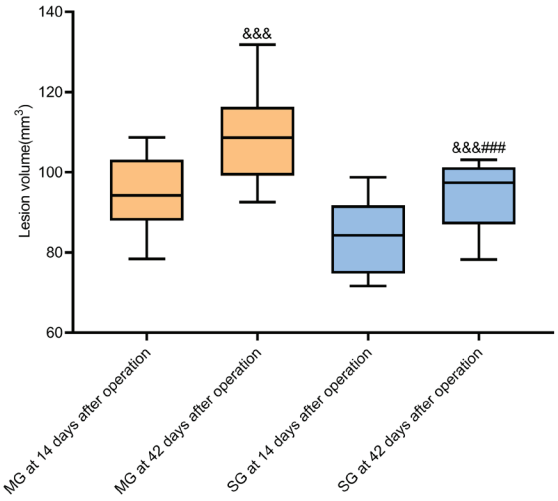

Fig. 1. Comparison of ectopic lesion volume in each group.

Shows that there was no significant difference in the volume of ectopic lesions between the model group and SU5416 group at 14 days after operation, while the volume of ectopic lesions in the SU5416 group was lower than that in the model group at 42 days after operation. Note: MG: model group; SG: SU5416 group. Compared within the group at 14 days after operation, &&&p<0.001; compared with the model group at 42 days after operation, ###p<0.001.

Morphological changes of normal and ectopic endothelial tissues in rats under light microscopy

Since the rats in the sham-operation group did not develop EMs and there was no presence of ectopic endometrial tissue, the comparison was made between normal endometrial tissue and ectopic endometrial tissue from the other groups. At 42 days after operation, the normal endometrial epithelial cells and glandular epithelium of the rats in the sham-operation group were arranged in a columnar shape with a complete structure, and the glands, blood vessels and interstitial cells of the lamina propria were neatly arranged and structurally complete. The ectopic endometrial epithelial cells and the glandular epithelium of the rats in the MG were high columnar; the endometrial structure was circular sawtooth closed, the numbers of lamina propria glands, stromal cells and blood vessels were large, and the nucleus oval was deeply stained. The ectopic endometrial epithelial cells of the SU5416 group showed atrophic changes, the structure of some epithelial cells is incomplete, the lamina propria gland epithelial cells are incomplete, the mesenchymal cells become smaller, the number of blood vessels is reduced and the arrangement is disordered (Fig. 2).

CD31-positive cell expression in endometrial tissue

Since the rats in the sham-operation group did not develop EMs and there was no presence of ectopic endometrial tissue, the comparison was made between normal endometrial tissue and ectopic endometrial tissue from the other groups. The staining of CD31 positive cells and the proportion of positive cells were detected by immunohistochemical method, which could show the changes of MVD of endometrium. The proportion of MVD of ectopic endometrial tissue (that is, CD31-positive cell expression) in the MG and SU5416 group was higher than that of normal endometrial tissues in the SOG ($p <$ 0.05); The proportion of CD31-positive cell

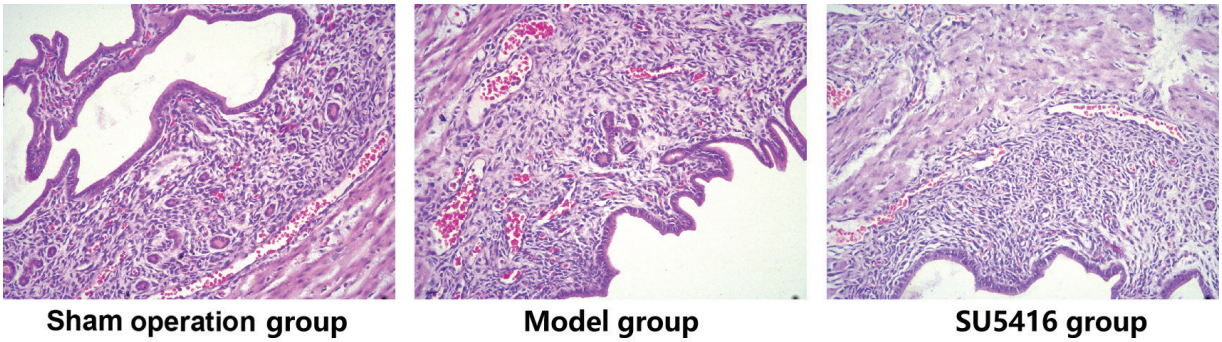

Fig. 2. Morphological changes of normal and ectopic endometrial tissues of rats under light microscopy (200×).

Shows that there was no endometriosis lesion in the sham-operation group, so the comparison was made between normal endometrial tissue and ectopic endometrial tissue from the other groups. At 42 days after operation, the normal endometrial epithelial cells and glandular epithelium of the rats in the sham-operation group were arranged in a columnar shape with a complete structure. The ectopic endometrial epithelial cells and the glandular epithelium of the rats in the model group were high columnar; the endometrial structure was circular sawtooth closed, the numbers of lamina propria glands, stromal cells and blood vessels were large, and the nucleus oval was deeply stained. The ectopic endometrial epithelial cells of the SU5416 group showed atrophic changes.

expression of ectopic endometrial tissues was lower in the SU5416 group than in the MG ($p<0.05$), which showed that SU5416 could effectively reduce the MVD of endometrial tissue in rats (Fig. 3).

Endometrial angiogenesis-related protein expression

Ang-1, Ang-2, and LN-5γ2 protein expression of ectopic endometrial tissues in the MG and SU5416 group were higher than those of normal endometrial tissues in the SOG ($p<0.05$); Ang-1, Ang-2, and LN-5γ2 protein expression in ectopic endometrial tissues of the SU5416 group were lower than that of the MG ($p<0.05$), indicating that SU5416 could effectively inhibit endometrial angiogenesis-related protein expression in rats (Fig. 4).

VEGF, MMP-9

The serum VEGF and MMP-9 levels and the expression of VEGF messenger RNA (mRNA) and MMP-9 mRNA in ectopic endometrial tissues of the MG and SU5416 group were higher than those of normal endometrial tissues in SOG ($p<0.05$); The serum VEGF and MMP-9 levels and the expression of VEGF mRNA and MMP-9 mRNA in ectopic endometrial tissues of the SU5416 group were lower than those of the MG ($p<0.05$), which showed that SU5416 could effectively inhibit the serum expression of VEGF and MMP-9 and endometrial tissues of rats (Fig. 5).

ERK-VEGF/MMP-9 pathway-related protein expression

The protein expression of P-ERK, VEGF, MMP-2 and MMP-9 of ectopic endometrial tissues in the MG and SU5416 group were higher than those of normal endometrial tissues in the SOG ($p<0.05$); The protein expression of P-ERK, VEGF, MMP-2 and MMP-9 in ectopic endometrial tissues of the SU5416 group were lower than that of the MG ($p<0.05$). It is evident that SU5416 can effectively inhibit the activation of ERK-VEGF/MMP-9 pathway in rats (Fig. 6).

Inflammatory factors

The levels of serum IL-1, IL-2, IL-6 and TNF-α were higher in the MG and SU5416 group than in the SOG ($p<0.05$); The levels of serum IL-1, IL-2, IL-6 and TNF-α were

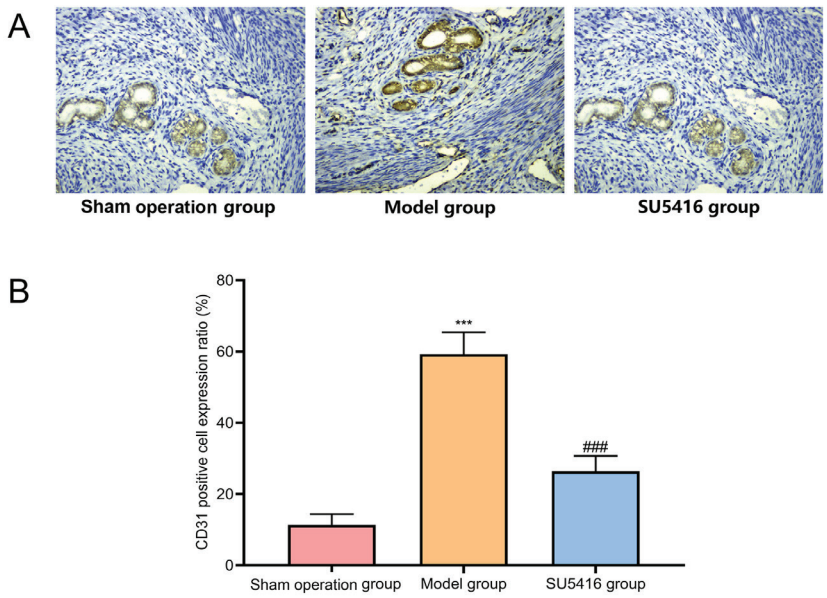

Fig. 3. Comparison of CD31-positive cell expression in endometrial tissues of rats in each group.

Shows that there was no endometriosis lesion in the sham-operation group, so the comparison was made between normal endometrial tissue and ectopic endometrial tissue from the other groups. (A) Staining of CD31-positive cells detected by immunohistochemistry (200×); (B) proportion of CD31-positive cell expression. Note: Compared with the sham operation group, $^{***}p<0.001$; Compared with the model group, $^{###}p<0.001$. Proportion of CD31-positive cell expression = number of CD31 positive cells/total number of cells × 100%.

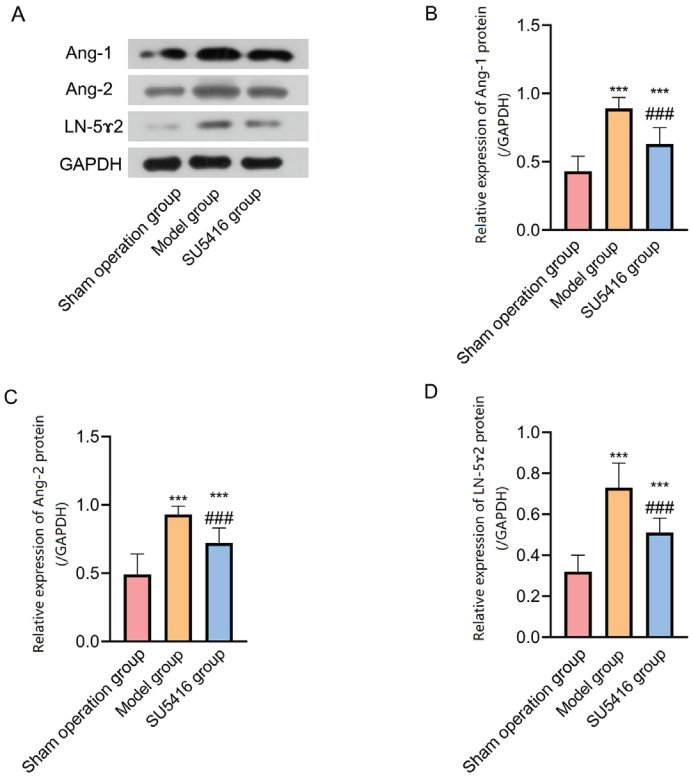

Fig. 4. Comparison of endometrial angiogenesis-related protein expression.

Shows that (B) Ang-1, (C) Ang-2, and (D) LN-5γ2 protein expressions in endometrial tissues of the SU5416 group were lower than those of the model group. Note: Ang-1: angiopoietin-1; Ang-2: angiopoietin-2; LN-5γ2: laminin-5γ2. Compared with the sham operation group, $^{***}p<0.001$; Compared with the model group, $^{###}p<0.001$.

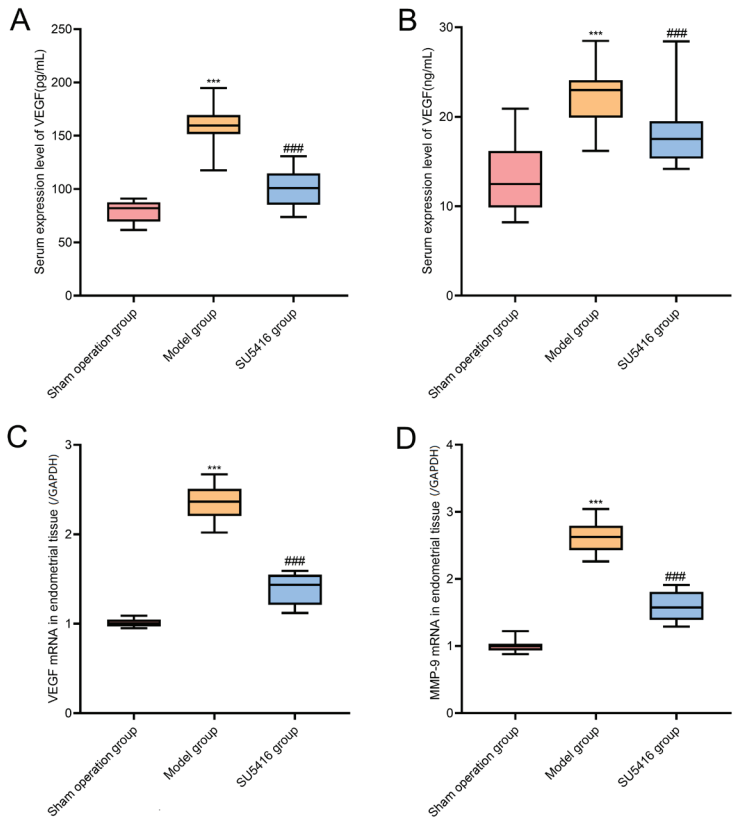

Fig. 5. Comparison of VEGF and MMP-9 expression in rats in each group.

Shows that the protein expression levels of serum (A) VEGF and (B) MMP-9 and the mRNA expression levels of (C) VEGF and (D) MMP-9 in endometrial tissue of the SU5416 group were lower than those of the model group. Note: VEGF: vascular endothelial growth factor; MMP-9: matrix metalloproteinase-9. Compared with the sham operation group, $^{***}p<0.001$; Compared with the model group, $^{###}p<0.001$.

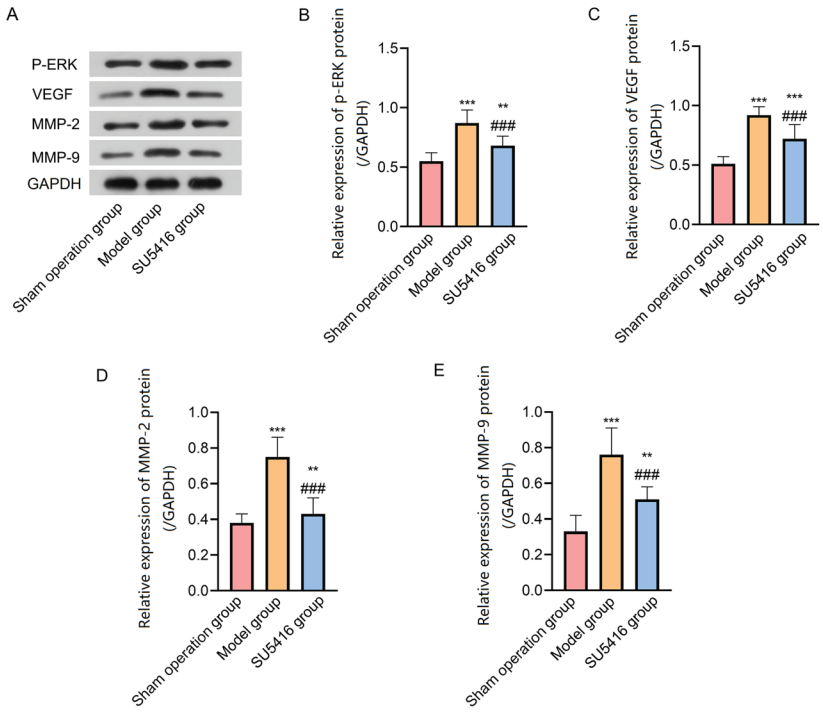

Fig. 6. Comparison of ERK-VEGF/MMP-9 pathway-related protein expression.

Shows that the expression levels of (B) P-ERK, (C) VEGF, (D) MMP-2, and (E) MMP-9 proteins in the endometrial tissue of the SU5416 group were lower than those of the model group. Note: P-ERK: phosphorylation of ERK; VEGF: vascular endothelial growth factor; MMP-2: matrix metalloproteinase-2; MMP-9: matrix metalloproteinase-9. Compared with the sham operation group, $^{**}p<0.01$, $^{***}p<0.001$; Compared with the model group, $^{###}p<0.001$.

lower in the SU5416 group than in the MG ($p<0.05$), which showed that SU5416 could effectively reduce the inflammatory response in rats (Fig. 7).

DISCUSSION

The etiology and mechanism of EMs are complex and diverse. The implantation theory of reverse flow of menstrual blood proposed by Sampson in 1921 is the most supported, that is, the exfoliated endometrial fragments flow back into the pelvic and abdominal cavity with the menstrual blood, and are implanted in the ovary and adjacent pelvic and abdominal cavity, causing a local inflammatory response in the peritoneum, leading to the establishment of a local microenvironment and angiogenesis, thereby providing a continuous angiogenesis stimulus for vascular remodeling [10-13]. However, either theory involves neovascularization and degradation and reconstruction of the extracellular matrix. The reason for the initiation of pathological angiogenesis lies in the unbalanced regulation of vascular inhibitory factors and promoting factors, among which the increase of pro-angiogenic factors such as VEGF and matrix metalloproteinase (MMP) is the main cause [14]. Therefore, anti-angiogenesis is of great importance in the prevention and treatment of EMs. SU5416 is a lipid-soluble small molecule VEGF receptor signal transduction inhibitor, which can block the interaction between VEGF and its receptor and inhibit angiogenesis [15]. However, there are no reports on the effect of SU5416 in EMs. In this experiment, an EMs model was established by autologous transplantation. The results showed that compared with the MG, the volume of ectopic lesions, the proportion of CD31 positive cells and the level of serum inflammatory factors in the SU5416 group were reduced

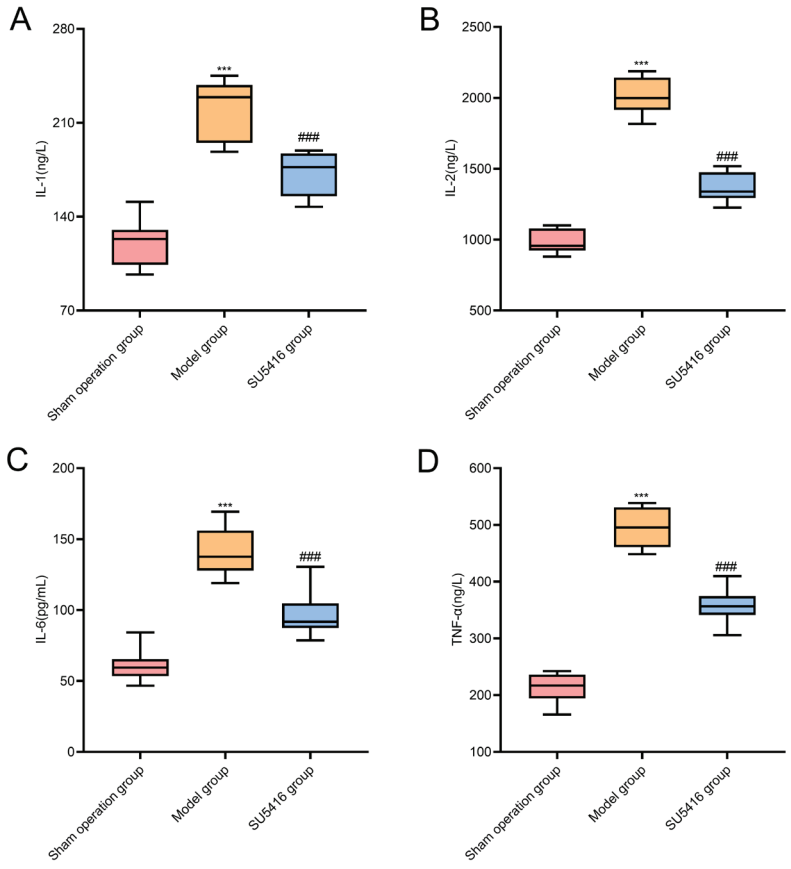

Fig. 7. Comparison of serum inflammatory factor levels in rats of each group.

Shows that the expression levels of (A) IL-1, (B) IL-2, (C) IL-6 and (D) TNF-α in endometrial tissue of the SU5416 group were lower than those of the model group. Note: IL-1: interleukin-1; IL-2: interleukin-2; IL-6: interleukin-6; TNF-α: tumor necrosis factor-α. Compared with the sham operation group, $^{***}p<0.001$; Compared with the model group, $^{###}p<0.001$.

at 42 days after operation. Membrane epithelial cells showed atrophic changes, mesenchymal cells became smaller, and the number of blood vessels decreased. It can be seen that SU5416 can reduce the volume of ectopic lesions and prevent the inflammatory response by inhibiting cell proliferation and angiogenesis.

The ERK signaling pathway is one of the mitogen-activated protein kinase (MAPK) pathways. Activated ERK can activate downstream targets such as the 90kD ribosomal S6 protein kinase family (RSKs), and promote the translocation of RSK1/2 and pERK1/pERK2 into the nucleus, activate early and immediate gene transcription, thereby regulating cell survival, apoptosis, proliferation, metabolism, transcription and other biological behaviors [16,17]. VEGF is one of the endothelial cell-specific vascular-derived proteins, which can promote fibrinogen exudation, increase trophoblast, endometrial and meconium permeability, promote endothelial cell proliferation and subperitoneal vascular network formation, thus inducing lesion growth and endothelial implantation; Moreover, VEGF can bind to relevant receptors on endothelial cells and initiate paracrine mechanisms via signaling pathways, which play an important role in endothelial implantation and placenta formation [18,19]. MMP-9 can degrade the main components of extracellular matrix such as collagen type IV, collagen V, and gelatin, destroy the integrity of the basement membrane, and promote the formation of new blood vessels and the sprouting of vascular endothelial cells [20]. Meanwhile, the degraded extracellular matrix protein fragments could regulate apoptosis, migration, and invasion of epithelial cells, leading to invasion into other parts of the eutopic endometrium [21]. Chen [22] *et al*. found that the ERK-VEGF/MMP-9 signaling pathway is closely related to angiogenesis, and down-regulating the expression of this signaling pathway can inhibit cell proliferation, invasion and angiogenesis. Guo [23] *et al.* found that inhibition of extracellular ERK activation downregulated MMP-9 and VEGF expression and signaling, thereby slowing down the rate of vascular invasion and growth. Yilmaz [24] *et al.* found increased expression of P-ERK, VEGF, and MMP-9 proteins in rats with EMs, while blocking cytokine binding to surface receptors and intercellular signaling pathways could control abnormal endometrial proliferation and angiogenesis. The results of this study revealed that the expression of P-ERK, VEGF, MMP-2, and MMP-9 proteins in the endometrial tissues of the MG was higher than that of the SOG, which was consistent with the above findings and again confirmed that the activation of ERK-VEGF/MMP-9 signaling pathway might be related to the development of EMs. The expression of P-ERK, VEGF, MMP-2, MMP-9 and Ang-1, Ang-2, LN-5γ2 proteins were reduced in the endometrial tissues of rats after SU5416 treatment, which showed that the VEGF receptor inhibitor SU5416 could reduce the synthesis and secretion of extracellular signal-regulated kinases and inhibit the activation of ERK-VEGF/MMP-9 signaling pathway in ectopic endometrial tissues, thus preventing angiogenesis and the growth, implantation and adhesion of abnormal proliferating cells in the pelvic and abdominal peritoneum.

In summary, the VEGF receptor inhibitor SU5416 inhibited angiogenesis and reduced inflammatory response in rat EMs, and its mechanism of action may be related to the downregulation of ERK-VEGF/MMP-9 pathway expression. This experiment confirmed the effects of SU5416 on angiogenesis, signaling pathway and inflammatory response in rats with EMs, providing new ideas for the clinical treatment and the development of new drugs. However, further in vivo experiments are needed to verify the therapeutic effects and specific mechanism of action of the VEGF receptor inhibitor.

Conflicts of interest

There are no conflicts to declare.

Funding

None.

Authors ORCID'number

- Danyang Zhao: 0000-0002-0668-9000
- Qiufang Bao: 0009-0008-1944-7431
- Lihong Chen: 0000-0003-2514-2913
- Lie Zheng: 0000-0002-9457-9003

Authors Contribution

Each author has made an important scientific contribution to the study and has assisted with the drafting or revising of the manuscript.

REFERENCES

1. **Chapron C, Marcellin L, Borghese B, Santulli P.** Rethinking mechanisms, diagnosis and management of endometriosis. Nat Rev Endocrinol 2019; 15(11): 666-682. *https://doi.org/10.1038/s41574-019-0245-z.*
2. **Jin Z, Zhang Y, Li J, Lv S, Zhang L, Feng Y.** Endometriosis stem cell sources and potential therapeutic targets: literature review and bioinformatics analysis. Regen Med 2021; 16(10): 949-962. *https://doi.org/10.2217/rme-2021-0039.*
3. **Ding L, Yang L, Ren C, Zhang H, Lu J, Wang S, Wu Z, Yang Y.** A review of aberrant DNA methylation and epigenetic agents targeting DNA methyltransferases in endometriosis. Curr Drug Targets 2020; 21(11): 1047-1055. *https://doi.org/10.2174/1389450121666200228112344.*
4. **Doroftei B, Ilie OD, Balmus IM, Ciobica A, Maftei R, Scripcariu I, Simionescu G, Grab D, Stoian I, Ilea C.** Molecular and clinical insights on the complex interaction between oxidative stress, apoptosis, and endobiota in the pathogenesis of endometriosis. Diagnostics (Basel) 2021; 11(8): 1434. *https://doi.org/10.3390/diagnostics11081434.*
5. **Mesquita J, Castro de Sousa JP, Vaz-Pereira S, Neves A, Tavares-Ratado P, Santos FM, Passarinha LA, Tomaz CT.** VEGF-B levels in the vitreous of diabetic and non-diabetic patients with ocular diseases and its correlation with structural parameters. Med Sci (Basel). 2017; 5(3): 17. *https://doi.org/10.3390/medsci5030017.*
6. **Pergialiotis V, Fanaki M, Bellos I, Stefanidis K, Loutradis D, Daskalakis G.** The impact of vascular endothelial growth factor single nucleotide polymorphisms in the development and severity of endometriosis: A systematic review of the literature. J Gynecol Obstet Hum Reprod 2020; 101732. *https://doi.org/10.1016/j.jogoh.2020.101732.*
7. **Huang H.** Matrix Metalloproteinase-9 (MMP-9) as a cancer biomarker and MMP-9 biosensors: recent advances. Sensors (Basel) 2018; 18(10): 3249. *https://doi.org/10.3390/s18103249.*
8. **Ye C, Sweeny D, Sukbuntherng J, Zhang Q, Tan W, Wong S, Madan A, Ogilvie B, Parkinson A, Antonian L.** Distribution, metabolism, and excretion of the antiangiogenic compound SU5416. Toxicol In Vitro 2006; 20(2): 154-162. *https://doi.org/10.1016/j.tiv.2005.06.047.*
9. **Sakao S, Tatsumi K.** The effects of antiangiogenic compound SU5416 in a rat model of pulmonary arterial hypertension. Respiration 2011; 81(3): 253-261. *https://doi.org/10.1159/000322011.*
10. **Bahrami A, Ayen E, Razi M, Behfar M.** Effects of atorvastatin and resveratrol against the experimental endometriosis; evidence for glucose and monocarboxylate transporters, neoangiogenesis. Life Sci 2021; 272: 119230. *https://doi.org/10.1016/j.lfs.2021.119230.*
11. **Rashidi BH, Sarhangi N, Aminimoghaddam S, Haghollahi F, Naji T, Amoli MM, Shahrabi-Farahani M.** Association of vascular endothelial growth factor (VEGF) Gene polymorphisms and expres-

sion with the risk of endometriosis: a case-control study. Mol Biol Rep 2019; 46(3): 3445-3450. *https://doi.org/10.1007/s11033-019-04807-6.*

12. **Li YZ, Wang LJ, Li X, Li SL, Wang JL, Wu ZH, Gong L, Zhang XD.** Vascular endothelial growth factor gene polymorphisms contribute to the risk of endometriosis: an updated systematic review and meta-analysis of 14 case-control studies. Genet Mol Res 2013;12(2): 1035-1044. *https://doi.org/10.4238/2013.April.2.20.*
13. **Qiu JJ, Lin XJ, Zheng TT, Tang XY, Zhang Y, Hua KQ.** The exosomal long noncoding RNA aHIF is upregulated in serum from patients with endometriosis and promotes angiogenesis in endometriosis. Reprod Sci 2019; 26(12): 1590-1602. *https://doi.org/10.1177/1933719119831775.*
14. **Liu S, Xin X, Hua T, Shi R, Chi S, Jin Z, Wang H.** Efficacy of anti-VEGF/VEGFR agents on animal models of endometriosis: A systematic review and meta-analysis. PLoS One. 2016; 11(11): e0166658. *https://doi.org/10.1371/journal.pone.0166658.*
15. **Mendel DB, Laird AD, Smolich BD, Blake RA, Liang C, Hannah AL, Shaheen RM, Ellis LM, Weitman S, Shawver LK, Cherrington JM.** Development of SU5416, a selective small molecule inhibitor of VEGF receptor tyrosine kinase activity, as an anti-angiogenesis agent. Anticancer Drug Des 2000; 15(1): 29-41.
16. **Guo YJ, Pan WW, Liu SB, Shen ZF, Xu Y, Hu LL.** ERK/MAPK signalling pathway and tumorigenesis. Exp Ther Med 2020; 19(3): 1997-2007. *https://doi.org/10.3892/etm.2020.8454.*
17. **Pashirzad M, Khorasanian R, Fard MM, Arjmand MH, LangariH, Khazaei M, Soleimanpour S, Rezayi M, Ferns GA, Hassanian SM, Avan A.** The therapeutic potential of MAPK/ERK inhibitors in the treatment of colorectal cancer. Curr Cancer Drug Targets 2021; 21(11): 932-943. *https://doi.org/10.2174/1568009621666211103113339.*
18. **Li Y, Fang L, Yu Y, Shi H, Wang S, Li Y, Ma Y, Yan Y, Sun YP.** Association between vascular endothelial growth factor gene polymorphisms and PCOS risk: a meta-analysis. Reprod Biomed Online 2020; 40(2): 287-295. *https://doi.org/10.1016/j.rbmo.2019.10.018.*
19. **Zhang H.** Expression and significance of MEK-5, ERK5, p-ERK, VEGF and MMP-9 in endometriosis [Master's thesis]. Tianjin: Tianjin Medical University; 2013.
20. **Mondal S, Adhikari N, Banerjee S, Amin SA, Jha T.** Matrix metalloproteinase-9 (MMP-9) and its inhibitors in cancer: A minireview. Eur J Med Chem. 2020;194:112260. *https://doi.org/10.1016/j.ejmech.2020.112260.*
21. **Dong H, Diao H, Zhao Y, Xu H, Pei S, Gao J, Wang J, Hussain T, Zhao D, Zhou X, Lin D.** Overexpression of matrix metalloproteinase-9 in breast cancer cell lines remarkably increases the cell malignancy largely via activation of transforming growth factor beta/SMAD signalling. Cell Prolif 2019; 52(5): e12633. *https://doi.org/10.1111/cpr.12633.*
22. **Chen Z, Xu DY, Yang K.** Association of ERK-VEG FMMP-9 signaling pathway with proliferation and angiogenesis in rectal cancer cells. Genomics and Applied Biology 2019; 38: 5828-5835. *https://doi: 10.13417/j.gab.038.005828.*
23. **Guo ML, Wang CE, Duan YM, Wang JG.** Gecko crude peptides inhibit migration and lymphangiogenesis by down regulating the expression of VEGF-C in human hepatocellular carcinoma cells and human lymphatic endothelial cells. Chin J Pharmacol Toxicol 2017; 31(10): 958-959. *https://doi: 10.3867/j.issn.1000-3002.201 7.10.025*
24. **Yilmaz B, Kilic S, Aksakal O, Ertas IE, Tanrisever GG, Aksoy Y, Lortlar N, Kelekci S, Gungor T.** Melatonin causes regression of endometriotic implants in rats by modulating angiogenesis, tissue levels of antioxidants and matrix metalloproteinases. Arch Gynecol Obstet 2015; 292(1): 209-216. *https://doi.org/10.1007/s00404-014-3599-4.*

Invest Clin 64(4): 495 - 504, 2023 https://doi.org/10.54817/IC.v64n4a6

Influence of different peritoneal incision closure methods on the operative outcomes and prognosis of patients undergoing laparoscopic inguinal hernia repair.

Bixiang Zheng, Xiaobin Luo, Changdong Wang, Rendong Zheng and Xiaofeng Yang

Department of General Surgery, Santai People's Hospital, Mianyang, Sichuan Province, China.

Keywords: Laparoscopic inguinal hernia repair; peritoneal rupture; bipolar coagulation.

Abstract. The aim was to investigate the effect of different peritoneal tear closure methods on the operative outcomes and prognosis of patients undergoing laparoscopic inguinal hernia repair (LIHR). Ninety patients who underwent LIHR in our hospital from August 2019 to December 2020 and had peritoneal tears during the operation were selected, and the patients were divided into a control group (CG) and the observation group (OG) according to different treatment plans, with 45 cases in each group. Patients in the CG were treated with absorbable sutures to repair the peritoneal tears, while patients in the OG were treated with bipolar coagulation to close and repair the peritoneal tears. The surgical conditions, postoperative pain scores, quality of life scores, complications, and recurrence were compared between the CG and OG groups. The operation time and hospital stay in the OG were shorter than those in the OG ($p<0.05$). The pain scores in the OG at 24 hours after operation were lower than those in the CG ($p<0.05$), and the pain scores of the two groups were not significantly different at two hours and 12 hours ($p>0.05$). Postoperative complications were not significantly different between the groups ($p>0.05$). The scores of material life, physical, social, and psychological function in the OG were higher than in the CG ($p<0.05$). There were no recurrences in the two groups during the 1-year follow-up. Closing repair of peritoneal rupture with bipolar coagulation reduces the operation time of patients with peritoneal rupture during TEP (total extraperitoneal hernioplasty) operations, reduces pain, and improves their quality of life. The treatment outcome is safe, effective, and has an excellent clinical application effect.

Corresponding author: Bixiang Zheng: Department of General Surgery, Santai People's Hospital, Mianyang, Sichuan Province, China. E-mail: yanhuizhong20@163.com

Influencia de diversos métodos de cierre de la incisión peritoneal en los resultados quirúrgicos y el pronóstico en pacientes sometidos a reparación laparoscópica de hernia inguinal.

Invest Clin 2023; 64 (4): 495 – 504

Palabras clave: reparación laparoscópica de la hernia inguinal; ruptura peritoneal; coagulación bipolar.

Resumen. El propósito de este trabajo fue investigar el efecto de distintos métodos de cierre de desgarros peritoneales sobre el resultado quirúrgico y el pronóstico en pacientes sometidos a la reparación laparoscópica de hernia inguinal (LIHR). Fueron elegidos un total de 90 pacientes sometidos a LIHR en nuestro hospital desde agosto de 2019 a diciembre de 2020 y que tuvieron desgarros peritoneales durante la operación; los pacientes fueron divididos en un grupo control (GC) y un grupo de observación (OG) según distintos planes de tratamiento, con 45 casos en cada grupo. Los pacientes del GC fueron tratados con suturas absorbibles para reparar los desgarros peritoneales, mientras que los pacientes del OG fueron tratados con coagulación bipolar para cerrar y reparar los desgarros peritoneales. Se realizó una comparación de ambas condiciones quirúrgicas, que incluyeron las puntuaciones de dolor posoperatorio y calidad de vida, las complicaciones y la recurrencia entre los grupos GC y OG. El tiempo de operación e ingreso en el hospital en el OG fueron más cortos que en el OG ($p<0,05$). Las puntuaciones de dolor en el OG a las 24 horas después de la operación fueron menores que las del GC ($p<0,05$) y las puntuaciones de dolor de ambos grupos no fueron diferentes de modo significativo a las 2 horas y 12 horas ($p>0,05$). Las complicaciones postoperatorias no fueron significativamente diferentes entre OG ($p>0,05$). Los puntajes de vida material, función física, función social y función psicológica en el OG fueron más elevados que los del GC ($p<0,05$). No hubo recurrencias en ninguno de los grupos durante el seguimiento de 1 año. En conclusión, la reparación de cierre de la ruptura peritoneal con coagulación bipolar redujo el tiempo de operación de los pacientes, redujo su dolor y mejoró su calidad de vida. El efecto del tratamiento es seguro, efectivo y tiene un excelente resultado en su aplicación clínica.

Received: 19-03-2023 Accepted: 21-05-2023

INTRODUCTION

An inguinal hernia is a common medical problem that develops when tissue, such as a portion of the intestine or abdominal fat, pushes through a weak area or hole in the abdominal wall [1]. This type of hernia is most common in men, but women can also develop them [2]. The lifetime risk of developing an inguinal hernia is 27-43% for men and 3-6% for women [3].

Inguinal hernias can be brought on by many things, such as heredity, age, persistent coughing, obesity, and physical stress[4,5]. Inguinal hernias often generate a visible bulge or swelling in the groin area, which

might become more noticeable while coughing or moving heavy things. The hernia may be painful or uncomfortable in certain circumstances, especially while standing or walking for extended periods [6,7].

Inguinal hernias can develop problems like incarceration or strangulation, in which the projecting tissue becomes trapped and loses blood flow, potentially resulting in tissue damage or even death. So, early diagnosis and treatment are essential in managing the condition and preventing complications [8].

Inguinal hernias are commonly treated with surgical repair, which may be done using laparoscopic or open methods. During surgery, the projecting tissue is pulled back into position, and the weak muscle wall is strengthened with sutures or synthetic mesh. Inguinal hernia surgery is frequently very successful and can offer long-lasting symptom alleviation [9,10].

However, during abdominal operations, peritoneal rips are a typical occurrence. Absorbable sutures and bipolar coagulation are two methods available to heal peritoneal injuries [11]. After a laparotomy or laparoscopy, the surgeon may close the peritoneum based solely on personal preference [12]. In order to minimize abdominal wall weakening and to prevent incisional hernias, it has been claimed by surgeons and in the standard surgical texts that the peritoneum should be sutured [13]. Nevertheless, clinical and experimental studies have shown that the raw peritoneal defect heals spontaneously, quickly, smoothly, and without apparent catastrophe because the peritoneum has no discernible impact on the healing process or the tensile strength of the laparotomy wound. So, after the laparoscopic hernia repair, the peritoneum should be left to heal spontaneously [14-16].

Since limited studies have compared these two techniques, and due to the existence of disagreements regarding the need to perform therapeutic measures and the need not to take action to repair the peritoneal rupture, this study was indicated to be conducted to compare the efficiency and safety of these two techniques and investigate the necessity or not of intervention in the repairment of peritoneal rupture during laparoscopic inguinal hernia surgery.

MATERIALS AND METHODS

General data

Ninety patients who underwent LIHR in our hospital from August 2019 to December 2020 and had peritoneal tears during the operation were selected and divided into the control group (CG) and the observation group (OG), with 45 cases in each group. The general data between the two groups was not significantly different ($p>0.05$) (Table 1). The ethics committee in the hospital approved this study, and all patients signed an informed consent form. Inclusion criteria: ①The age range considered for

Table 1
General data.

Groups	Cases	Sex		Age (years)	Disease course (months)	BMI (kg/m²)	Type (cases)			
		Male	Female				I	II	III	IV
Observation group	45	40 (88.8%)**	5 (11.12%)	63.56±7.76*	50.52±10.25	24.75±2.47	7 (15.5%)**	14 (31.1%)	13 (28.8%)	11 (24.6%)
Control group	45	38 (84.4%)	7 (15.6%)	62.23±7.85*	52.56±9.58	24.95±2.82	9 (20%)	12 (26.7%)	15 (33.3%)	9 (20%)
χ^2/t/Z		0.385		0.808	-0.975	-0.358	-0.377			
$p^{\&}$		0.535		0.421	0.332	0.721	0.706			

*Quantitative variables expressed by mean ± standard deviation. ** Qualitative variables expressed by frequency (percent). &P-value based on t-test / chi-square χ^2. *Significance level ≤ 0.05.*

this study was between 30 and 80 years old; ②Patients who were diagnosed with a direct inguinal hernia by clinical symptoms, signs, B-ultrasound, and other examinations[17], and who underwent TEP surgery and had peritoneal rupture during the operation; ③They fell within the American Society of Anesthesiologists grade I-II score; ④Patients with complete clinical medical records. Exclusion criteria: ①Patients with a history of mid-lower abdominal surgery; ②those with indirect inguinal hernia, incarcerated or strangulated hernia, or recurrent hernia; ③those with contraindications to general anesthesia; ④those with severe cardiac, hepatic, and renal dysfunction.

Operation methods

All patients received general anesthesia after entering the operating room. Surgeons performed all operations in the same group, and the specific operation steps strictly followed the "Guidelines for Standardized Operation of Laparoscopic Surgery for Inguinal Hernia". All patients were treated with TEP. In the observation group, a small incision of about 1.5 cm in length was made at 1 cm below the umbilicus to the line alba, followed by an incision of the skin, subcutaneous tissue, and anterior sheath of the *rectus abdominis*. The skin retractor was used to pull the *rectus abdominis* fiber to both sides until the posterior sheath was exposed, a one cm cannula was inserted, and the pneumoperitoneum was created. The other two five-mm cannulas were located five cm and ten cm below the median line umbilicus, respectively. The endoscope push method enlarged the preperitoneal space, and the pubic symphysis and the pubic ligament were exposed, turning laterally to isolate the Bogros space in the groin area.

After the direct hernia sac was freed and restored under direct vision, it was ligated at its base, and the distal end of the ligation line was cut off. The spermatic cord components were then abdominally walled, the iliac vessels were exposed, and the Bogros space in the groin area was fully exposed. The edge of the peritoneum cephalad was freed as much as possible to make room for patch placement. A 10 cm×15 cm polypropylene mesh was used as the repair material, and the mesh was rolled into a "cigarette" shape with the long axis as the edge and was placed in the casing. After entirely unfolding, the mesh was centered on the myopubic foramen to cover the inguinal foramen. The spermatic vessels and the *Vas deferens* were freed by 6 to 8 cm to expose the spermatic cord fully. The abdominal wall suture straight needle was used with No. 7 silk thread to enter the preperitoneal space twice; at the hernia ring, a needle thread and a needle and hook thread were successively passed on the patch, and the patch was subcutaneously fixed.

Peritoneal rupture closure methods

After the peritoneal rupture occurred during the operation, the peritoneum was closed by the corresponding methods: CG patients were treated with absorbable suture to repair the peritoneal tears, after entering the abdominal cavity, continuous suture with micro-wire or continuous suture was used with absorbable line, and then closed; while the patients in the OG were treated with bipolar coagulation to close and repair the peritoneal tears: the peritoneal rupture was repaired by bipolar electrocoagulation and hemostasis, and then the mesh was placed extraperitoneally.

Observation indicators

Operation situation

We observed and recorded both groups' operation time, intraoperative blood loss, and hospital stay.

Postoperative pain

At 2 h, 12 h, and 24 h after surgery, patients were evaluated using the visual analog scale (VAS) [18]. A 10 cm long straight line was used to show the degree of pain, and the scores ranged from 0 to 10 points, with 0 representing no pain and 10 as the most painful.

Complications

Patients' complications (including postoperative puncture hernia, intestinal fistula, intestinal obstruction, and chronic pain) were recorded.

Quality of life

The Comprehensive Assessment Questionnaire for Quality of Life (GQOL-74) [19] evaluated the patient's quality. Material life, physical function, social function, and psychological function were rated on a scale of 0 - 100 points, with higher scores being a better patient quality of life.

Recurrence conditions

The recurrence of hernia sac in the two groups after one year of treatment was recorded.

Statistical methods

SPSS 20.0 was used for statistical analysis, enumeration data were compared by X^2 test, rank data were compared by rank sum test, measurement data were expressed by mean±standard deviation ($\bar{x} \pm s$), and a *t*-test was used for comparison. The statistical result was regarded as statistically significant when $p<0.05$.

RESULTS

Comparison of operation conditions

The operation time and hospital stay in the OG were reduced compared to the CG ($p<0.05$), and in both groups, the intraoperative blood loss was not significantly different ($p>0.05$), as seen in Table 2.

Comparison of postoperative pain scores

The pain scores in the OG at 24 hours after the operation were reduced than those in the CG ($p<0.05$), and the pain scores at two hours and 12 hours in both groups were not significantly different ($p>0.05$), seen in Table 2.

Incidence of complications

The incidence of postoperative complications between the OG was not significantly different ($p>0.05$), as shown in Table 3.

Postoperative quality of life between the two groups

The scores of material life, physical function, social function, and psychological function in the OG were higher than those in the CG ($p<0.05$), as seen in Table 4.

Table 2
Operation conditions and postoperative pain scores in two groups.

Groups	Cases	Operation conditions			Postoperative pain scores		
		Operation time (min)	Intraoperative blood loss (mL)	Hospital stay (d)	Postoperative 2 h	Postoperative 12 h	Postoperative 24 h
Observation group	45	40.56±6.52*	24.45±4.74	3.54±1.22	3.58±1.34	2.27±0.75	1.20±0.28
Control group	45	60.35±10.74*	25.12±4.23	4.22±1.54	3.83±1.55	2.43±0.68	1.43±0.30
t		-10.566	-0.708	-2.322	-0.819	-1.060	-3.760
p[&]		0.001	0.471	0.023	0.415	0.292	0.001

*Quantitative variables expressed by mean ± standard deviation.
[&]P-value based on t-test. *Significance level* ≤ 0.05.

Table 3
Incidence of complications between the two groups.

Groups	Cases	Postoperative Puncture hernia	Intestinal fistula	Intestinal obstruction	Chronic pain	Total
Observation group	45	0 (0.00) *	0 (0.00)	1 (2.22)	1 (2.22)	2 (4.44)
Control group	45	1 (2.22) *	2 (4.44)	0 (0.00)	2 (4.44)	5 (11.11)
χ^2						0.620
$p^{\&}$						0.431

* Qualitative variables expressed by frequency (percent). &P-value based chi-square χ^2. *Significance level* ≤ 0.05.

Table 4
Postoperative quality of life between the two groups.

Groups	Cases	Psychological function	Social function	Physical function	Material life
Observation group	45	72.40±6.45*	75.62±5.46	77.46±6.72	73.46±6.85
Control group	45	67.58±7.52*	70.32±7.14	73.34±5.76	68.63±7.03
t		3.264	3.956	3.123	3.301
$p^{\&}$		0.002	0.000	0.002	0.001

*Quantitative variables expressed by mean ± standard deviation. &P-value based on t-test. *Significance level* ≤ 0.05.

Comparison of postoperative quality of life between the two groups

There were no recurrences in the two groups during a one-year follow-up.

DISCUSSION

Laparoscopic inguinal hernia repair has become increasingly popular due to its minimally invasive nature, faster recovery times, and lower postoperative complications than open surgical methods. The peritoneal incision's closure, which might affect the patient's recovery and general prognosis, is a crucial component of this treatment. The two main methods for closing the peritoneal incision are bipolar coagulation and absorbable sutures [11,20]. This study compared the operative outcomes and prognosis of patients undergoing laparoscopic inguinal hernia repair with these two different peritoneal incision closure methods.

This bipolar coagulation during TEP operation (OG) offers several advantages compared to the absorbable suture method (CG). The results showed a significantly shorter operation time and hospital stay, reduced pain scores at 24 hours' post-operation, and improved quality of life in various aspects for patients in the OG. Importantly, no significant difference was observed in the incidence of postoperative complications between the groups, indicating that the bipolar coagulation method is safe and effective.

The findings of this study are consistent with previous research, which has reported various benefits of using bipolar coagulation for the repair of peritoneal rupture. The study's results by Meyer *et al.* [21], showed that the rate of complications in the TEP method is low, and this laparoscopic hernia repair technique is repeatable and reliable.

The bipolar coagulation sealing technology converts electrical energy into heat energy to dissolve and denature tissue proteins, resulting in a permanent lumen or ruptured tissue coagulation and closure effect [22,23]. This technology can safely close tissue bundles, ligaments, and blood vessels with a <0.7 cm [24] diameter. The peritoneal injury stimulates the release of cytokines, activates the coagulation cascade, and deposits fibrin as a temporary matrix [25]. When bipolar electrocoagulation sealing technology is used to repair peritoneal ruptures, it rapidly dissolves and denatures fibrin and collagen to form new peritoneal tissue, resulting in a better sealing effect. Precautions should be taken during the operation to ensure the entire edge of the breach is closed, and the size of the bipolar energy and use time are critical to the closure effect [26]. The results of the study by Liang *et al.* [27], showed that compared with ultrasonic and bipolar electrocoagulation techniques, advanced bipolar use was more reliable for mesenteric vessels in laparoscopic surgery; however, bipolar electrocoagulation with optimal power can be used for its simplicity of operation and low cost. Various new electrosurgical devices will cause less damage as laparoscopic technology progresses, making surgery more accurate and less damaging. Although bipolar electrocoagulation has a broad thermal damage breadth, it is nevertheless relatively safe.

Oguz *et al.* [28], conducted a study to compare peritoneal closure techniques in laparoscopic transabdominal inguinal hernia repair. This study analyzed tucker and suture techniques to close the peritoneum based on the patient results. The results showed that tucker and suture have comparable safety for peritoneal closure in laparoscopic TAPP inguinal hernia surgery. However, what can be seen is that no study has simultaneously examined the variables of operation time and hospitalization, pain level, physical function, social function, and psychological function.

The results of our study showed that the use of bipolar coagulation reduces the operation time and hospitalization and also leads to a reduction in the pain score 24 hours after the operation. In addition, this study showed that patients who underwent closing repair with bipolar coagulation improved their scores in material life, physical functioning, social functioning, and psychological functioning, indicating an improvement in their overall quality of life.

The reduced operation time in the OG group can lead to increased patient satisfaction, decreased anesthesia-related complications, and reduced healthcare costs. Additionally, the shorter hospital stay observed in the OG group may further reduce healthcare costs and improve patient satisfaction.

The lower pain scores observed in the OG group may be attributed to the reduced tissue trauma and inflammation associated with bipolar coagulation compared to sutures [29]. This reduction in pain may contribute to a faster return to normal activities and improved postoperative quality of life.

The lack of significant differences in the incidence of postoperative complications between the two groups indicates that both methods are safe and effective in repairing peritoneal rupture. However, the improved quality of life scores in the OG group further emphasizes the potential benefits of the bipolar coagulation method.

Several factors can explain the preference for bipolar coagulation over spontaneous release of the peritoneum. Bipolar coagulation allows for better control of bleeding during the process, which can assist in shortening the operation time and lower the risk of complications [30]. Reduced operation time and bleeding can also contribute to a shorter hospital stay and lower pain scores, as observed in the study results.

Bipolar coagulation can accomplish hemostasis by denaturing proteins in the tissues, resulting in coagulation and closure of tiny blood vessels. This shortens the duration of the procedure by minimizing blood loss and lowering bleeding from the location of the peritoneal rupture. In contrast, spon-

taneous release of the peritoneum may result in ongoing bleeding from the rupture, lengthening the time needed for surgery [31].

Bipolar coagulation is a quick and simple technique that does not require suturing. It reduces operation complexity without compromising efficacy. In conclusion, bipolar coagulation is a simple and effective method for managing peritoneal rupture during TEP inguinal hernia repair with significant benefits over the spontaneous release of the peritoneum [32]; so, it should be considered as the first-line treatment option for this intraoperative complication.

Funding

None

Conflict of interests

The authors declared that they have no competing interests.

Authors' ORCID

- Bixiang Zheng (BZ): 0000-0002-8546-7472
- Xiaobin Luo (XL): 0000-0002-1986-5819
- Changdong Wang (CW): 0000-0001-8944-1280
- Rendong Zheng (RZ): 0000-0003-4912-6758
- Xiaofeng Yang (XY): 0000-0002-4334-2356

Contribution of authors

BZ played a crucial role in study design and conducted expertise in laparoscopic surgery. XL provided the statistical analysis and critical insights. CW contributed to the literature review and information synthesis. RZ conducted data collection and data analysis. XY contributed to the manuscript.

REFERENCES

1. **Rao G, Rao A, Pujara N, Pujara P, Patel S.** Prevalence of hernia among fishermen population in kutch district. India. National J Integrated Res Med 2015;6(4):44-51.
2. **Öberg S, Andresen K, Rosenberg J**. Etiology of inguinal hernias: A comprehensive review. Front Surg 2017;4:52.
3. **Köckerling F, Simons MP**. Current concepts of inguinal hernia repair. Visceral Medicine 2018;34(2):145-150. *https://doi.org/10.1159/000487278.*
4. **Warsinggih, Ulfandi D, Fajar A, Faruk M**. Factors associated with TNF-alpha levels in patients with indirect inguinal hernia: A cross-sectional study. Ann Med Surg 2022;78:103858. *https://doi.org/10.1016/j.amsu.2022.103858.*
5. **Elango S, Perumalsamy S, Ramachandran K, Vadodaria K**. Mesh materials and hernia repair. BioMed 2017;7(3):16. *https://doi.org/ 10.1051/bmdcn/2017070316.*
6. **Wozniewska P, Golaszewski P, Pawluszewicz P, Hady HR**. Inguinal hernias–the review of literature. Post N Med 2018;31(5):287-291.
7. **Kumar S**. Analysis of cases of inguinal hernia patients visited to department of surgery: A clinical study. IJBAMR 2012;1: 369-373.
8. **Heniford BT**. Hernia handbook. 2015.
9. **Shakil A, Aparicio K, Barta E, Munez K.** Inguinal hernias: Diagnosis and management. Am Fam Physician 2020;102(8):487-492.
10. **Taşdelen HA.** The extended-view totally extraperitoneal (ETEP) approach for incisional abdominal wall hernias: Results from a single center. Surg Endosc 2022;36(6):4614-4623. *https://doi.org/10.1007/s00464-021-08995-w.*
11. **Triantafyllidis I**. Totally extraperitoneal approach (TEP) for inguinal hernia repair. 2022. *Doi: 10.5772/intechopen.104638*
12. **Gurusamy KS, Cassar Delia E, Davidson BR**. Peritoneal closure versus no peritoneal closure for patients undergoing non-obstetric abdominal operations. Cochrane Database Syst Rev 2013; (7). *https://doi.org/10.1002/14651858.CD010424.pub2.*

13. **Wales E, Holloway S.** The use of prosthetic mesh for abdominal wall repairs: A semi-systematic-literature review. Int Wound J 2019;16(1):30-40. *https://doi.org/10.1111/iwj.12977.*
14. **Bamigboye AA, Hofmeyr GJ.** Closure versus non-closure of the peritoneum at caesarean section: Short -and long- term outcomes. Cochrane Database Syst Rev 2014; (8). *https://doi.org/10.1002/14651858.CD000163.pub2.*
15. **Elkins TE, Stovall T, Warren J, Ling FW, Meyer NL.** A histological evaluation of peritoneal injury and repair: Implications for adhesion formation. Obstet Gynecol 1987;70(2):225-228.
16. **Gemer SD, Dorfman D, Cardozo J, Rivas L, Mora la Cruz E, Marcano C, Lombardi M.** Description of the spontaneous repair of the internal rectus abdominis muscle sheath and peritoneum in dogs. Surgical implications. Revista Científica FCV-LUZ 2000;10(1):42-46.
17. **Aiolfi A, Cavalli M, Del Ferraro S, Manfredini L, Lombardo F, Bonitta G, Bruni PG, Panizzo V, Campanelli G, Bona D.** Total extraperitoneal TEP) versus laparoscopic transabdominal preperitoneal (TAPP) hernioplasty: Systematic review and trial sequential analysis of randomized controlled trials. Hernia 2021;25(5):1147-1157. *https://doi.org/10.1007/s10029-021-02407-7.*
18. **Molegraaf M, Lange J, Wijsmuller A.** Uniformity of chronic pain assessment after inguinal hernia repair: A critical review of the literature. Eur Surg Res 2017;58(2):1-19.
19. **Xu Q, Zhang G, Li L, Xiang F, Qian L, Xu X, Yan Z.** Non-closure of the free peritoneal flap during laparoscopic hernia repair of lower abdominal marginal hernia: A retrospective analysis. Front Surg 2021;8. *https://doi.org/ 10.3389/fsurg.2021.748515.*
20. **Koning GG, Wetterslev J, Van Laarhoven CJ, Keus F.** The totally extraperitoneal method versus lichtenstein's technique for inguinal hernia repair: A systematic review with meta-analyses and trial sequential analyses of randomized clinical trials. PloS One 2013;8(1): e52599. *https://doi.org/10.1371/journal.pone.0052599.*
21. **Meyer A, Blanc P, Balique JG, Kitamura M, Juan RT, Delacoste F, Atger J.** Laparoscopic totally extraperitoneal inguinal hernia repair: Twenty-seven serious complications after 4565 consecutive operations. Rev Col Bras Cir 2013;40:32-36.
22. **Wakasugi M, Nakahara Y, Hirota M, Matsumoto T, Kusu T, Takemoto H, Takachi K, Oshima S**. Efficacy of single-incision laparoscopic totally extraperitoneal inguinal hernia repair for overweight or obese patients. Surg Laparosc Endosc Percutan Tech 2019;29:200–202. *https://doi.org/10.1097/SLE.0000000000000628.*
23. **Asgari Z, Rouholamin S, Hosseini R, Sepidarkish M, Hafizi L, Javaheri A.** Comparing ovarian reserve after laparoscopic excision of endometriotic cysts and hemostasis achieved either by bipolar coagulation or suturing: A randomized clinical trial. Arch Gynecol Obstet 2016;293(5):1015-1022. *https://doi.org/10.1007/s00404-015-3918-4.*
24. **Kostov GG, Dimov RS.** Total extra peritoneal inguinal hernia repair: A single-surgeon preliminary findings report. Folia Med (Plovdiv) 2021;63:183-188.
25. **Camerlo A, Magallon C, Vanbrugghe C, Chiche L, Gaudon C, Rinaldi Y, Fara R.** Robotic hepatic parenchymal transection: A two-surgeon technique using ultrasonic dissection and irrigated bipolar coagulation. J Robot Surg 2021;15(4):539-546. *https://doi.org/10.1007/s11701-020-01138-8.*
26. **Ciavattini A, Clemente N, Delli Carpini G, Saccardi C, Borgato S, Litta P.** Laparoscopic uterine artery bipolar coagulation plus myomectomy vs traditional laparoscopic myomectomy for "large" uterine fibroids: Comparison of clinical efficacy. Arch Gynecol Obstet 2017;296(6):1167-1173. *https://doi.org/10.1007/s00404-017-4545-z.*
27. **Liang J, Xing, H, Chang Y.** Thermal damage width and hemostatic effect of bipolar electrocoagulation, ligasure, and ultracision

techniques on goat mesenteric vessels and optimal power for bipolar electrocoagulation. BMC Surgery 2019;19(1):1-7. *https://doi.org/10.1186/s12893-019-0615-4.*

28. **Oguz H, Karagulle E, Turk E, Moray G.** Comparison of peritoneal closure techniques in laparoscopic transabdominal preperitoneal inguinal hernia repair: A prospective randomized study. Hernia 2015;19(6):879-885. *https://doi.org/10.1007/s10029-015-1431-0.*
29. **Awad Osama G, Abdel-Naby Hafez MA, Hasan MM.** Use of bipolar coagulation diathermy for the management of recurrent pediatric epistaxis. Egy J Otolaryngol 2016;32(1):7-12. *https://doi.org/10.4103/1012-5574.175795.*
30. **Seehofer D, Mogl M, Boas-Knoop S, Unger J, Schirmeier A, Chopra S, Eurich D.** Safety and efficacy of new integrated bipolar and ultrasonic scissors compared to conventional laparoscopic 5-mm sealing and cutting instruments. Surg Endosc 2012;26:2541-2549. *https://doi.org/10.1007/s00464-012-2229-0.*
31. **Pogorelić Z, Katić J, Mrklić I, Jerončić A, Šušnjar T, Jukić M, Vilović K, Perko Z.** Lateral thermal damage of mesoappendix and appendiceal base during laparoscopic appendectomy in children: Comparison of the harmonic scalpel (ultracision), bipolar coagulation (ligasure), and thermal fusion technology (miseal). J Surg Res 2017;212:101-107. *https://doi.org/10.1016/j.jss.2017.01.014.*
32. **Mathew KG, Pokhrel G**. Closing peritoneal tear during laparoscopic inguinal hernia repair: Simple and effective technique. Hernia 2020;24(5):1121-1124. *https://doi.org/10.1007/s10029-020-02237-z.*

Invest Clin 64(4): 505 - 512, 2023 https://doi.org/10.54817/IC.v64n4a7

Nuclear and cytoplasmic expressions of the receptor for advanced glycation end products (RAGE) in the rat central nervous system.

Jesús Mosquera-Sulbarán[1], Adriana Pedreáñez[2], Yenddy Carrero[1] and Catherina Peña[1]

[1] Instituto de Investigaciones Clínicas "Dr. Américo Negrette", Facultad de Medicina, Universidad del Zulia, Maracaibo, Venezuela.
[2] Cátedra de Inmunología, Escuela de Bioanálisis, Facultad de Medicina, Universidad del Zulia, Maracaibo, Venezuela.

Keywords: RAGE; ligands; nucleus; cerebral cortex; cerebellum.

Abstract. The receptor for advanced glycation end products (RAGE) is a transmembrane protein involved in the induction of inflammatory processes and oxidative stress after interacting with its ligands on the cell surface. Localization on the cell surface is necessary for interaction with the ligands. This study aimed to determine the expression of RAGE in different parts of the normal rat brain and cerebellum using the immunofluorescence technique. Several cerebral cortex layers (molecular/granular layers: M/GL; pyramidal layer: PL) and the hypothalamus were analyzed, as well as the molecular layer (CML) and the granular layer (CGL) of the cerebellum. Cells with RAGE-positive nuclei were generally observed in the brain's cerebral cortex and cerebellum**.** In the M/GL, cells with different degrees of positivity in the nucleus and cytoplasm accompanied by RAGE-positive material in the adjacent extracellular space were observed, and RAGE-positive material in the neuropile. Pyramidal neurons presenting various degrees of nuclear RAGE-positive material budding and cells with different degrees of nuclear and cytoplasmic positivity were observed in PL. The hypothalamus showed a high number of cells with RAGE-positive granules adjacent to the nucleus and in the cytoplasm; nuclei remained negative. Many positive nuclei were observed in CML; they were scarce in CGL. These data suggest the storage of RAGE at the nuclear and cytoplasmic levels in healthy rats and hypothesize the possible translocation of this molecule to the cell surface in pathological conditions.

Corresponding autor. Jesús Alberto Mosquera-Sulbarán. Instituto de Investigaciones Clínicas "Dr. Américo Negrette", Facultad de Medicina, Universidad del Zulia, Maracaibo, Venezuela. E-mail: mosquera99ve@yahoo.com

Expresión nuclear y citoplasmática del receptor para compuestos de glicosilación avanzada en el sistema nervioso central de la rata.

Invest Clin 2023; 64 (4): 505 – 512

Palabras clave: RAGE; ligandos; núcleo; corteza cerebral; cerebelo.

Resumen. El receptor para compuestos de glicosilación avanzada (RAGE) es una proteína transmembrana involucrada en la inducción de procesos inflamatorios y en el estrés oxidativo después de su interacción con sus ligandos en la superficie celular. La localización de este receptor en la superficie celular es necesaria para su interacción con sus ligandos. El objetivo de este estudio fue determinar la expresión de RAGE en las diferentes partes del cerebro y cerebelo de la rata normal. Mediante la utilización de técnicas de inmunofluorescencia se analizaron varias capas de la corteza cerebral (capas molecular/granular: CM/G; capa piramidal: CP) y el hipotálamo. Las capas molecular (CMC) y la capa granular (CGC) del cerebelo fueron también analizadas. Se observaron células con el núcleo positivo para RAGE tanto en cerebro como cerebelo. En CM/G se apreciaron células con diversos grados de positividad para RAGE acompañadas de material positivo para RAGE en el espacio extracelular adyacente y en la neuropila. En la CP se observaron neuronas piramidales presentando diversos grados de gemación de material nuclear positivo para RAGE y diversas células con diferentes grados de positividad nuclear y citoplasmática. En el hipotálamo se apreciaron gran número de células expresando gránulos positivos a RAGE tanto adyacente al núcleo como en el citoplasma; el núcleo permaneció negativo. Alto número de núcleos positivos se apreciaron en la capa CMC a diferencia de la capa CGC del cerebelo. Estos hallazgos sugieren el almacenamiento del RAGE en el núcleo y en el citoplasma en la rata normal e hipotetizan una posible translocación de esta molécula a la superficie celular en condiciones patológicas.

Received: 26-11-2023 Accepted: 06-08-2023

INTRODUCTION

The receptor for advanced glycation end products (RAGE) is a transmembrane protein and a multireceptor belonging to the immunoglobulin superfamily, expressed on the cell surface and capable of binding to various ligands, inducing cell activation, cell dysfunction, and tissue damage [1, 2]. RAGE has been implicated in various pathophysiological processes such as neurodegenerative diseases and infectious processes [1-3]. After RAGE binds to its ligand, pro-inflammatory processes increase with the induction of pro-inflammatory cytokines and oxidative stress, determining a vicious circle of inflammation mediated by the overexpression of the nuclear transcription factor kB (NF-kB) that leads to cell damage [1,3]. Traditionally, the interaction of RAGE with its ligands at the cell surface level inducing intracellular signals leading to pro-inflammatory processes has been reported [4,

[5]. The interaction of RAGE with its ligands in the central nervous system is of paramount importance in the induction of neurodegenerative diseases [3, 6-8]; however, there is little information about the location of RAGE in central nervous system cells in non-pathological conditions. The present study is focused on determining by immunohistochemical methods the location of RAGE in the rat central nervous system under healthy conditions.

MATERIAL AND METHODS

This study used healthy male Sprague-Dawley rats (weight 150 to 200 g) (N=10). All rats had unlimited access to tap water and food. All animals were euthanized, and samples from rat cerebrum (including the hypothalamus) and cerebellum were embedded in Tissue-Tek (Miles, Inc, Diagnostic Division, Kankakee, Illinois, United States), frozen in acetone and dry ice, and stored at -70 ºC until use. Cryostat sections (4 μm) from samples were treated with a rabbit anti-rat RAGE antibody (5μg/mL: ab3611; Abcam, Cambridge, United Kingdom) to analyze RAGE brain expression. Rabbit immunoglobulin G (IgG) in tissues was localized by a secondary rhodamine-conjugated goat anti-rabbit IgG at 5μg/mL (Sigma-Aldrich, St. Louis, Missouri, USA). Antibody against a nonrelevant antigen or normal rabbit serum was used as the negative control. Sections were mounted in a solution of p-phenylenediamine in phosphate-buffered saline–glycerol and viewed under an epifluorescent microscope (Axioskop, Zeiss, Wetzlar, Germany). Positive cells were expressed as the number of cells per 0.0625 μ^2 from 20 randomly selected fields of the brain or cerebellum. Experiments were performed according to the ethical guidelines of the committee of bioethical and biosecurity of FONACIT (Caracas, Venezuela) following the Guide for the Care and Use of Laboratory Animals (National Institutes of Health Publication No. 8023, revised 1978) and the committee of bioethics of the Universidad del Zulia School of Medicine.

Statistical analysis was performed using GraphPad Prism, version 7.0 (GraphPad Software, San Diego, USA). Measurement data with normal distribution is represented as mean ± standard deviation. For continuous variables that were normally distributed, differences between groups were determined by ANOVA and the posttest of Bonferroni. A p-value < 0.05 was considered to be statistically significant.

RESULTS

The analysis of different rat cerebrum and cerebellum areas showed high reactivity to the anti-RAGE antibody in several areas. At the level of the cerebral cortex, positive cells were observed in the molecular/granular layer (M/GL) and the pyramidal layer (PL). Positive cells were seen in the cerebellum in the molecular layer (CML) and less frequently in the cerebellar granular layer (CGL). A high number of positive cells was observed in the hypothalamus (Fig. 1). Histological analysis showed numerous cells with high nuclear reactivity to the anti-RAGE antibody in M/GL (Fig. 2). Likewise, cells with negative or scarcely positive nuclei were found accompanied by cytoplasmic and adjacent extracellular positive reactivity to RAGE, simulating a comet.

Interestingly, extracellular RAGE-positive areas without cell presence were observed (Fig. 3). Pyramidal neurons with highly positive nuclei and positive glial cells were observed in PL (Figs. 4 and 5). RAGE-positive nuclei presenting structures resembling nuclear buds in pyramidal neurons were observed (Fig. 5). The cells of the hypothalamus showed a high frequency of cytoplasmic RAGE-positive granules but no nuclear positivity (Figs. 1 and 6).

Nuclear expression of RAGE in the cerebellum was observed mainly in the CML, with a low frequency of positive nuclei in CGL; however, some cells showed granular cytoplasmic positivity in this layer. Purkinje cells were found to be negative (Figs. 1 and 7).

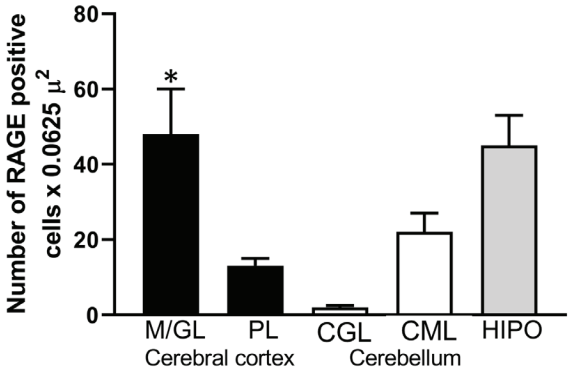

Fig. 1. Expression of the receptor for advanced glycation end products (RAGE) in the rat central nervous system. High nuclear expression of RAGE was observed in the molecular/granular layer of cerebral cortex and in the molecular layer of the cerebellum. Cells from the hypothalamus did not express nuclear RAGE but a high number expressed cytoplasmic RAGE in a granular form. M/GL: molecular/granular layer; PL: pyramidal layer; CGL: cerebellar granular layer; CML: cerebellar molecular layer; HIPO: hippocampus. * $p<0.01$ vs. PL, CGL, CML.

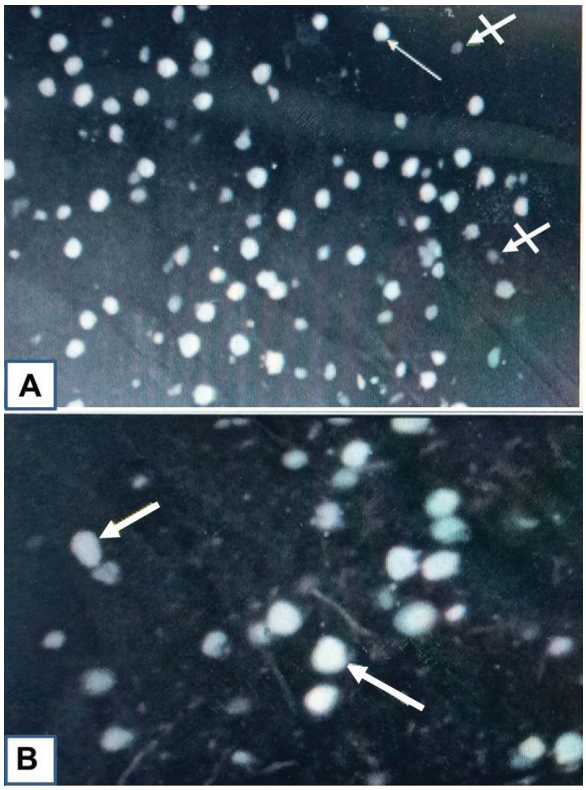

Fig. 2. Expression of the receptor for advanced glycation end products (RAGE) in the molecular/granular layer of the cerebral cortex. A) Panoramic view where a large number of positive nuclei can be observed. B) Detail. Arrows: positive nuclei. Cross arrows: negative nuclei. Original magnification: A: x600; B: x1000.

DISCUSSION

In this study, the expression of RAGE in the rat central nervous system was mainly limited to the cell nucleus and cytoplasm. Functionally, RAGE is expressed on the cell surface, where it interacts with various ligands to activate intracellular pathways that produce a pro-inflammatory and oxidative stress state [1-3, 6-8].

The presence of this receptor within the cell nucleus observed in this study suggests a nuclear function or represents a storage site for a subsequent trajectory of this receptor from the nucleus to the cell surface to exert its functions. Previous studies have shown the passage of intranuclear molecules to the cytoplasm [9-13], suggesting a possible cell surface expression pathway for RAGE. In this regard, the immunohistochemical findings of this report show cerebral cells showing decreased expression of nuclear RAGE accompanied by increased cytoplasm expression and adjacent extracellular RAGE-positive material. In addition, pyramidal neurons showed budding of RAGE-positive nuclear material, and cells with cytoplasm RAGE-positive granules were observed, suggesting a possible nuclear-to-cytoplasmic pathway.

The presence of RAGE in the nucleus suggests its nuclear localization prior to its synthesis, possibly as a storage site, as occurs with the non-histone chromosomal proteins "high mobility group" (HMG) that are present in the cell nucleus bound to DNA [10, 12] and perform functions such as determination of nucleosomal structure and stability, and binding of transcription factors to their cognate DNA sequences [14]. HMG can be localized in the nucleus, cytoplasm, and the extracellular space during some pathological processes where it can interact with

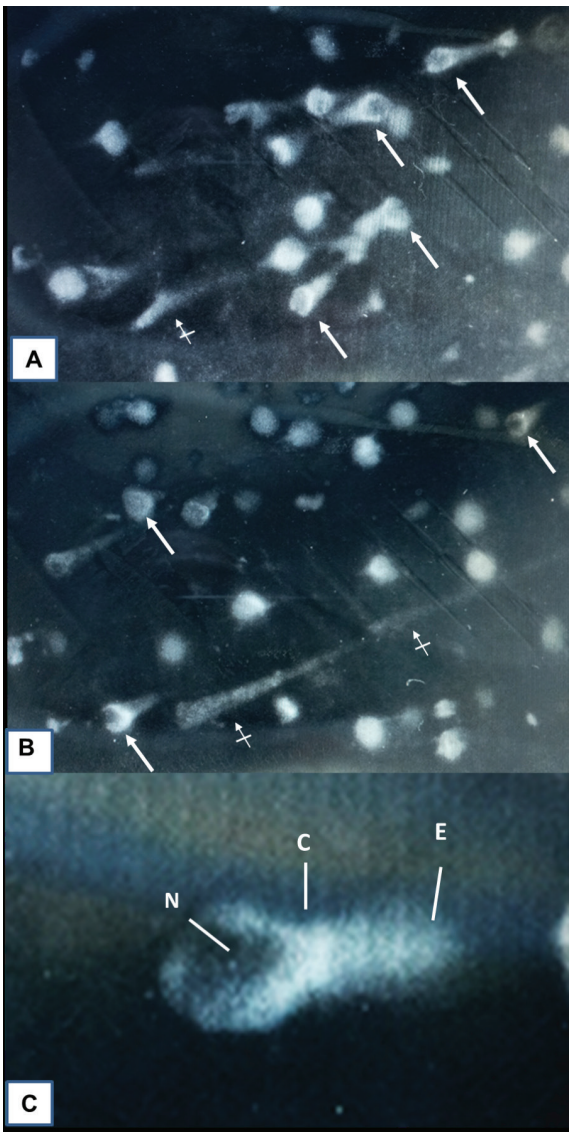

Fig. 3. Expression of the receptor for advanced glycation end products (RAGE) in the molecular/granular layer of the cerebral cortex. A and B) Cells with different degrees of nuclear and cytoplasmic positivity to RAGE (arrows). RAGE-reactive extracellular material is seen in the neuropile (crossed arrow). C) Detail of cell showing weak nuclear RAGE positivity and high positivity for cytoplasmic. Note the presence of RAGE-positive material adjacent to the cell. N: nucleus; C: cytoplasm; E: extracellular space. Original magnification: A and B: x600; C: x1000.

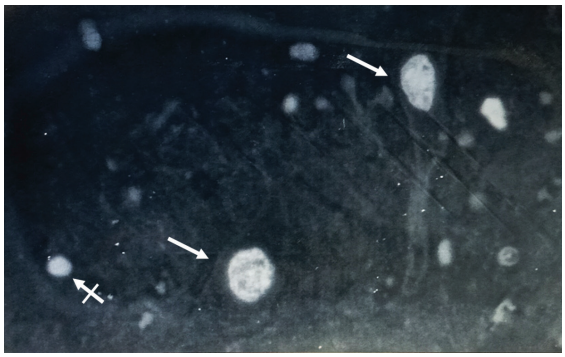

Fig. 4. Expression of the receptor for advanced glycation end products (RAGE) in the pyramidal layer of the cerebral cortex. Pyramidal neurons with high nuclear positivity for RAGE are appreciated. Arrows: Positive neurons. Cross arrow: probably a positive glial cell nucleus. Original magnification: x1000.

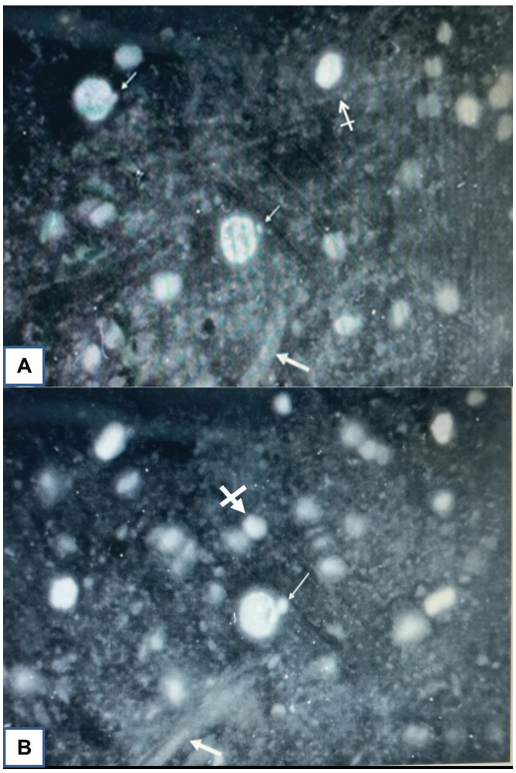

Fig. 5. Expression of the receptor for advanced glycation end products (RAGE) in the pyramidal layer of the cerebral cortex. A) Nuclear RAGE-positive pyramidal neurons showing nuclear budding (small arrows). Cross arrow: positive neuron without nuclear budding. Thick arrow: pyramidal neuron dendrite. B) Nuclear RAGE-positive pyramidal neuron showing nuclear budding (small arrow). Cross arrow: positive glial cell nucleus. Thick arrow: neuron axon. Original magnification: x1000.

RAGE [9, 11, 13]. There is no information available on the presence of RAGE in the nucleus, and possibly the expression of nuclear RAGE on the cell surface obeys mechanisms similar to those of HMG. Binding to DNA may represent the storage mechanism of RAGE in the nucleus. In this regard, RAGE's ability to bind to DNA [15] and its role in participating in DNA double-strand repair processes [16] has been reported. Another point of analysis is the intranuclear role of RAGE and HMG since the latter represents one of the RAGE's ligands [17].

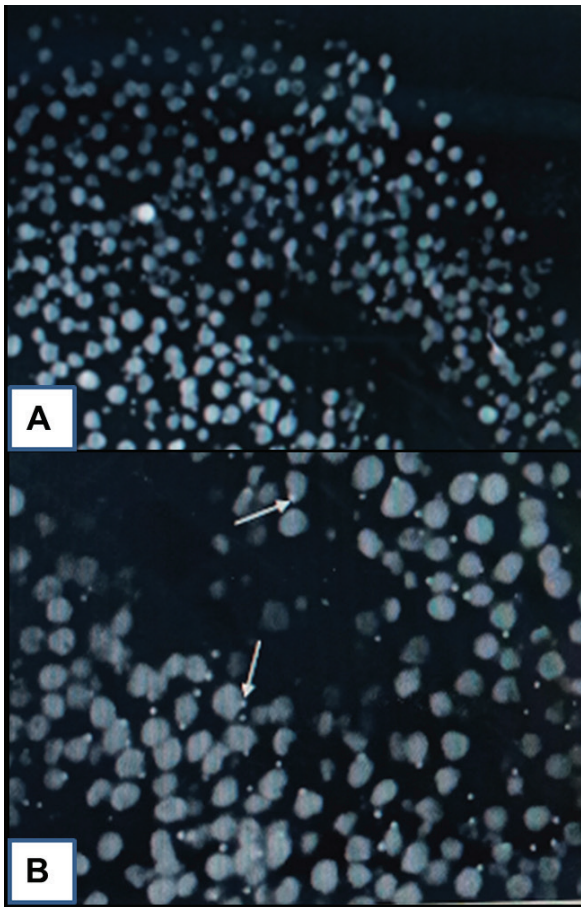

Fig. 6. Expression of the receptor for advanced glycation end products (RAGE) in hippocampus. A) Overview of hypothalamic cells, the majority of which are positive for cytoplasmic granular expression of RAGE. B) Hippocampal cells presenting positive RAGE granules adjacent to the nucleus or in the cytoplasm (arrows). Original magnification: A: x200; B:x600.

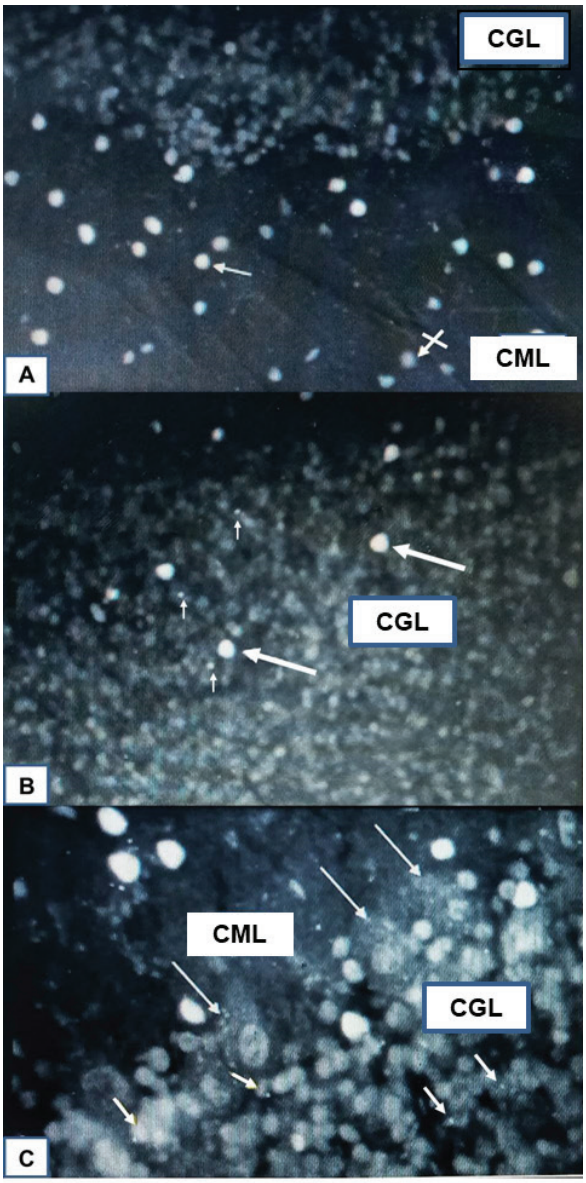

Fig. 7. Expression of the receptor for advanced glycation end products (RAGE) in the cerebellum of normal rats. A) High number of cells expressing RAGE-positive nuclei (arrow) in the molecular layer, compared to low number in the granular layer. Arrow: positive nucleus. Cross arrow: negative nucleus. B) Scarce presence of RAGE-positive nuclei (thick arrows) and RAGE-positive granules (small arrows) in cells of the granular layer. C) Scarce presence of RAGE-positive nuclei and RAGE-positive granules (small arrows) in the granular layer. Negativity was observed in Purkinje cells (arrows). Cerebellar molecular layer: CML. Cerebellar Granular layer: CGL. A and B: x200; C: x600.

The expression of RAGE in the central nervous system makes this tissue vulnerable to inflammatory processes. The role of RAGE in neurodegenerative processes, neuroinflammation, Parkinson's, and Alzheimer's diseases, among other encephalopathies, has been reported [1, 3, 18, 19]. Cerebral and cerebellar nuclear and cytoplasmic RAGE could play a role in these pathologies. Perhaps the factors that induce those pathologies induce the passage of nuclear and cytoplasmic RAGE to the cell surface.

In conclusion, this report demonstrates the presence of RAGE as a nuclear protein and its cytoplasmic expression in the cerebrum and cerebellum of normal rats. These data highlight possible studies on the translocation of RAGE from the nucleus to the cell surface, on nuclear functions, and on the interaction of RAGE with HMG in the nucleus.

Conflict of interest

Authors report no conflict of interest

Funding statement

This investigation has no financial support.

Author's ORCID

- Jesús A Mosquera-Sulbarán (JMS): 0000-0002-1496-5511
- Adriana Pedreáñez (AP): 0000-0002-3937-0469
- Yenddy Carrero (YC): 0000-0003-4050-4468
- Caterina Peña (CP): 0009-0009-2824-2566

Author Contributions

JMS: conceptualization, methodology, data curation, writing - original draft, writing - review & editing. AP: methodology, software, formal analysis, writing - review & editing. YC: resources, conceptualization, methodology, writing - review & editing. CP: methodology, software, formal analysis.

REFERENCES

1. **Mosquera JA.** Role of the receptor for advanced glycation end products (RAGE) in inflammation. Review. Invest Clin 2010; 51(2): 257-268.
2. **Muñoz N, Pedreañez A, Mosquera J.** Angiotensin II induces increased myocardial expression of Receptor for Advanced Glycation End products, monocyte/macrophage infiltration and circulating endothelin-1 in rats with experimental diabetes. Can J Diabetes 2020; 44(7): 651-656. *https://doi: 10.1016/j.jcjd.2020.03.010.*
3. **Tóbon-Velasco JC, Cuevas E, Torres-Ramos MA.** Receptor for AGEs (RAGE) as mediator of NF-kB pathway activation in neuroinflammation and oxidative stress. CNS. Neurol Disord Drug Targets 2014; 13(9): 1615-1626. *https://doi: 10.2174/1871527313666140806144831.*
4. **Serratos IN, Castellanos P, Pastor N, Millán-Pacheco C, Rembao D, Pérez-Montfort R, Cabrera N, Reyes-Espinosa F, Díaz-Garrido P,** López-Macay **A, Martínez-Flores K, López-Reyes A, Sánchez-García A, Cuevas E, Santamaria A.** Modeling the interaction between quinolinate and the Receptor for Advanced Glycation End Products (RAGE): relevance for early neuropathological processes. PLoS ONE 2015; 10(3): e0120221. *https://doi.org/10.1371/journal.pone.012022.*
5. **Hudson BI, Kalea AZ, Arriero MM, Harja E, Boulanger E, D'Agati V, Schmid AM.** Interaction of the RAGE cytoplasmic domain with Diaphanous-1 is required for ligand-stimulated cellular migration through activation of Rac1 and Cdc42. J Biol Chem 2008;283(49): 34457-34468. *https://doi.org/10.1074/jbc.M801465200.*
6. **Culig L, Chu X, Bohr VA.** Neurogenesis in aging and age-related neurodegenerative diseases. Ageing Res Rev 2022; 78:101636. *https://doi: 10.1016/j.arr.2022.101636.*

7. **Brahadeeswaran S, Sivagurunathan N, Calivarathan L.** Inflammasome signaling in the aging brain and age-related neurodegenerative diseases. Mol Neurobiol 2022; 59(4):2288-2304. *https://doi: 10.1007/s12035-021-02683-5.*
8. **Chellappa RC, Palanisamy R, Swaminathan K.** RAGE isoforms, its ligands and their role in pathophysiology of Alzheimer's Disease. Curr Alzheimer Res 2020; 17(14):1262-1279. https:// *doi: 10.2174/1567205018666210218164246.*
9. **Fan H, Tang HB, Chen Z, Wang HQ, Zhang L, Jiang Y, Li T, Yang CF, Wang XY, Li X, Wu SX, Zhang GL.** Inhibiting HMGB1-RAGE axis prevents pro-inflammatory macrophages/microglia polarization and affords neuroprotection after spinal cord injury. J Neuroinflammation 2020; 17(1): 295. *https://doi: 10.1186/s12974-020-01973-4.*
10. **Ge Y, Huang M, Yao YM**. The Effect and regulatory mechanism of high mobility Group Box-1 Protein on immune cells in inflammatory diseases. Cells 2021; 10(5): 1044. *https://doi.org/10.3390/ 10.3390/cells10051044.*
11. **Chen R, Kan R, Tang D.** The mechanism of HMGB1 secretion and release. Exp Mol Med 2022; 54(2): 91–102. *https://doi: 10.1038/s12276-022-00736-w.*
12. **Wang H.** Regulation of HMGB1 Release in Health and Diseases. Cells 2022; 12(1): 46. *https://doi: 10.3390/cells12010046.*
13. **Wang S, Yi Z.** HMGB1 in inflammation and cancer. J Hematol Oncol 2020; 13(1): 116. *https://doi:10.1186/s13045-020-00950-x.*
14. **Bustin M.** Regulation of DNA-dependent activities by the functional motifs of the high-mobility-group chromosomal proteins. Mol Cell Biol 1999; 19(8): 5237–5246. *https://doi: 10.1128/MCB.19.8.5237.*
15. **Sirois CM, Jin T, Miller A, Bertheloot D, Nakamura H, Horvath GL, Mian A, Jiang, J, Schrum J, Bossaller L, Pelka K, Garbi N, Brewah Y, Tian J, Chang, C, Chowdhury PS.** RAGE is a nucleic acid receptor that promotes inflammatory responses to DNA. J Exp Med 2013; 210(11): 2447–2463. *https://doi: 10.1084/jem.20120201.*
16. **Tsai KYF, Tullis B, Breithaupt KL, Fowers R, Jones N, Grajeda S, Arroyo JA.** A role for RAGE in DNA double strand breaks (DSBs) detected in pathological placentas and trophoblast cells. Cells 2021; 10(4): 857. *https://doi: 10.3390/cells10040857.*
17. **Lee BW, Chae HY, Kwon SJ, Park SY, Ihm J, Ihm SH.** RAGE ligands induce apoptotic cell death of pancreatic β-cells via oxidative stress. Int J Mol Med 2010; 26(6): 813-818. *https://doi.org/10.3892/ijmm_00000529.*
18. **Byun K, Yoo YC, Son M, Lee J, Jeon GB, Park YM, Salekdeh G, Lee B**. Advanced glycation end-products produced systemically and by macrophages: A common contributor to inflammation and degenerative diseases. Pharmacol Ther 2017; 177:44-55. *https://doi:10.1016/j.pharmthera.2017.02.030.*
19. **Sathe K, Maetzler W, Lang JD, Mounsey RB, Fleckenstein C, Martin HL, Schulte C, Mustafa S, Synofzik M, Vukovic Z, Itohar, S, Berg D, Teismann P.** S100B is increased in Parkinson's disease and ablation protects against MPTP-induced toxicity through the RAGE and TNF-α pathway. Brain 2012; 135(Pt 11): 3336-3347. *https://doi: 10.1093/brain/aws250.*

Invest Clin 64(4): 513 - 523, 2023 https://doi.org/10.54817/IC.v64n4a8

Stress-associated ovarian damage, infertility, and delay in achieving pregnancy and treatment options.

Gulsah Aynaoglu Yildiz[1], Omer Erkan Yapca[2], Kemal Dinc[3], Cebrail Gursul[4], Betul Gundogdu[5], Mehmet Aktas[6], Zeynep Suleyman[7], Seval Bulut[7] and Halis Suleyman[8]

[1]Department of Perinatology, Etlik Zubeyde Hanim Maternity and Women's Health Teaching and Research Hospital, Ankara-Turkey.
[2]Department of Obstetrics and Gynaecology, Faculty of Medicine, Ataturk University, Erzurum-Turkey.
[3]Department of Obstetrics and Gynaecology, Faculty of Medicine, Erzincan Binali Yildirim University, Erzincan-Turkey.
[4]Department of Physiology, Faculty of Medicine, Erzincan Binali Yildirim University, Erzincan-Turkey.
[5]Department of Pathology, Faculty of Medicine, Ataturk University, Erzurum-Turkey.
[6]Department of Biochemistry, Faculty of Medicine, Erzincan Binali Yildirim University, Erzincan, Turkey.
[7]Department of Pharmacology, Health Sciences Institute, Erzincan Binali Yildirim University, Erzincan, Turkey.
[8]Department of Pharmacology, Faculty of Medicine, Erzincan Binali Yildirim University, Erzincan, Turkey.

Keywords: ovarian damage; sertraline; cerebrolysin; stress; rats.

Abstract. Many types of stress, including psychological stress, negatively affect reproductive health. This study aimed to investigate the effects of sertraline (a selective serotonin reuptake inhibitor), cerebrolysin (neuroprotective/neurotrophic), and a combination of both against stress-induced ovarian damage, infertility and pregnancy delay in female rats. The rats were divided into five groups (n=14/each group) as healthy (HG), stress control (StC), stress+sertraline (SS), stress+cerebrolysin (SC), and stress+sertraline+cerebrolysin (SSC). To induce stress, animals (except the HG) were kept in a supine position with their forelimbs and hindlimbs (FIM) tied for one hour. Then, sertraline (20mg/kg) was given orally to the SS. Cerebrolysin (2.5ml/kg) was injected into the SC subcutaneously. Sertraline+cerebrolysin was administered to SSC with the same methods and doses. FIM and drug administration continued for 30 days. Six rats from each

Corresponding Author. Halis Suleyman. Department of Pharmacology, Faculty of Medicine, Erzincan Binali Yildirim University, Erzincan, Turkey, Post code: 24100, Phone: +90 4462261818, Fax: +90 5309211909, E-mail: halis.suleyman@gmail.com

group were euthanized with high-dose anesthesia, right and left ovarian tissues were removed, and tissues were examined biochemically and histopathologically. The remaining rats were taken for breeding. Exposure to stress in rats caused an increase in malondialdehyde (MDA), tumor necrosis factor-alpha (TNF-α), interleukin-1β (IL-1β), and interleukin-6 (IL-6) levels and a decrease in total glutathione (tGSH). Stress was related to histopathological damage, infertility, and delayed birth. The sertraline and cerebrolysin combination was the most effective in preventing these changes, with sertraline and cerebrolysin alone in second and third places, respectively. Regarding efficacy, selective serotonin reuptake inhibitors (SSRIs) and related drugs may be beneficial in treating stress-related ovarian damage, infertility, and delay in pregnancy.

Daño ovárico, infertilidad y retraso en la concepción relacionados con el estrés y opciones de tratamiento.

Invest Clin 2023; 64 (4): 513 – 523

Palabras clave: daño ovárico; sertralina; cerebrolisina; estrés; ratas.

Resumen. Muchos tipos de estrés, incluido el estrés psicológico, afectan negativamente a la salud reproductiva. El objetivo de este estudio fue investigar los efectos de la sertralina (un inhibidor selectivo de la recaptación de serotonina), la cerebrolisina (neuroprotector/neurotrófico) y una combinación de ambos contra el daño ovárico, la infertilidad y el retraso del embarazo inducido por el estrés en ratas hembra. Las ratas se dividieron en cinco grupos (n=14/cada grupo), como sanas (HG), control de estrés (StC), estrés+sertralina (SS), estrés+cerebrolisina (SC) y estrés+sertralina+cerebrolisina (SSC) . Para inducir el estrés, los animales (excepto el HG) se mantuvieron en posición supina con las extremidades anteriores y posteriores (FIM) atadas durante una hora. Luego, se administró sertralina (20 mg/kg) por vía oral al grupo SS. Cerebrolysin (2,5 mL/kg) se inyectó al grupo SC por vía subcutánea. Se administró sertralina+cerebrolisina al grupo SSC con los mismos métodos y dosis. La FIM y la administración de fármacos continuaron durante 30 días. Se sacrificaron seis ratas de cada grupo con anestesia de dosis alta, se extirparon los tejidos de los ovarios derecho e izquierdo y se examinaron bioquímica e histopatológicamente. Las ratas restantes se tomaron para reproducción. La exposición al estrés en ratas provocó un aumento de los niveles de malondialdehído (MDA), factor de necrosis tumoral alfa (TNF-α), interleucina-1β (IL-1β) e interleucina-6 (IL-6) y una disminución del glutatión total (tGSH). El estrés se relacionó con daño histopatológico, infertilidad y retraso en el parto. La combinación de sertralina y cerebrolisina fue la más efectiva para prevenir estos cambios, con sertralina y cerebrolisina solas en segundo y tercer lugar, respectivamente. Los inhibidores selectivos de la recaptación de serotonina (ISRS) y los medicamentos relacionados pueden ser beneficiosos en el tratamiento del daño ovárico relacionado con el estrés, la infertilidad y el retraso en el embarazo.

Received: 13-05-2023 Accepted: 08-08-2023

INTRODUCTION

One of the fundamental reasons for psychological stress is socioeconomic factors[1]. It has been known that chronic stress is related to numerous diseases [2]. Abnormalities that cause infertility, such as ovulation, implantation disorders, and tube damage, have also been connected with psychological stress [3]. Many types of stress, including psychological stress, harm fertility and reproductive functions [4]. There is information in the literature that stress triggers depression and anxiety [5].

Furthermore, it is stated that depression and anxiety lead to infertility [6]. It has been observed that oxidative stress and pro-inflammatory cytokine production increase in depression and anxiety [7]. Degeneration, infiltration, and histopathological damage , such as atretic follicles, are seen in response to stress in rat ovaries [8]. Kadioglu *et al*. revealed that stress, which leads to infertility, increases total oxidant levels and decreases antioxidant levels in rat ovarian tissue [9]. This literature recommends that drugs with antioxidant, antidepressant, anti-inflammatory, and anxiolytic effects may be beneficial in treating stress-related ovarian damage and reproductive dysfunction.

Sertraline, is an antidepressant drug with selective serotonin re-uptake inhibitor antioxidant properties [10]. It has been experimentally revealed that sertraline exerts an anti-inflammatory effect by reducing tumor necrosis factor-alpha (TNF-α) levels [11]. It has been suggested that the antidepressant and anxiolytic effect of sertraline is based on the suppression of excessive production of TNF-α, interleukin-6 (IL-6), interleukin-1beta (IL-1β), and other pro-inflammatory cytokines [12,13]. Cerebrolysin is another drug we would like to see for its effects on stress-related ovarian damage, infertility, and preventing delay in maternity. Cerebrolysin is a porcine brain-derived drug with neuroprotective and neurotrophic effects and contains low molecular weight peptides and amino acids [9]. It has been defended that the antidepressant effect of cerebrolysin is based on its reducing oxidative stress and cytokine-related inflammation [14]. In addition, it has been argued that using an antidepressant drug with a drug with neuroprotective properties increases the effectiveness of antidepressant treatment [15]. All this information shows that sertraline, cerebrolysin, and a combination of both may be beneficial against increased stress, ovarian damage, infertility, and delay in achieving pregnancy in animals. This study aimed to investigate the effects of sertraline, cerebrolysin, and the combination of both on stress-induced ovarian injury, infertility, and pregnancy delay in rats.

MATERIALS AND METHODS

Animals

Seventy albino Wistar female rats provided by the Medical Experimental Application and Research Center of Ataturk University weighing between 272-288 grams at 6 months of age were utilized in our study. Rats were placed in a laboratory with a 12-hour light/12-hour dark cycle at appropriate humidity (45%) and temperature (22°C) and fed *ad libitum* before experimentation. Experimental applications were carried out considering the ARRIVE guidelines. The implementation of the experiment was started after the procedures were approved by the Atatürk University Animal Experiments Local Ethics Committee (date: 27.12.2018, meeting no: 13/253).

Chemicals

Sertraline was procured from PFIZER (Turkey), cerebrolysin from EVER Pharma (Austria), and sodium thiopental from IE Ulagay (Turkey).

Animal groups

The rats were randomly separated into healthy controls (HG), stress-applied control (StC), stress+sertraline (SS), stress + cerebrolysin (SC), and stress+ sertraline +

cerebrolysin (SSC) groups, with [14] animals in each group.

Experiment procedure

Stress was induced in rats by the forced immobilization method (FIM). For the implementation of this experiment, all animals except the HG group were placed in the supine position; their hindlimb and forelimbs were tied and kept in this position for one hour. After one hour, sertraline (20 mg/kg) was given to the SS rat group by oral gavage. SC group was injected with cerebrolysin (2.5 mL/kg) subcutaneously. Sertraline+cerebrolysin was administered to the SSC group at the indicated doses under the same method. The HG and StC groups were given the same volume of distilled water. FIM and drug applications were continued once a day for 30 days. Six rats from each group were euthanized (ip, 50 mg/kg thiopental sodium), and the right and left ovarian tissue were removed for biochemical and histopathological examination. The rest of the animals were kept in the same environment with mature male rats for two months for pregnancy.

The rats that were found to be pregnant were taken into separate cages and fed. Rats that did not become pregnant and give birth during this period were considered infertile. In addition, the time from the day the female rats were placed in the same cage with the male rats to the day they gave birth was determined. The delay in maternity was determined by subtracting the standard gestational period (21 days) from this period.

Biochemical analyses

Preparation of samples

Ovarian tissues were weighed. Tissues were made up to 2 mL with 1.15% potassium chloride solution for MDA determination and phosphate buffer with pH=7.5 for GSH determination and homogenized in an ice-cold medium, it was centrifuged for 15 minutes (10000 rpm, +4 °C). The supernatant portion was utilized as an analysis sample.

Malondialdehyde (MDA) and Total Glutathione (tGSH) Analysis

Malondialdehyde was measured to establish the oxidation level, tGSH was measured to determine the antioxidant level. MDA measurements were made according to the method defined by Ohkawa *et al.* [16]. tGSH measurement was performed in line with the method defined by Sedlak and Lindsay [17].

Tumor Necrosis Factor-α (TNF-α), Interleukin 1-β (IL-1β), and Interleukin-6 (IL-6) Analysis

Tumor Necrosis Factor-α, IL-1β, and IL-6 were measured to assess the pro-inflammatory status. The samples were weighed, and then all tissue was cut. These samples were then snap-frozen with liquid nitrogen and homogenized using a mortar and pestle. After the samples were melted, they were kept at 2-8 °C. PBS (pH 7.4), 1/10 (w/v) was added; after this, vortexed for 10 seconds, centrifuged at 10000 xg for 20 minutes, and supernatants were aliquoted. TNF-α, IL-1β, and IL-6 levels were measured using a commercial kit (Eastbiopharm Co Ltd ELISA kit, China).

Histopathological Examination

After the tissue samples were defined in 10% formaldehyde solution, they were washed in the cassettes under tap water for 24 hours. They were then treated with conventional-grade alcohol to remove water from the tissues, passed through xylol, and embedded in paraffin. Sections of 4-5 microns were taken from these paraffin blocks and subjected to hematoxylin-eosin staining. Tissues were examined under a light microscope, and then photographs were taken (Olympus® Inc. Tokyo, Japan, DP2-SAL firmware program). Ovarian tissues were evaluated regarding congestion, hemorrhage, degeneration in follicle cells, water accumulation in follicle cells, cystic changes in follicles, and edema. The severity of histopathological findings was graded from 0-3 (0-normal, 1-mild injury, 2-moder-

ate injury, and 3-severe injury). Histopathological evaluation was performed by a pathologist who was blinded to treatment and group allocations.

Statistical Analysis

This study used the "IBM SPSS 22® (Armonk, NY: IBM Corp.)" program for statistical analysis. Since the biochemical data were numeric, the analysis was done with one-way ANOVA, Tukey was used as a post hoc test, and the results were presented as Mean ± Standard error (X±SEM). Since the histopathological data were sequential, Kruskal-Wallis was preferred for analysis, and then the Dunn's test was used. Data were presented as Median (Minimum-Maximum), $p<0.05$ was accepted as statistical significance.

RESULTS

Biochemical Results

MDA and tGSH Analysis

The levels of MDA in the StC group (5.87±0.02) were significantly higher than in the HG (1.34±0.06), SS (2.85±0.02), SC (3.45±0.08) and SSC (1.52±0.06) groups as can be seen in Fig. 1A ($p<0.001$). The increase in MDA levels in the SSC group was observed to be significantly lower than in the SS and SC groups ($p<0.001$). For MDA, the HG and SSC groups were similar ($p=0.123$). The amount of tGSH measured in the ovarian tissue of the StC (1.30±0.05) group was observed to be significantly lower than the values measured in the HG (6.00±0.19), SS (3.64±0.08), SC (2.37±0.05) and SSC (5.42±0.18) groups ($p<0.001$). In the treatment combination group, inhibition in the decrease of tGSH was more significant than in the sertraline and cerebrolysin groups (Fig. 1B).

TNF-α, IL-1β and IL-6 Analysis

As seen in Fig. 2, TNF-α (Fig. 2A), IL-1β (Fig. 2B) and IL-6 (Fig. 2C) levels in the StC group (6.73±0.05, 8.05±0.17, 8.52±0.23, respectively) were significantly increased compared to HG (1.73±0.17, 2.25±0.04, 2.87±0.12, respectively), SS (3.27±0.04, 4.28±0.11, 4.89±0.03, respectively), SC (4.66±0.05, 5.81±0.04, 6.82±0.03, respectively) and SSC (2.04±0.10, 2.39±0.05, 3.14±0.03, respectively) groups ($p<0.001$). The increase in TNF-α, IL-1β, and IL-6 levels was significantly lower in the combination group when compared with the SS and SC groups alone ($p<0.001$). Cytokine levels were similar in SSC and HG groups ($p>0.05$).

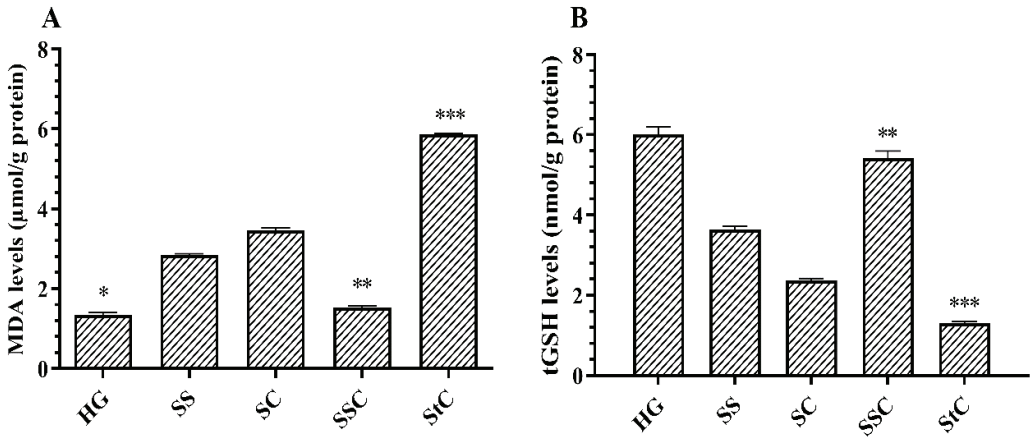

Fig. 1. MDA (A) and tGSH (B) levels in the ovarian tissue of study groups.
*p=0.123 vs SSC group; **p<0.001 vs SS and SC groups; ***p<0.001 vs HG, SS, SC and SSC groups. Statistical analysis was done with one-way ANOVA, followed by the Tukey test. HG, healthy group; StC, stress-treated control group; SS, stress+sertraline group; SC, stress+cerebrolysin group; SSC, stress+sertraline+cerebrolysin group.

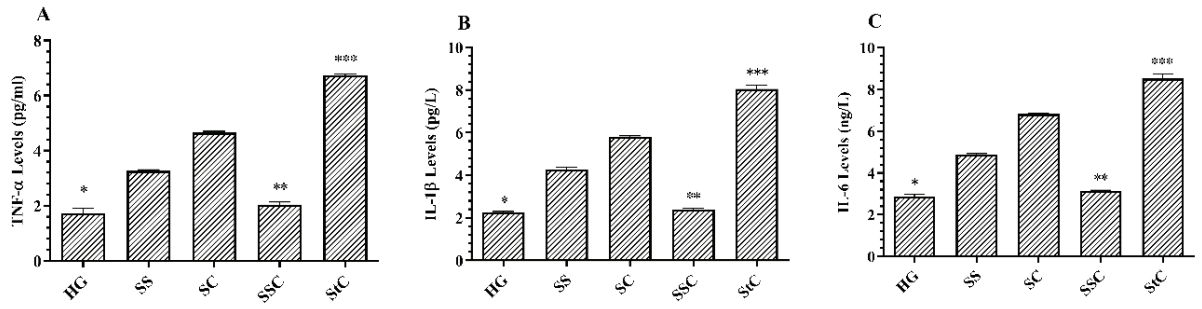

Fig. 2. TNF-α (A), IL-1β (B), and IL-6 (C) levels in the ovarian tissue of study groups. *p>0.05 vs SSC group; **p<0.001 vs. SS and SC groups; ***p<0.001 vs. HG, SS, SC and SSC groups. Statistical analysis was done with one-way ANOVA, followed by the Tukey test. HG, healthy group; StC, stress-treated control group; SS, stress+sertraline group; SC, stress+cerebrolysin group; SSC, stress+sertraline+cerebrolysin group.

Reproduction Test Results

Animals in the HG group gave birth within 23-26 days, as observed in Table 1. Six of the eight rats in the SS group gave birth within 27-36 days, while two did not give birth within two months. Three of the eight rats in the SC group gave birth within 33-38 days, but three did not give birth within two months. In the SSC group, all eight female rats gave birth on days 24-28. One of eight female rats in the StC group gave birth on day 49, but the remaining seven did not give birth during this time.

Histopathological findings

As seen in Fig. 3A and Table 2, no pathological findings were found in the ovarian tissue of the HG group; corpus luteum and follicle structure were observed within normal limits. Grade-3 degenerated secondary follicle and congestion were observed in the ovarian tissue of the StC group (Fig. 3E, Table 2). Moreover, grade-3 dilated congested vessels, hemorrhage, and edema were seen in the ovarian tissue of the StC group (Fig. 3F, Table 2). Vascular congestion (grade-1) and relatively normal follicle and corpus luteum structure (grade-0) were seen in the ovarian tissue of the SS group treated with sertraline (Fig. 3B, Table 2). In the SC group, mild fluid accumulation in the lumen, cystic changes (grade-1), minimal vascular congestion (grade-1), and corpus luteum damage (grade-1) were detected (Fig. 3C, Table 2). There were no histopathological signs other than mild vascular congestion (grade-1) and relatively normal corpus luteum (grade-0) in the SSC group (Fig. 3D, Table 2).

DISCUSSION

The effects of sertraline, cerebrolysin, and their combination against FIM-related stress-associated ovarian damage, infertility, and delay in achieving pregnancy in female rats were investigated in this study. Various stress factors lead to damage to all organs and tissues of the body, as can be understood from the literature [18]. Previous studies have revealed that psychological or physiological stress is related to oxidative stress [19]. Stress increased the levels of MDA, known as the toxic product of lipid peroxidation (LPO), and decreased the antioxidant tGSH levels in the ovarian tissue of animals, as can be observed in our results. These biochemical findings show that stress changes the oxidant-antioxidant balance in favor of oxidants in the ovarian tissue. In the literature, it has been shown that stress increases oxidants in ovarian tissue while decreasing antioxidants [20]. As it is known, membrane lipids are oxidized by reactive oxygen species (ROS), and a toxic product, MDA, is formed. MDA resulting from LPO greatly disrupts the structure and functions of the cell membrane

Table 1
Infertility and reproductive process in rats preproductiveprocess in rats.

Groups	Non-infertile rats n %		İnfertile rats n %		Reproductive process (RP) (day)	Delay in maternity (RP-21 days)
HG (n=8)	8	100	-	-	24.63 ± 0.42*	3.63 ± 0.42*
SS (n=8)	6	75	2	25	30.17 ± 1.45**	9.17 ± 1.45**
SC (n=8)	3	37.7	5	62	36.00 ± 1.53***	15.00 ± 1.53***
SSC(n=8)	8	100	-	-	25.75 ± 0.59	4.75 ± 0.59*
StC (n=8)	1	12	7	88	49.00	28.00

*, p>0.05 vs SSC; **, p<0.05 vs SC and SSC, ***; p<0.05 vs SS and SSC. Statistical analysis was done with one-way ANOVA, followed by the Tukey test. Results are expressed as mean±standard error of the mean. HG, healthy group; StC, stress-treated control group; SS, stress+sertraline group; SC, stress+cerebrolysin group; SSC, stress+sertraline+cerebrolysin group; n, number of animals.

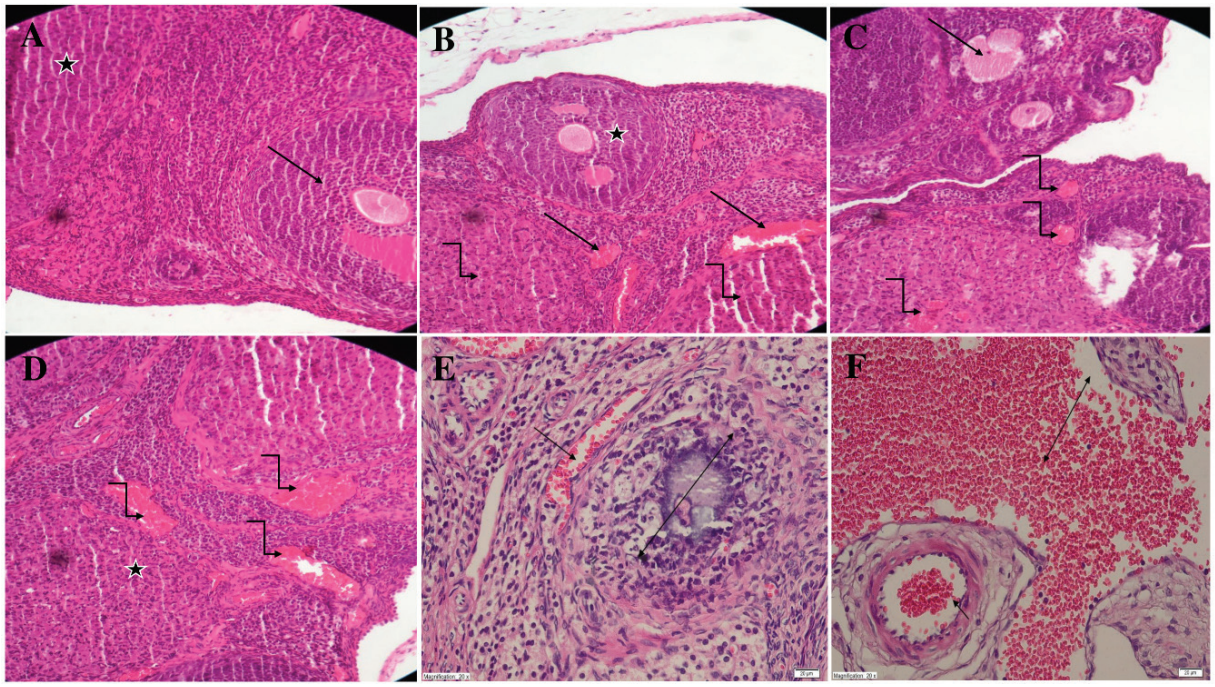

Fig. 3 (A-F). Histopathological examination of ovarian tissues in study groups. **A.** Ovarian tissue of the SG group; view of healthy corpus luteum (star) and follicle structure (arrow) within normal limits. **B.** Ovarian tissue of the StC group; Section showing degenerated secondary follicle (bilateral arrow), dilated congested blood vessel (straight arrow). **C.** Ovarian tissue of the StC group; section showing dilated congested blood vessel (straight arrow), hemorrhage, and edema (bilateral arrow). **D.** Ovarian gland of the SS group; Section showing congested blood vessels (arrows), the follicle (star), and corpus luteum (zigzag arrow). **E.** Ovarian tissue of the SC group; Follicle structure with fluid accumulation in the lumen and cystic change (arrow), section showing mild congestion (zigzag arrow). **F.** Ovarian tissue of the SSC group; Section, showing mildly congested blood vessel (zigzag arrow), corpus luteum (star). H&E x 200. HG, healthy group; SS, stress+sertraline group; SC, stress+cerebrolysin group; SSC, stress+sertraline+cerebrolysin group; StC, stress-treated control group. H&E x 200.

Table 2
Histopathological examination of ovarian tissues.

Groups	Congestion	Hemorrhage	Follicle cell degeneration	Water accumulation in follicle cells	Cystic change in follicles	Edema
HG (n=6)	0(0-0)*	0(0-0)*	0(0-0)*	0(0-0)*	0(0-0)*	0(0-0)*
SS (n=6)	1(0-2)*	0(0-0)*	0(0-1)*	0(0-0)*	0(0-0)*	0(0-0)*
SC (n=6)	1(0-2)*	0(0-0)*	0(0-0)*	1(0-2)**	1(1-1)**	0(0-0)*
SSC (n=6)	1(0-1)*	0(0-0)*	0(0-0)*	0(0-0)*	0(0-0)*	0(0-0)*
StC (n=6)	3(2-3)**	3(3-3)**	3(2-3)**-	0(0-0)*	0(0-0)*	3(2-3)**

Histopatological grading; 0-normal, 1- mild injury, 2-moderate injury, and 3-severe injury. *, $p>0.05$ vs other groups with the same sign; **, $p<0.05$ vs other groups. Kruskal Wallis test was used. Results are expressed as median (minimum -maximum). HG, healthy group; SS, stress+sertraline group; SC, stress+cerebrolysin group; SSC, stress+sertraline+cerebrolysin group; StC, stress-treated control group.

and leads to further destruction [21]. As such, MDA level is known as a marker of oxidative stress and antioxidant status in patients [22]. Our results, which align with these previous findings, showed that the amount of tGSH decreased significantly. At the same time, MDA increased in the ovarian tissues of animals exposed to stress. GSH is a tripeptide that can be found in most cells. GSH protects cells from the toxic effect of ROS by detoxifying hydrogen peroxide and organic oxides [23].

It is known that pro-inflammatory cytokine production plays a role in parallel with excessive oxidant production in the pathogenesis of ovarian damage, infertility, and delay in achieving pregnancy that develops due to stress and other factors [9,24]. Our results, accordingly, showed that TNF-α, L-1β and IL-6 levels increased in the ovarian tissue of animals with infertility and delay in achieving pregnancy. In studies with patients, it has been reported that TNF-α, IL-6, and other pro-inflammatory cytokines are among the factors that lead to infertility in ovarian pathologies [25]. Oxidative stress and pro-inflammatory cytokines increase in psychological disorders such as depression and anxiety, as mentioned above [7].

It has been reported that stress is associated with depression, and depression may lead to ovarian dysfunction [26]. Sertraline was more effective than cerebrolysis against stress-related ovarian damage, infertility, and pregnancy delay. The fact that sertraline is more effective than cerebrolysin may be due to its more significant inhibition of overproduction of oxidant and pro-inflammatory cytokines than cerebrolysin. Sertraline has antioxidant properties as mentioned hereinabove [10]. Moreover, it is argued that the antidepressant and anxiolytic effect of sertraline is based on suppressing excessive production of TNF-α, L-1β, IL-6, and other pro-inflammatory cytokines [12,13]. It has been documented that the antidepressant effect of cerebrolysin is due to the reduction of oxidative stress and cytokine-related inflammation [14]. Cerebrolysin is also a neuroprotective and neurotrophic drug [27]. The fact that the use of an antidepressant drug together with a drug with neuroprotective properties increases the effectiveness of the treatment has been reported in the literature [15]. The administration of sertraline and cerebrolysin in combination suppressed oxidant and inflammatory markers in ovarian tissue better than sertraline and cerebrolysin administered alone. It also better prevented stress-related infertility and delay in achieving pregnancy in our study.

Severe histopathological injury was seen in the ovarian tissue of the stress group. In addition, mild cystic changes in

the follicles and water accumulation in the follicle cells were observed in the stress and cerebrolysin group, while adding sertraline to the treatment prevented these changes. Combination therapy, sertraline, and cerebrolysin were the best suppressors of histopathological damage, respectively. It is known that oxidant and pro-inflammatory cytokines lead to hemorrhage, congestion, follicle degeneration, inflammatory cell infiltration, and necrosis in the ovarian tissue [24]. Infertility and delay in achieving pregnancy developed in the stress-treated control group in which severe histopathological damage was detected in the ovarian tissue, as can be understood from our results. Ince et al. reported severe follicle degeneration in ovaries with high MDA and low tGSH levels [28]. In another study by Ince et al. stated that severe degeneration was found in the ovarian follicles of animals in which sterility and delay in achieving pregnancy developed [29]. It was revealed in the study of Kadioglu et al. that the stress induced by the forced immobilization method causes widespread congestion, hemorrhage, accumulation of fluid, and inflammatory infiltration in the subcapsular area in the ovaries. Infertility, delay in achieving pregnancy, decrease in the number of offspring, and intrauterine physical developmental retardation were found in the animal group with these histopathological signs [9]. The stress induced by the FIM has led to oxidative and inflammatory damage in the ovarian tissue of animals, sterility, and delay in achieving pregnancy. The combination therapy of sertraline and cerebrolysin were the drugs that best prevented ovarian damage, infertility, and delay in achieving pregnancy, respectively. This information has revealed the fact that antidepressant drugs with antioxidant and anti-inflammatory effects might be useful in the treatment of stress-related ovarian damage, infertility and delay in achieving pregnancy. It has been revealed particularly that the combination of antidepressant (sertraline) and neuroprotective / neurotrophic (cerebrolysin) drug combination may be more beneficial. In line with this information sertraline, cerebrolysin and their combination may be preferred in treating stress-associated ovarian damage, infertility, and delay in achieving pregnancy. However, it is required to investigate antidepressant and neuroprotective/neurotrophic drug combinations from different groups in the future to confirm these findings.

ACKNOWLEDGMENTS

We want to thank Erzincan Binali Yildirim University Experimental Animals Application and Research Center for their contributions.

Conflict of interest

There is no conflict of interest among the authors.

ORCID number of authors

- Gulsah Aynaoglu Yildiz (GAY): 0000-0002-3283-7783
- Omer Erkan Yapca (OEY): 0000-0002-5578-0126
- Kemal Dinc (KD): 0000-0003-4955-455X
- Cebrail Gursul CG): 0000-0001-6521-6169
- Betul Gundogdu (BG): 0000-0002-3786-3286
- Mehmet Aktas (MA): 0000-0003-1931-8353
- Zeynep Suleyman (ZS): 0000-0003-0128-7990
- Seval Bulut (SB): 0000-0003-4992-1241
- Halis Suleyman (HS): 0000-0002-9239-4099

Participation of authors

Substantial contribution to conception and design: GAY, HS; Acquisition of data: MA, HS; Analysis and interpretation of data: KD, ZS, SB; Drafting of the manuscript: GAY, OEY, HS; Critical revision of the manuscript for important intellectual content: GAY, HS; Statistical analysis: ZS, SB; Research group leadership: GAY, HS; Have given final approval of the submitted manuscript: GAY, OEY, KD, CG, BG, MA, ZS, SB, HS.

REFERENCES

1. **Nargund VH.** Effects of psychological stress on male fertility. Nat Rev Urol 2015;12:373-382.
2. **Sominsky L, Hodgson DM, McLaughlin EA, Smith R, Wall HM, Spencer SJ.** Linking Stress and Infertility: A Novel Role for Ghrelin. Endocr Rev 2017;38:432-467.
3. **Abdel Hafez SMN, Allam F, Elbassuoni E.** Sex differences impact the pancreatic response to chronic immobilization stress in rats. Cell Stress Chaperones 2021;26:199-215.
4. **Mamgain A, Sawyer IL, Timajo DAM, Rizwan MZ, Evans MC, Ancel CM, Inglis MA, Anderson GM.** RFamide-related peptide neurons modulate reproductive function and stress responses. J Neurosci 2021;41:474-488.
5. **Damone AL, Joham AE, Loxton D, Earnest A, Teede HJ, Moran LJ.** Depression, anxiety and perceived stress in women with and without PCOS: a community-based study. Psychol Med 2019;49:1510-1520.
6. **Lakatos E, Szigeti JF, Ujma PP, Sexty R, Balog P.** Anxiety and depression among infertile women: a cross-sectional survey from Hungary. BMC Womens Health 2017;17:48.
7. **Li M, Li C, Yu H, Cai X, Shen X, Sun X, Wang J, Zhang Y, Wang C.** Lentivirus-mediated interleukin-1β (IL-1β) knockdown in the hippocampus alleviates lipopolysaccharide (LPS)-induced memory deficits and anxiety- and depression-like behaviors in mice. J Neuroinflammation 2017;14:190.
8. **Chukwuebuka NB, Emeka OA, Irukefe OS, Iju WJ, Godsday OU, Temitope OG, Nneamaka EC, Peter AC.** Stress-Induced Morphological Changes of Ovarian Histology in Female Wistar Rats. Biomedical & Pharmacology Journal. 2020;13:1625-1643.
9. **Kadioglu B, Gundogdu B, Kurt N, Bilgin AO, Suleyman H, Suleyman Z.** The effect of rhodiola rosea root extract on stress-induced ovarian damage, infertility and reproductive disorders in female rats. Clinical and Experimental Obstetrics & Gynecology. 2020;47:530-536.
10. **Abdel Salam OM, Mohammed NA, Sleem AA, Farrag AR.** The effect of antidepressant drugs on thioacetamide-induced oxidative stress. Eur Rev Med Pharmacol Sci 2013;17:735-744.
11. **Baharav E, Bar M, Taler M, Gil-Ad I, Karp L, Weinberger A, Weizman A.** Immunomodulatory effect of sertraline in a rat model of rheumatoid arthritis. Neuroimmunomodulation 2012;19:309-318.
12. **Shulyak A, Gorpynchenko I, Drannik G, Poroshina T, Savchenko V, Nurimanov K.** The effectiveness of the combination of rectal electrostimulation and an antidepressant in the treatment of chronic abacterial prostatitis. Cent European J Urol 2019;72:66-70.
13. **Hou R, Ye G, Liu Y, Chen X, Pan M, Zhu F, Fu J, Fu T, Liu Q, Gao Z, Baldwin DS, Tang Z.** Effects of SSRIs on peripheral inflammatory cytokines in patients with Generalized Anxiety Disorder. Brain Behav Immun 2019;81:105-110.
14. **El-Marasy SA, El Awdan SA, Hassan A, Ahmed-Farid OA, Ogaly HA.** Anti-depressant effect of cerebrolysin in reserpine-induced depression in rats: Behavioral, biochemical, molecular and immunohistochemical evidence. Chem Biol Interact 2021;334:109329.
15. **Safarova T, Gavrilova S.** The use of neuroprotectors in the treatment of late depression. Zhurnal Nevrologii i Psikhiatrii Imeni SS Korsakova 2020;120:46-53.

16. **Ohkawa H, Ohishi N, Yagi K**. Assay for lipid peroxides in animal tissues by thiobarbituric acid reaction. Anal Biochem 1979;95:351-358.
17. **Sedlak J, Lindsay RH.** Estimation of total, protein-bound, and nonprotein sulfhydryl groups in tissue with Ellman's reagent. Anal Biochem 1968;25:192-205.
18. **Cakir B, Kasımay O, Kolgazi M, Ersoy Y, Ercan F, Yegen BC.** Stress-induced multiple organ damage in rats is ameliorated by the antioxidant and anxiolytic effects of regular exercise. Cell Biochem Funct 2010;28:469-479.
19. **Islam MT.** Oxidative stress and mitochondrial dysfunction-linked neurodegenerative disorders. Neurol Res 2017;39:73-82.
20. **Aynaoglu Yildiz G, Yildiz D, Yapca OE, Suleyman B, Arslan YK, Kurt N, Suleyman H**. Effect of diazepam, sertraline and melatonin on the stress-induced reproductive disorders and intrauterine growth restriction in female rats. J Matern Fetal Neonatal Med 2021;34:4103-4109.
21. **Yuceli S, Suleyman B, Yazici GN, Mammadov R, Cankaya M, Kunak CS, Bulut S, Suleyman H, Altuner D.** Effect of taxifolin on ischemia/reperfusion-induced oxidative injury of sciatic nerve in rats. Transplant Proc 2021;53:3087-3092.
22. **Gaweł S, Wardas M, Niedworok E, Wardas P.** Malondialdehyde (MDA) as a lipid peroxidation marker. Wiadomosci lekarskie (Warsaw, Poland: 1960) 2004;57:453-455.
23. **Forman HJ, Zhang H, Rinna A.** Glutathione: overview of its protective roles, measurement, and biosynthesis. Mol Aspects Med 2009;30:1-12.
24. **Unlubilgin E, Suleyman B, Balci G, Atakan Al R, Cankaya M, Arslan Nayki U, Suleyman H.** Prevention of infertility induced by ovarian ischemia reperfusion injury by benidipine in rats: Biochemical, gene expression, histopathological and immunohistochemical evaluation. J Gynecol Obstet Hum Reprod 2017;46:267-273.
25. **Wang XM, Ma ZY, Song N.** Inflammatory cytokines IL-6, IL-10, IL-13, TNF-α and peritoneal fluid flora were associated with infertility in patients with endometriosis. Eur Rev Med Pharmacol Sci 2018;22:2513-2518.
26. **Senashova O, Reddy AP, Cameron JL, Bethea CL.** The effect of citalopram on midbrain CRF receptors 1 and 2 in a primate model of stress-induced amenorrhea. Reprod Sc. 2012;19:623-632.
27. **Berent D, Zboralskı K, Macander M.** Antioxidant properties of cerebrolysin–an old drug with newly discovered capabilities. The Polish Journal of Aviation Medicine and Psychology. 2014;20:25.
28. **Ince S, Ozer M, Goktug Kadioğlu B, Kuzucu M, Karahan Yilmaz S, Özkaraca M, Gezer A, Suleyman H.** The effect of adenosine triphosphate on bevacizumab-induced ovarian damage and reproductive dysfunction in rats. Gen Physiol Biophys. 2021;40:71-78.
29. **Ince S, Ozer M, Kadioglu BG, Kuzucu M, Ozkaraca M, Gezer A, Suleyman H, Cetin N.** The effect of taxifolin on oxidative ovarian damage and reproductive dysfunctions induced by antipsychotic drugs in female rats. J Obstet Gynaecol Res. 2021;47:2140-2148.

Invest Clin 64(4): 524 - 532, 2023 https://doi.org/10.54817/IC.v64n4a9

Uropatógenos multirresistentes y con resistencia extendida a los antimicrobianos aislados en pacientes adultos de la comunidad de Barinas, Venezuela.

Poema Salazar[1,2] *y María Araque*[2]

[1]Laboratorio Clínico Microbiología Barinas, CA, Barinas, Venezuela.
[2]Laboratorio de Microbiología Molecular, Facultad de Farmacia y Bioanálisis, Universidad de Los Andes, Mérida, Venezuela.

Palabras clave: infección urinaria; uropatógenos; resistencia antimicrobiana; multirresistencia; resistencia extendida.

Resumen. El objetivo de este estudio fue determinar la frecuencia de uropatógenos multirresistentes (MDR) y con resistencia extendida (XDR) aislados de pacientes adultos de la comunidad de Barinas, Venezuela, durante el año 2022. De un total de 1019 urocultivos provenientes de pacientes que asistieron al Laboratorio Clínico Microbiológico Barinas, 337 (33,07%), fueron seleccionados según criterios de inclusión. El procesamiento microbiológico de las muestras se realizó por métodos convencionales. Las pruebas de susceptibilidad antimicrobiana y la determinación de betalactamasas de espectro extendido, se realizaron por métodos fenotípicos estandarizados. La clasificación en cepas MDR y XDR se llevó a cabo según criterios internacionales. Los datos fueron procesados mediante estadística descriptiva y análisis de frecuencia. De los 337 urocultivos analizados, el 70,92% correspondió a pacientes del sexo femenino, de edades comprendidas entre 31 y 60 años. De los uropatógenos identificados, el 93,17% estuvo representado por Enterobacterales, donde *Escherichia coli* destacó con un 87,54%, seguido por *Pseudomonas aeruginosa* (2,67%) y *Enterococcus faecalis* (1,48%). El 87,12% de las cepas de *E. coli* presentaron resistencia por lo menos a un antibiótico, 46,78% era del fenotipo MDR y 5,42% del XDR. En general, más de la mitad de los uropatógenos identificados se distribuyeron entre los fenotipos MDR y XDR. Los resultados evidencian la necesidad de desarrollar investigaciones locales que permitan mejorar las terapias empíricas y dirigidas en las infecciones del tracto urinario, además de realizar acciones de concienciación para el uso racional de los antibióticos y mejorar la vigilancia epidemiológica de cepas multirresistentes circulantes en la región.

Autor de correspondencia: María Araque. Laboratorio de Microbiología Molecular, Departamento de Microbiología, Facultad de Farmacia y Bioanálisis, Universidad de Los Andes, Mérida, Venezuela. Teléfono: +58 414 7170637. Correo electrónico: araquemc@ula.ve

Multidrug-resistant and extensively antimicrobial-resistant uropathogens isolated from adult patients in Barinas, Venezuela.

Invest Clin 2023; 64 (4): 524 – 532

Keywords: urinary infection; uropathogens; antimicrobial-resistance; multidrug-resistance; extensive-drug resistance.

Abstract. This study aimed to determine the frequency of multidrug-resistant (MDR) and extensively drug-resistant (XDR) uropathogens isolated from adult patients in Barinas City, Venezuela, in 2022. Of 1019 urine cultures from patients who attended the Barinas Clinical Microbiological Laboratory, 337 (33.07%) were selected according to inclusion criteria. The microbiological processing of urine was carried out through conventional methods. Antimicrobial susceptibility tests and extended-spectrum beta-lactamase determination were performed using standardized phenotypic methods. The classification of MDR and XDR strains was conducted according to international criteria. Data were processed through descriptive statistics and frequency analysis. Of 337 urine cultures analyzed, 70.92% corresponded to female patients, and the age groups between 31 and 60 years were the most frequent. Of the uropathogens identified, 93.17% were represented by Enterobacterales, where *Escherichia coli* stood out with 87.54%, followed by *Pseudomonas aeruginosa* (2.67%) and *Enterococcus faecalis* (1.48%). Of the *E. coli* strains, 87.12% presented resistance to at least one antibiotic, with 46.78% MDR and 5.42% XDR. In general, more than half of the uropathogens identified were distributed either as MDR or XDR phenotypes. The results show the need to develop local research to improve empirical and targeted therapies in urinary tract infections, in addition to awareness actions for the rational use of antibiotics and epidemiological surveillance of multiresistant strains circulating in the region.

Received: 15-01-2023 *Accepted: 18-05-2023*

INTRODUCCIÓN

La infección del tracto urinario (ITU), es uno de los principales motivos de consulta en la atención primaria y se considera una de las causas más frecuentes para la prescripción de antibióticos [1]. El aumento de la resistencia a los antimicrobianos, junto con las consecuencias negativas que confiere el uso de antibióticos de amplio espectro sobre la salud de la microbiota del hospedero, han resaltado las desventajas del tratamiento empírico para las ITU [1,2]. La razón del avance de la resistencia a los antibióticos en las bacterias uropatógenas es multifactorial, pero pueden identificarse como causas importantes el uso indebido de los antibióticos, la falta de adherencia al tratamiento y la automedicación [3].

La resistencia antimicrobiana es un fenómeno dinámico en expansión, que varía de acuerdo a la región geográfica, así

como a las diferentes áreas de un hospital [3,4]. En este contexto, conocer el patrón de susceptibilidad de los uropatógenos frente a los antibióticos es importante, no solo para elaborar guías de tratamiento empírico que permitirían iniciar un tratamiento eficaz, sino también para determinar la complejidad del fenotipo de resistencia de los microrganismos, conocidos como multirresistentes, con resistencia extendida o panresistentes (MDR, XDR, y PDR por sus siglas en inglés, respectivamente) [1-5]. En consecuencia, la probabilidad de adecuación de la terapia antimicrobiana disminuye con el aumento de la resistencia antimicrobiana, y el desarrollo de nuevos agentes antibacterianos no es tan rápido como el incremento de la tasa de microorganismos resistentes[2,6]. Por consiguiente, es indispensable realizar una evaluación periódica, preferiblemente anual, de la prevalencia y la resistencia bacteriana de los uropatógenos más frecuentes e implementar redes de vigilancia regional de susceptibilidad antimicrobiana, como ha sugerido la Organización Mundial de la Salud [7].

En Venezuela son pocos los reportes que describen los patrones complejos de susceptibilidad de uropatógenos aislados en pacientes no hospitalizados [3,8,9]. Por tal motivo, en este trabajo se determinó la frecuencia de uropatógenos multirresistentes (MDR) y con resistencia extendida (XDR), aislados de pacientes adultos de la comunidad, en la ciudad de Barinas, Venezuela, durante el año 2022.

MATERIALES Y MÉTODOS

Diseño del estudio y selección de la muestra. Se realizó un estudio observacional y retrospectivo en el laboratorio privado Microbiología Barinas C.A., donde se analizaron los datos clínicos, epidemiológicos y microbiológicos de pacientes adultos con diagnóstico de infección del tracto urinario (ITU), procedentes del área urbana y semiurbana de la ciudad de Barinas, Venezuela, durante el período de enero a diciembre del 2022. La fuente de información fue obtenida a través de la base de datos del laboratorio y estos transcritos a fichas de trabajo diseñadas para tal fin.

La selección de los pacientes se realizó de acuerdo a los siguientes criterios de inclusión:

- Pacientes mayores de 18 años.
- Pacientes sintomáticos con ITU con urocultivo positivo a partir de muestras clínicas tomadas por micción espontánea, con contaje $\geq 10^5$ UFC/mL en mujeres y $\geq 10^3$UFC/mL en hombres.
- Datos clínicos y epidemiológicos completos para cada paciente

Criterios de exclusión:

- Pacientes pediátricos
- Urocultivos negativos o contaminados
- Pacientes hospitalizados o con historia de hospitalización en los últimos 3 meses
- Pacientes con tratamiento antibiótico
- Pacientes con catéter vesical
- Pacientes embarazadas
- Pacientes con datos incompletos

Procesamiento microbiológico. El aislamiento e identificación microbiológica de los uropatógenos se realizó utilizando metodologías convencionales basadas en pruebas bioquímicas y fisiológicas de acuerdo a los procedimientos recomendados por la Sociedad Americana de Microbiología [10].

Pruebas de susceptibilidad antimicrobiana. La susceptibilidad antimicrobiana se determinó mediante el método de difusión del disco, y la interpretación de los perfiles de susceptibilidad se basó en los puntos de cortes vigentes, establecidos por el Instituto de Estandarización de Laboratorios Clínicos (CLSI por sus siglas en inglés, 2022) [11]. Los antibióticos (Oxoid) ensayados fueron: ampicilina (AMP 10 μg), amikacina (AMK 30 μg), cefazolina (CFZ 30 μg), ciprofloxa-

cina (CIP 5 μg), fosfomicina (FOS 200 μg), gentamicina (GEN 10 μg), nitrofurantoina (NIT 300 μg) y trimetoprim/sulfametoxazol (SXT 1,25/23,75 μg). La detección fenotípica de betalactamasas de espectro extendido (BLEE), se realizó utilizando la prueba del doble disco combinado (DDC), también de acuerdo a lo descrito en el CLSI, 2022. Las definiciones de las cepas multirresistentes (MDR) y con resistencia extendida (XDR), se basaron en la terminología internacional estandarizada, propuesta por el Centro de Control de Enfermedades (CDC) y el Centro Europeo para la Prevención y el Control de Enfermedades (ECDC) [5]. La categoría no MDR se definió como aquellas cepas que presentaron resistencia a un máximo de dos grupos de antimicrobianos y las que demostraron sensibilidad a todos los antibióticos ensayados se denominaron pansensibles.

Análisis estadístico. Los datos fueron analizados utilizando el programa SPSS versión 21 (IBM Corporation, New York, USA). Las variables continuas se describieron como promedio y desviación estándar y las nominales y ordinales se señalaron con porcentajes.

Consideraciones bioéticas. Este estudio fue aprobado por el Comité de Investigación y Ética de la Facultad de Medicina, Postgrado en Ciencias Médicas Fundamentales, Universidad de Los Andes, Mérida, Venezuela (Acta Nº PCMF09-CDV-02-2022) y fue considerado "sin riesgo" de acuerdo los principios éticos internacionales descritos en la Declaración de Helsinki 7º Ed. 2013. Se protegió la privacidad de los datos de los pacientes y estos fueron manejados con estricta confidencialidad solo para fines de investigación y académicos.

RESULTADOS

Durante el año 2022 se procesaron 1019 urocultivos. Posteriormente, al aplicar los criterios de inclusión determinados para este estudio, la población definitiva seleccionada estuvo constituida por 337 urocultivos positivos, representando el 33,07% del total de muestras analizadas. El 70,92% (244/337) de los urocultivos estudiados correspondió a pacientes del sexo femenino de edades comprendidas entre 21 y 60 años. Por el contrario, las muestras de orina de pacientes masculinos procedían marcadamente de personas mayores de 61 años (Tabla 1).

Los uropatógenos identificados en este estudio se señalan en la Tabla 2. Se aisló un total de 337 microorganismos, el 93,17% de estos estuvo representado por las Enterobacterales, donde destacó *Escherichia coli* con un 87,54%. El segundo lugar lo ocuparon los bacilos Gram negativos no fermentadores (3,86%), distinguiéndose *Pseudomonas aeruginosa* con un 2,67%, mientras que los cocos Gram positivos se ubicaron en el tercer lugar (2,97%), *Enterococcus faecalis fue* el más frecuentemente aislado de este grupo (1,48%).

En la Tabla 3, se muestra el perfil de susceptibilidad antimicrobiana de las cepas de *E. coli,* el principal uropatógeno aislado en las muestras analizadas.

Tabla 1
Distribución de las muestras de orina positivas al estudio microbiológico de acuerdo al grupo etario y sexo.

		Sexo	
Grupo etario (años)	Total Nº (%)	Femenino Nº (%)	Masculino Nº (%)
18-20	9 (2,67)	8 (3,35)	1 (1,02)
21-30	28 (8,31)	27 (11,30)	1 (1,02)
31-40	49 (14,54)	47 (19,66)	2 (2,04)
41-50	37 (10,98)	33 (13,81)	4 (4,08)
51-60	58 (17,21)	49 (20,50)	9 (9,18)
61-70	63 (18,69)	33 (13,81)	30 (30,61)
71-80	65 (19,29)	32 (13,39)	33 (33,67)
> 80	28 (8,31)	10 (4,18)	18 (18,37)
Total	337 (100)	239 (70,92)	98 (29,08)

Tabla 2
Uropatógenos aislados en pacientes adultos con infección del tracto urinario provenientes de la comunidad.

Microorganismos aislados (n= 337)	Nº	%
Enterobacterales	**314**	**93,17**
Escherichia coli	295	87,54
Proteus mirabilis	11	3,26
Klebsiella spp	4	1,19
Complejo *Enterobacter cloacae*	4	1,19
Bacilos Gram Negativos no fermentadores	**13**	**3,86**
Pseudomonas aeruginosa	9	2,67
Complejo *Acinetobacter baumannii*	4	1,19
Cocos Gram positivos	**10**	**2,97**
Enterococcus faecalis	5	1,48
Staphylococcus aureus	3	0,89
Enterococcus spp	1	0,30
Staphylococcus spp	1	0,30

Los resultados indican que solo el 12,88% (38/295) de las cepas *E. coli* fue totalmente sensibles al panel de antibióticos probados, mientras que el resto, 87,12% (257/295) presentó por lo menos un marcador de resistencia. Veintiséis cepas (26/257; 10,12%), mostraron resistencia a algunos de los antibióticos ensayados, sin presentar producción de BLEE. Por el contrario, 231 (85,88%) *E. coli,* mostraron diferentes patrones de resistencia, donde la producción de BLEE fue una característica común. Al respecto, resalta que más de la mitad (154/231; 66,67%) de las cepas productoras de BLEE desplegaron fenotipos complejos de multirresistencia (138/231; 59,74%) y con resistencia extendida (16/231; 6,93%). Las cepas MDR mostraron por lo menos 6 patrones diferentes con la asociación de varios marcadores de resistencia, donde la presencia de BLEE, la resistencia a ciprofloxacina y trimetoprim/sulfametoxazol fueron las más comunes.

Tabla 3
Patrones de susceptibilidad antimicrobiana de 295 cepas de *Escherichia coli*, aisladas de pacientes con infección del tracto urinario provenientes de la comunidad.

Patrón de susceptibilidad	N°	%
Pansensible	**38**	**12,88**
Resistente	**257**	**87,12**
Total no multirresistentes (no MDR) (n= 103)		
Resistentes sin BLEE		
CIP	8	30,77
AMP	1	3,85
SXT	6	23,08
CIP; SXT	4	15,38
GEN; SXT	1	3,85
SAM; SXT	1	3,85
SAM; NIT	1	3,85
GEN; CIP; FOS	1	3,85
GEN; CIP, SXT	2	7,69
AMP; CIP, SXT	1	3,85
BLEE sin otros marcadores de resistencia	6	2,60
BLEE+ con asociación a un marcador de resistencia		
BLEE+ CIP	29	12,66
BLEE+ SXT	24	10,66
BLEE+ NIT	18	8,00
Multirresistentes (MDR) (n= 138)		
BLEE+ CIP; SXT; FOS	42	30,43
BLEE+ CIP; SXT; NIT	36	26,09
BLEE+ CIP; SXT; GEN	24	17,39
BLEE+ CIP; SXT; NIT	16	11,59
BLEE+ CIP; GEN; AMK	12	8,70
BLEE+ CIP; GEN; SXT	8	5,80
Resistencia extendida (XDR) (n= 16)		
BLEE+ CIP; SXT; NIT; GEN; AMK; FOS	15	93,75
BLEE+ CRE; CIP; SXT; NIT; GEN; FOS	1	6,25

BLEE: betalactamasa de espectro extensivo; CRE: carbapenemasa; AMP: ampicilina; AMK: amikacina; CIP: ciprofloxacina; FOS: fosfomicina; GEN: gentamicina; NIT: nitrofurantoina; SXT: trimetoprim/sulfametoxazol.

En relación a las cepas XDR, solo se observaron dos patrones de resistencia conformados por la combinación de 7 grupos de antibióticos.

Los niveles o categorías de susceptibilidad de los uropatógenos aislados se muestran en la Tabla 4. Del total de 337 uropatógenos aislados, el 15,13% fue pansensible y ninguna cepa mostró resistencia a todos los antibióticos probados, es decir no hubo uropatógenos panresistentes. Las cepas no MDR (resistentes entre 1 a 3 grupos de antibióticos) solo fueron observadas en *E. coli* (34,92%). En el grupo de MDR, todas las especies bacterianas identificadas en este estudio presentaron cepas con esta categoría, excepto *Enterococcus* spp y *Staphylococcus* spp, cuyos únicos representantes fueron pansensibles. La categoría XDR, además de *E. coli*, fue observada en cepas de *K. pneumoniae*, *P. aeruginosa* y en el complejo *Acinetobacter baumannii.* En general, los uropatógenos aislados se distribuyeron con mayor frecuencia en la categoría MDR (48,37%). *E.coli* fue la única especie que presentó cepas en todas las categorías de susceptibilidad estudiadas (pansensible, no MDR, MDR y XDR) excepto en la panresistente.

DISCUSIÓN

Las infecciones del tracto urinario (ITU) se encuentran entre las causas de consulta ambulatoria y de urgencias más frecuentes [2]. Estas infecciones son causadas predominantemente por *E. coli*, y cuando son adquiridas en la comunidad y la presentación clínica no es complicada, son tratadas empíricamente [12]. Sin embargo, en los últimos años, se ha observado un aumento de *E. coli* uropatógenas con perfiles de MDR y con resistencia extendida (XDR), que no solo dificultan el tratamiento de las ITU, sino que también aumentan el riesgo de una enfermedad prolongada y de mortalidad [1-3].

Tabla 4
Distribución de los uropatógenos aislados de pacientes adultos con infección del tracto urinario de acuerdo a categorías de susceptibilidad.

Uropatógeno	Total Nº (%)	Pansensible Nº (%)	No MDR Nº (%)	MDR Nº (%)	XDR Nº (%)	PDR Nº (%)
Enterobacterales						
Escherichia coli	295 (87,54)	38 (12,88)	103 (34,92)	138 (46,78)	16(5,42)	0
Proteus mirabilis	11 (3,26)	6 (54,55)	0	5 (45,45)	0	0
Complejo *Klebsiella pneumoniae*	4 (1,19)	0	0	3 (75,00)	1 (25,00)	0
Complejo *Enterobacter cloacae*	4 (1,19)	0	0	4 (100)	0	0
Bacilos Gram negativos no fermentadores						
Pseudomonas aeruginosa	9 (2,67)	2 (22,22)	0	6 (66,66)	1 (11,11)	0
Complejo *Acinetobacter baumannii*	4 (1,19)	0	0	2 (50,00)	2 (50,00)	0
Cocos Gram positivos						
Enterococcus faecalis	5 (1,48)	3 (60,00)	0	2 (40,00)	0	0
Complejo *Staphylococcus aureus*	3 (0,89)	0	0	3 (100)	0	0
Enterococcus spp.	1 (0,29)	1 (100)	0	0	0	0
Staphylococcus spp.	1 (0,29)	1 (100)	0	0	0	0
Total	337 (100)	51 (15,13)	103 (30,56)	163 (48,37)	20 (5,94)	0

No MDR: resistencia entre 1 a 2 grupos de antimicrobianos; MDR: multirresistencia antimicrobiana; XDR: resistencia extendida a los antimicrobianos; PDR: panresistentes a los antimicrobianos.

Es conocido que las ITU no complicadas, adquiridas en la comunidad, son particularmente frecuentes entre las mujeres jóvenes, en edad reproductiva y en una gran mayoría de estas, es común que experimenten al menos un episodio de infección urinaria en su vida [2]. Uno de los factores más importantes que afectan el manejo de la ITU en los últimos años, ha sido la aparición de la resistencia a los antimicrobianos, implicando este fenómeno un verdadero reto para el médico tratante [1-9].

E. coli fue el uropatógeno más frecuente identificado en este estudio y el que mostró más resistencia Por otra parte, de todas las cepas de *E. coli* aisladas, las productoras de BLEE predominaron en más del 85%. Similares resultados han sido reportados en otras regiones del país, de manera que *E. coli* uropatógena productora de BLEE, aislada en ambientes intra o extra hospitalarios, es una característica común en el ámbito nacional [8,9,13-15]. Es importante destacar que las cepas de *E. coli*, además de ser productoras de BLEE, presentaron resistencia asociada a otros antibióticos, conformando distintos patrones de resistencia complejos, los cuales se distribuyeron en fenotipos compatibles con MDR y XDR. Es probable que estos fenotipos particulares se deban, además de las BLEE, a la presencia de determinantes de resistencia adicionales que median la producción de enzimas modificadoras de aminoglucósidos, bombas de expulsión y alteraciones de la permeabilidad de la pared celular, entre otros mecanismos [2,9,14].

La resistencia a los antimicrobianos es un fenómeno creciente en expansión que no conoce fronteras geográficas ni ecológicas. Hasta hace poco se pensaba que los uropatógenos multirresistentes causaban infecciones urinarias complicadas solo en pacientes hospitalizados, como lo demostraron Quijada-Martínez y col. [14,15], cuando reportaron una variedad de cepas de Enterobacterales XDR en los diferentes servicios de Medicina Interna del Hospital Universitario de Los Andes (Mérida, Venezuela). Ahora, y con base en los hallazgos obtenidos en este estudio, no solo *E. coli* ,sino la mayoría de los uropatógenos aislados en esta investigación, demostraron tener resistencias compatibles con fenotipos MDR y XDR, lo que hace pensar que la urobiota del tracto urinario se ha convertido en uno de los principales reservorios de genes de resistencia [2,3,14,15]. Aunque desde el punto de vista genético, la resistencia de estos uropatógenos a diferentes antibióticos, puede explicarse en parte, por la selección de mutaciones cromosómicas. El mecanismo más importante y comúnmente involucrado, es la adquisición de genes exógenos localizados en elementos genéticos transferibles como los plásmidos y los transposones. Entre estos genes, el papel fundamental lo desempeñan los que codifican para la producción de BLEE, carbapenemasas y las betalactamasas tipo AmpC [1,3,8,9,14,15].

Desafortunadamente, cuando se comparan con las infecciones atribuibles a microorganismos susceptibles, las ITU causadas por uropatógenos MDR y XDR, tienen un mayor riesgo de evolucionar hacia la cronicidad, la severidad de la infección o la muerte [1-3,12]. Este hecho se debe, principalmente, al aumento de las probabilidades de iniciar una terapia antimicrobiana empírica ineficaz y al fracaso clínico de la terapia dirigida, incluso cuando se prescriben antibióticos con actividad *in vitro* [2]. Al respecto, la mayoría de las guías internacionales para el diagnóstico y tratamiento de las infecciones urinarias, señala que la selección de la antibioterapia empírica inicial, se basará en el perfil local de susceptibilidad de los uropatógenos, evitando aquellos antibióticos donde el registro de resistencia supere el 20% [2,13,16].

Si bien este estudio, probablemente, puede no reflejar la situación epidemiológica a nivel nacional, los resultados de esta investigación son relevantes para establecer parámetros de referencia local, especialmente en aquellos casos que permitan mejorar la calidad y seguridad de la asistencia médica, así como la optimización de las conductas

terapéuticas, dada la importancia que tiene la ITU como una patología frecuente en la consulta ambulatoria.

En conclusión, una variedad de uropatógenos fue aislada en las muestras de orina de pacientes adultos, provenientes de las zonas urbanas y semiurbanas de la ciudad de Barinas. Sin embargo, *E. coli* destacó como principal agente etiológico. La mayor parte de estas cepas mostró diversos patrones de resistencia, en los que se incluyeron fenotipos productores de BLEE asociados a la resistencia a diferentes antibióticos, que generaron fenotipos complejos de resistencia tipo MDR y XDR. Cepas con estas categorías de resistencia, generan gran preocupación y evidencian la necesidad de desarrollar investigaciones locales urgentes que permitan monitorizar los perfiles de susceptibilidad de patógenos de interés epidemiológico para orientar las terapias empíricas y las dirigidas, además de realizar acciones de concienciación para el uso racional de los antibióticos y la vigilancia epidemiológica de cepas multirresistentes circulantes en la región.

Financiamiento

El trabajo fue autofinanciado. No se recibió financiamiento externo.

Conflicto de interés

Los autores declaran no tener ningún conflicto de intereses.

Números ORCID de los autores

- Poema Salazar (PS): 0009-0002-1621-1585
- María Araque (MA): 0000-0001-6517-953X

Contribuciones de autoría

PS: Procesamiento microbiológico, recolección de datos, obtención de resultados, análisis e interpretación de datos, redacción inicial del manuscrito. Aprobación del manuscrito en su versión final. **MA:** Concepción, diseño del trabajo, discusión y análisis de resultados, corrección y revisión crítica del manuscrito. Aprobación del manuscrito en su versión final.

REFERENCIAS

1. **Silago V, Moremi N, Mtebe M, Komba E, Masoud S, Mgaya FX, Mirambo MM, Nyawale HA, Mshana SE, Matee MI.** Multidrug-resistant uropathogens causing community acquired urinary tract infections among patients attending health facilities in Mwanza and Dar es Salaam, Tanzania. Antibiotics 2022; 11: 1718. *https://doi.org/10.3390/antibiotics11121718*
2. **Klein RD, Hultgrena SJ**. Urinary tract infections: microbial pathogenesis, host-pathogen interactions and new treatment strategies. Nat Rev Microbiol 2020; 18(4): 211–226. *https://doi:10.1038/s41579-020-0324-0.*
3. **Guzmán M, Salazar E, Cordero V, Castro A, Villanueva A, Rodulfo H, De Donato M.** Multidrug resistance and risk factors associated with community-acquired urinary tract infections caused by *Escherichia coli* in Venezuela. Biomédica 2019; 39(Supl.1):96-106. *https://doi.org/10.7705/biomedica.v39i2.4030*
4. **Yábar MN, Curi-Pesantes B, Torres CA, Calderón-Anyosa R, Riveros M, Ochoa TJ.** Multirresistencia y factores asociados a la presencia de betalactamasas de espectro extendido en cepas de *Escherichia coli* provenientes de urocultivos. Rev Peru Med Exp Salud Pública 2017; 34(4):660-665. *https://doi:10.17843/rpmesp.2017.344.2922*
5. **Magiorakos AP, Srinivasan A, Carey RB, Carmeli Y, Falagas ME, Giske CG, Harbarth S, Hindler JF, Kahlmeter G, Olsson-Liljequist B, Paterson DL, Rice LB, Stelling J, Struelens MJ, Vatopoulos A, Weber JT, Monnet DL.** Multidrug-resistant, extensively drug-resistant and pandrug-resistant bacteria: an international expert proposal for interim standard

definitions for acquired resistance. Clin Microbiol Infect 2012; 18: 268–281.

6. **León-Buitimea A, Morones-Ramírez JR, Yang JH. Peña-Miller R.** Editorial: Facing the upcoming of multidrug-resistant and extensively drug-resistant bacteria: novel antimicrobial therapies (NATs). Front Bioeng Biotechnol 2021; 9:636278. *https://doi: 10.3389/fbioe.2021.636278.*
7. **World Health Organization**. Antimicrobial resistance: global report on surveillance 2014. WHO; 2014. Geneva.
8. **Millán Y, Hernández E, Millán B, Araque M**. Distribución de grupos filogenéticos y factores de virulencia en cepas de *Escherichia coli* uropatógena productora de beta-lactamasa CTX-M-15 aisladas de pacientes de la comunidad en Mérida, Venezuela. Rev Argent Microbiol 2014; 46(3):175-181.
9. **Hernández E, Araque M, Millán Y, Millán B, Vielma S.** Prevalencia de β-lactamasa CTX-M-15 en grupos filogenéticos de *Escherichia coli* uropatógena aisladas en pacientes de la comunidad de Mérida, Venezuela. Invest Clín 2014; 55(1):32-43.
10. **Karen C. Carroll; Michael A. Pfaller; Marie Louise Landry; Robin Patel; Alexander J. McAdam; Sandra S. Richter; D. W. Warnock.** Eds. Manual of Clinical Microbiology (ASM Books) 12th Ed. 2019. Washington (DC).
11. **Clinical and Laboratory Standards Institute.** Performance Standards for Antimicrobial Susceptibility Testing; 32th. Informational Supplement. CLSI Document M100-S27. Clinical and Laboratory Standards Institute, Wayne, PA.USA. 2022.
12. **Marcos-Carbajal P, Galarza-Pérez M, Huancahuire-Vega S, Otiniano-Trujillo S, Soto-Pastrana J.** Comparación de los perfiles de resistencia antimicrobiana de *Escherichia coli* uropatógena e incidencia de la producción de betalactamasas de espectro extendido en tres establecimientos privados de salud de Perú. Biomédica 2020; 40(Supl.1): 139-147. *https://doi.org/10.7705/biomedica.4772.*
13. **Quijada-Martínez P, Flores-Carrero A, Labrador I, Araque M**. Estudio clínico y microbiológico de las infecciones urinarias asociadas a catéter en los servicios de medicina interna de un hospital universitario venezolano. Rev Peru Med Exp Salud Pública 2017; 34(1):52-61.
14. **Quijada-Martínez P, Flores-Carrero A, Labrador I, Millán Y, Araque M.** Molecular characterization of multidrug-resistant Gram-negative bacilli producing catheter–associated urinary tract infections in internal medicine services of a Venezuelan University Hospital. Austin J Infect Dis 2017; 4(1): id1030.
15. **Millán Y, Araque M. Ramírez A.** Distribución de grupos filogenéticos, factores de virulencia y susceptibilidad antimicrobiana en cepas de *Escherichia coli* uropatógena. Rev Chilena Infect. 2020; 37(2):117-23.
16. **Anger, JT, Bixler BR, Holmes, RS, Lee, UJ, Santiago-Lastra, Y, Selph SS**. Updates to recurrent uncomplicated urinary tract infections in women: AUA/CUA/SUFU Guideline. J Urology 2022; 208: 536-54. *https://doi.org/10.1097/JU.0000000000002860.*

Invest Clin 64(4): 533 - 538, 2023 https://doi.org/10.54817/IC.v64n4a10

Evaluation of myocardial infarction by a 12-lead routine electrocardiogram: a case report of an ST-segment elevation.

Huayong Jin, Lijiang Ding, Binglei Li and Jianming Zhang

Department of ECG Room, Shaoxing People's Hospital, Zhejiang Province, China.

Keywords: electrocardiogram; spiked helmet sign; ST-segment elevation; myocardial infarction.

Abstract. The spiked helmet sign (SHS) is a type of ST-segment elevation associated with critical cardiac disease and a high risk of death. We report a case of SHS caused by an ECG artifact. A 60-year-old male patient presented to the clinic after suffering an electric shock. The initial 12-lead routine electrocardiogram showed an SHS. The patient received appropriate intravenous fluid replacement therapy, and after 30 minutes, the ST-T changes of the 12-lead electrocardiogram were all restored to normal. The patient was discharged after a 24-hour observation period in the emergency room. Recent studies have pointed out that there may be two different types of SHS. One is the mechanical factor, and the other is the significant prolongation of the QT interval. The two types have different clinical significance. In our report, the radial artery of the patient's right wrist pulsed strongly, and after the occurrence of SHS, the SHS disappeared after adjusting the contact position of the electrode in his right arm. This SHS caused by mechanical traction was an ECG artifact. Although the SHS may be an essential indicator of critical illness, there are mechanical factors that lead to the appearance of ECG artifacts. Therefore, in clinical work, obtaining a complete medical history and primary conditions of the patient at the time of ECG sampling is necessary to help the diagnosis and thus avoid erroneous treatment.

Corresponding author: Jianming Zhang. Department of ECG Room, Shaoxing People's Hospital, Shaoxing 312000, Zhejiang Province, China. E-mail: zjsxzjm@163.com

Evaluación del infarto de miocardio mediante un electrocardiograma de rutina de 12 derivaciones: reporte de un caso de elevación del segmento ST.

Invest Clin 2023; 64 (4): 533 – 538

Palabras clave: electrocardiograma; signo del casco prusiano; elevación del segmento ST; infarto del miocardio.

Resumen. El signo del casco prusiano (signo del casco con púa-SHS) es un tipo de elevación del segmento ST asociado con enfermedad cardíaca crítica y un alto riesgo de muerte. Presentamos un caso de SHS causado por un artefacto del ECG. Un paciente varón de 60 años acudió a la clínica tras sufrir una descarga eléctrica. El electrocardiograma de rutina inicial de 12 derivaciones mostró un SHS. El paciente recibió una terapia de reposición de líquidos por vía intravenosa adecuada y, después de 30 minutos, los cambios ST-T del electrocardiograma de 12 derivaciones se normalizaron. El paciente fue dado de alta después de un período de observación de 24 horas en la sala de emergencias. Estudios recientes han señalado que puede haber dos tipos diferentes de SHS. Uno debido a un factor mecánico y el otro es la prolongación significativa del intervalo QT. Los dos tipos tienen un significado clínico diferente. En nuestro reporte, la arteria radial de la muñeca derecha del paciente pulsaba con fuerza, y después de la aparición del SHS, este desapareció después de ajustar la posición de contacto del electrodo en su brazo derecho. Este SHS causado por tracción mecánica era un artefacto del ECG. Aunque el SHS puede ser un indicador esencial de enfermedad crítica, existen factores mecánicos que conducen a la aparición de artefactos en el ECG. Por lo tanto, en la práctica clínica, es necesario obtener una historia clínica completa y observar las condiciones primarias del paciente en el momento de la toma de muestras del ECG para ayudar al diagnóstico y así evitar un tratamiento erróneo.

Received: 19-06-2023 Accepted: 05-08-2023

INTRODUCTION

The ST-segment elevation is typical in acute myocardial infarction. In 2011, Littmann et al. reported a particular type of ST-segment elevation, which presented as ST-segment inferior oblique elevation with baseline superior oblique elevation of the QRS wavefront and a sharp R wave. Because of its graphic characteristics similar to the shape of the pointed helmet used by German soldiers, this electrocardiogram (ECG) finding was named the spiked helmet sign (SHS) [1]. In the existing literature, SHS is usually associated with critical illnesses such as acute myocardial infarction and predicts very poor clinical outcomes, including death[2,3]. However, the mechanism and clinical significance of SHS is still unclear.

ECG artifacts caused by various interferences are often encountered in clinical work [4]. Although common interferences can be identified in combination with ECG morphology and clinical manifestations of

patients, some can also manifest as severe heart diseases, such as acute myocardial infarction, which is difficult for even experienced clinicians to identify. This case reports the ECG manifestations of a patient who initially developed false SHS after an electric shock.

CASE DESCRIPTION

A 60-year-old man with no previous history of critical illness presented with head, chest, hip, and left elbow pain one hour after a fall. The patient was found lying on the ground at work one hour before. The patient's co-workers claimed that he was injured due to a fall. The patient recalled the scene then and claimed that an electric shock caused it. The patient had an episode of transient coma and recovered spontaneously without nausea, vomiting, convulsions, or dyspnea. At the time of presentation, the patient's temperature was 36.6 ℃, heart rate was 90 beats per minute, blood pressure was 150/70 mmHg, and oxygen saturation was 95%. The results of the physical examination were mild respiratory sounds in both lungs, normal heart sounds, no evident murmur, warm limbs, about 1% of a third-degree burn area on the forearm of the left upper limb, movable limbs, and palpable *dorsalis pedis* artery pulsation. A CT scan of the skull revealed swelling of the right scalp soft tissue. Creatine kinase and creatine kinase-MB were 953.7U/L and 27U/L, respectively, which were higher than normal values. A 12-lead electrocardiogram (Fig. 1) revealed an SHS: lead (I, II, AVL, and AVF) showed an ST elevation of 0.05–0.1 mV with T-wave inversion, the lead AVR showed an ST depression of 0.05mm with T-wave bidirectional changes, and QT interval extended to 460 ms. During this period, the radial artery of the patient's right wrist pulsated strongly, and the SHS phenomenon disappeared after adjusting the contact position of the right arm electrode. After that, the patient received appropriate intravenous rehydration therapy. After 30 minutes, the 12-lead electrocardiogram (Fig. 2) was reviewed, and all the ST-T changes in the electrocardiogram returned to normal. The patient was discharged without any abnormality after 24 hours of observation in the emergency department.

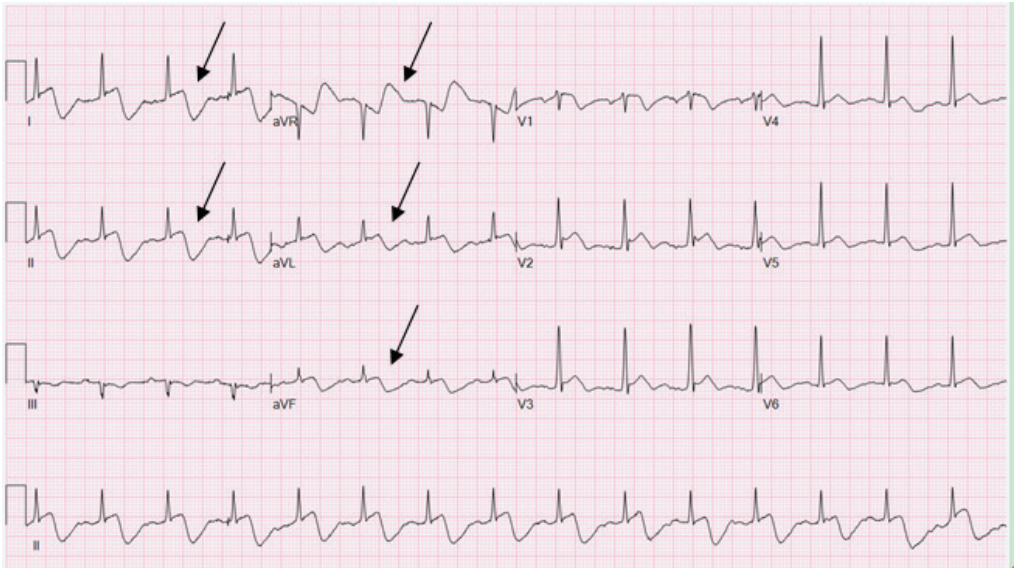

Fig. 1. The patient presented with a 12-lead routine ECG. Arrows indicate ST elevation of 0.05-0.1mv with T-wave inversion in leads I, II, AVL, and AVF, and ST depression of 0.05mv in lead AVR with bidirectional changes in T-wave.

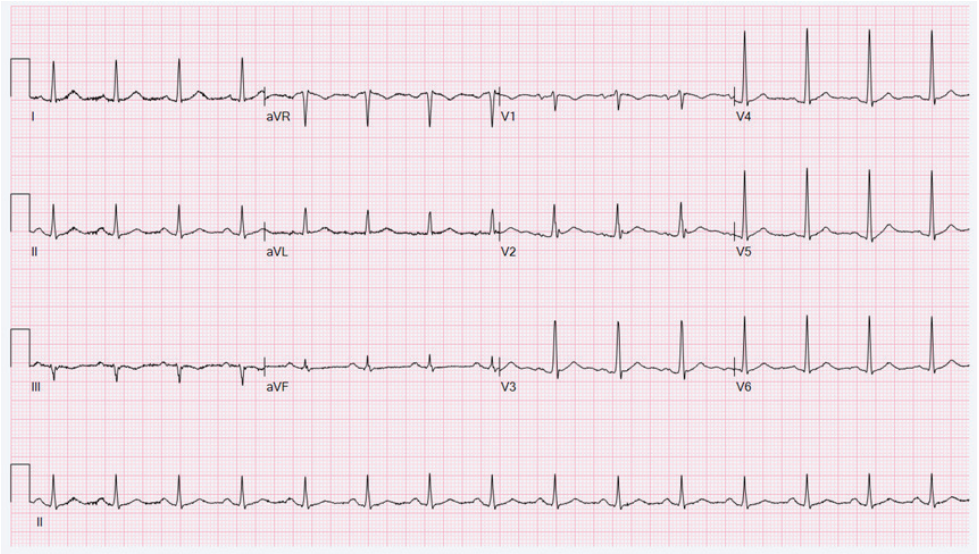

Fig. 2. The patient's ECG reviewed after 30 minutes. ST-T in leads I, II, AVR, AVL, and AVF returned to normal.

DISCUSSION

In the twelve years since the SHS was first reported in 2011, several communications have portrayed the SHS as an indicator of critical illness and poor prognosis, with an alarming post-emergence mortality rate of 59% [5]. However, recent studies have divided the SHS into two types. The prolongation of the QT interval causes one, and the other is caused by the superposition of mechanical factors, which may be an ECG artifact [6].

Experimental data show that physical stretching of the skin can produce a voltage of several millivolts [7]. The conductivity of ion channels in the heart will be changed under the pull of different tensions, affecting myocardial cells' action potential and changing the ECG pattern [8]. In addition, recent studies support the conclusion that mechanical factors contribute to the SHS. When Tomcsányi et al. placed the ECG lead over the arteriovenous fistula in the left arm of a hemodialysis patient, the ECG showed SHS, whereas when the electrodes were placed further on the normal epidermis, the SHS disappeared, meaning that SHS was caused by pulsatile epidermal stretching [6]. Agarwal *et al.* reported that an SHS appeared in the ECG of a 77-year-old male patient who used mechanical ventilation when the pressure in the chest cavity increased, obviously due to excessive positive end-expiratory pressure, but disappeared after reducing positive end-expiratory pressure [9]. In this case, when compared with the ECG image in Fig. 1, we found no dynamic changes in ST-T in Lead III. According to Einstein's triangle theory, Lead III was the potential difference between the left arm and left leg. When the artifact came to the right arm, there was an interference artifact in leads I and II, and Lead III remained normal. The patient's right wrist radial artery was beating strongly, and the ECG showed SHS, whereas the ECG disappeared after adjusting the position of the right arm electrode contact, similar to the case reported by Tomcsányi [10]. Therefore, in our case, the SHS was an ECG artifact caused by mechanical traction.

The SHS phenomenon can be produced when limb lead electrodes are placed on the radial artery, indicating acute ST-segment elevation muscular infarction (STEMI). Although an SHS may be an essential indicator of critical diseases, we must identify other

conditions that can cause SHS and remain vigilant. Obtaining a complete medical history and the patient's basic situation during ECG sampling can help clarify the truth of ECG performance, thus avoiding wrong diagnosis and over-treatment.

Conflict of competence

The authors declare no conflict of interest.

Funding

The research is supported by 2022 Zhejiang Provincial Health Science and Technology Plan, Promotion and Application of ECG Remote Intelligent Network Transmission and Report Writing Standards in Grassroots Hospitals (No.: 2022ZH061).

Authors' Orcid Number

- Huayong Jin (HJ): 0009-0008-2326-5884
- Lijiang Ding (LD): 0009-0006-1889-1384
- Binglei Li (BL): 0009-0005-5803-120X
- Jianming Zhang (JZ): 0009-0007-1433-8087

Contribution of authors to the papers

Substantial contributions to conception and design: HJ, LD. Data acquisition, data analysis, and interpretation: BL, JZ. Drafting the article or critically revising it for important intellectual content: HJ, LD. Final approval of the version to be published**:** All authors. Agreement to be accountable for all aspects of the work in ensuring that questions related to the accuracy or integrity of the work are appropriately investigated and resolved: Huayong Jin, Lijiang Ding, Binglei Li, Jianming Zhang. Huayong Jin and Lijiang Ding contributed equally to this work as co-first authors.

REFERENCES

1. **Littmann L, Monroe MH**. The "spiked helmet" sign: A new electrocardiographic marker of critical illness and high risk of death. In: *Mayo Clin Proc 2011;*86:1245-1246. *https://doi.org/10.4065/mcp.2011.0647*.
2. **Hamade H, Jabri A, Yusaf A, Nasser MF, Karim S**. The spiked helmet sign: a concerning electrocardiographic finding. JACC Case Reports 2021; 3(11): 1370-1372. *https://doi.org/10.1016/j.jaccas.2021.04.048*.
3. **Oluyadi F, Theetha Kariyanna P, Jayarangaiah A, Celenza-Salvatore J, M. McFarlane I**. Helmet sign on EKG: a rare indicator of poor prognosis in critically ill patients. Am J Med Case Reports 2019; 7(10): 260-263. *https://doi.org/10.12691/ajmcr-7-10-9*.
4. **Littmann L**. Electrocardiographic artifact. J Electrocardiol 2021; 64: 23-29. *https://doi.org/10.1016/j.*jelectrocard.*2020.11.006*.
5. **Mahmoudi E, Hui JMH, Leung KSK, Satti DI, Athena Lee YH, Christien Li KH, Hei Lau DH, Ming Kot TK, Ciobanu A, Bazoukis G, Kai Chan JSh, Baranchuk A.** Spiked helmet rlectrocardiographic sign-A systematic review of case reports. Curr Probl Cardiol 2023; 48(3): 101535. *https://doi.org/10.1016/j.cpcardiol.2022.101535*.
6. **Tomcsányi J, Bózsik B**. Two forms of the spiked helmet sign are caused by two separate mechanisms. J Electrocardiol 2022; 73: 129-130. *https://doi.org/10.1016/j.jelectrocard.*2019*.07.012*.
7. **Edelberg R**. Local electrical response of the skin to deformation. J Appl Physiol 1973; 34(3): 334-340. *https://doi.org/10.1152/jappl.1973.34.3.334*.
8. **Weise LD, Panfilov AV.** Correction: A discrete electromechanical model for human cardiac tissue: Effects of stretch-activated currents and stretch conditions on restitution properties and spiral wave dynamics. PLoS One 2013; 8(6): e59317. *https://doi.org/10.1371/*annotation*/9ceadf50-eb8f-4051-9e41-772884d47385*.

9. Agarwal A, Janz TG, Garikipati N V. Spiked helmet sign: An under-recognized electrocardiogram finding in critically ill patients. Indian J Crit Care Med 2014; 18(4): 238-240. *https://doi.org/10.4103/0972-5229.130576*.

10. Tomcsányi J. EKG-gyöngyszem: akut coronaria szindróma gyanúját keltő EKG-műtermék–poroszsisak-jel. Orv Hetil 2021; 162(34): 1383-1385.

Invest Clin 64(4): 539 - 556, 2023 https://doi.org/10.54817/IC.v64n4a11

Antifúngicos: lo que tenemos, lo que tendremos, lo que queremos.

Dilia Martínez-Méndez[1], Mariolga Bravo-Acosta[2] y Neomar Semprún-Hernández[1]

[1]Unidad de Inmunología "Nola Montiel". Maracaibo. Venezuela.
[2]Servicio de Medicina Interna, Hospital General Guasmo Sur. Guayaquil, Ecuador.

Palabras clave: antimicóticos; micosis; enfermedad fúngica invasiva; resistencia antimicrobianos; nuevos antifúngicos.

Resumen. Se estima que 300 millones de personas padecen alguna infección fúngica y 1,5 millones fallecen anualmente a consecuencia de ella, similar a la mortalidad por tuberculosis y tres veces más que por malaria. Cifras que pueden ser mayores pues las micosis no son de denuncia obligatoria. Con las lecciones aprendidas durante la pandemia por SARS-CoV-19, el brote 2022 por viruela del mono, la resistencia a los antibacterianos y el reconocimiento por la OMS que las micosis reciben poca atención y recursos, sumado a que los antifúngicos disponibles poseen importantes efectos adversos, escasa biodisponibilidad oral y creciente resistencia, se hace imperativo el desarrollo de nuevos antifúngicos con mejores características farmacocinéticas y farmacodinámicas, amplio espectro a costos accesibles y disponibles a nivel mundial. Es lo que queremos. Todo un reto.

Autor de correspondencia: Dilia Martínez-Méndez. Unidad de Inmunología "Nola Montiel". Maracaibo. Venezuela. Correo electrónico: dkmartinez.mw@gmail.com

Antifungals: what we have, what we will have, what we want.

Invest Clin 2023; 64 (4): 539 – 556

Keywords: antifungals; mycoses; invasive fungal disease; antimicrobial resistance; Novel antifungals.

Abstract. It is estimated that 300 million people have some fungal infection, and 1.5 million die annually because of it, similar to the mortality from tuberculosis and three times more than malaria. These numbers may be higher since mycoses are not mandatory reporting. With the lessons learned during the SARS-CoV-19 pandemic, the 2022 outbreak of Monkeypox, the resistance to antibacterial, and the recognition by the WHO that mycoses receive very little attention and resources, added to the fact that available antifungals have significant adverse effects, poor oral bioavailability and growing resistance, it is imperative to develop new antifungals with better pharmacokinetics and pharmacodynamic characteristics, a broad spectrum at affordable costs and worldwide supply. It is what we want. A huge challenge.

Recibido: 21-02-2023 Aceptado: 01-05-2023

INTRODUCCIÓN

Se estima que 300 millones de personas padecen alguna infección fúngica (aproximadamente 3.000.000 de casos de aspergilosis pulmonar crónica y 250.000 de aspergilosis pulmonar invasiva, 223.100 casos de meningitis criptocóccica complicada con VIH/SIDA, 700.000 con candidosis invasiva, 500.000 con neumonía por *Pneumocystis jirovecii*, 100.000 con histoplasmosis diseminada, 1.000.000 con keratitis fúngica y cerca de 200.000.000 con *Tinea capitis*) y al menos 1,5 millones fallecen anualmente a consecuencia de ella, cifra similar a la de mortalidad por tuberculosis y aproximadamente tres veces más a la de muertes producidas a consecuencia de la malaria, lo que las convierte en un problema de salud pública mundial [1-3]. Números alarmantes que pueden ser mayores debido a que las enfermedades fúngicas no son de denuncia obligatoria en la mayoría de los sistemas de salud con el consiguiente subregistro de casos [4].

No obstante la creciente resistencia a los antifúngicos, los disponibles poseen importantes efectos adversos y escasa biodisponibilidad oral, por lo que se hace imperativo el desarrollo de nuevos antifúngicos con mejores características farmacocinéticas y farmacodinámicas y menos efectos adversos[5]. A continuación, se describen los antifúngicos disponibles actualmente en el mercado mundial, los que están en estudios fase 3 y brevemente otras alternativas en estudio para el tratamiento de las micosis.

LO QUE TENEMOS

Polienos: (nistatina, natamicina, anfotericina B)

Los miembros de esta familia son insolubles en agua e inestables en presencia de luz. Comparten características químicas: cadenas insaturadas (tetraenos y heptaenos los de importancia clínica), un éster interno, un grupo carboxilo libre y una hexosamina lateral denominada micosamina, que es la

estructura química que se une al ergosterol formando canales o poros, lo cual permite la pérdida de iones y altera la estructura de la membrana, incrementando su permeabilidad con pérdida de proteínas y glúcidos citoplasmáticos causando la muerte celular[6] (Fig. 1). Además, se ha reportado que la anfotericina B y la nistatina, promueven la producción de especies reactivas de oxígeno (ROS) e interleucina-1β (IL-1β) alterando la viabilidad de las biopelículas de hongos filamentosos y levaduras incluso antes de la formación de los poros de membrana, confiriéndoles efectos directos e indirectos en la destrucción de los hongos [7,8]. El mecanismo de resistencia a los polienos consiste en reducir la síntesis de ergosterol (C5-6 esterol desaturasa) y reducir la producción de ROS con alteración mitocondrial; efecto observado en *Candida tropicalis* y algunas especies de *Aspergillus* [9,10].

La nistatina (1951), aislada a partir de cultivos de *Streptomyces noursei*, tiene actividad sobre levaduras del género *Candida*. No se absorbe por vía oral ni cutánea, empleándose la vía tópica en la candidosis vaginal, orofaríngea y en la infección gastrointestinal en inmunocomprometidos[11]. En modelos murinos, los ensayos combinando nistatina con Intralipid® (emulsión lipídica para perfusión intravenosa), demostraron que puede administrarse de forma sistémica con muy buena respuesta contra la candidosis y aspergilosis sistémica [12,13], pero su uso endovenoso no ha sido autorizado en humanos.

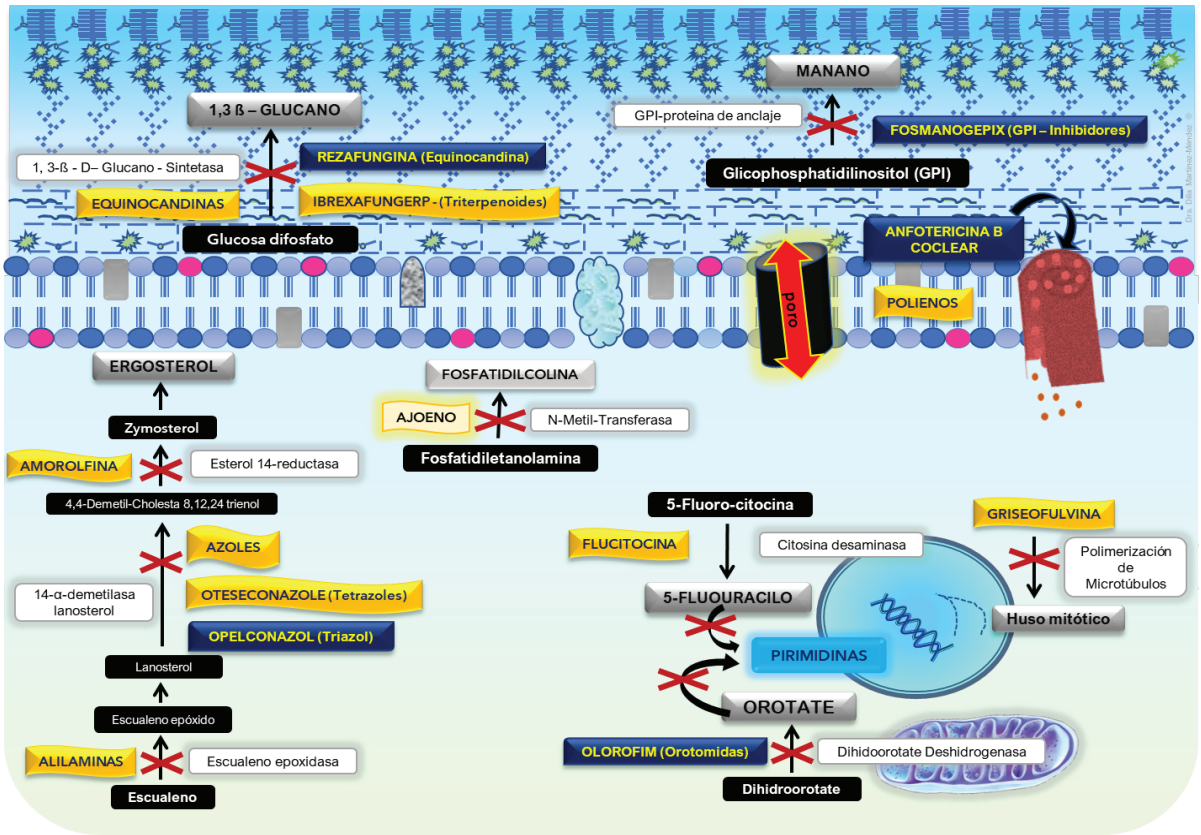

Fig. 1. Mecanismos de acción y dianas de los antifúngicos disponibles (rectángulo amarillo) y los antifúngicos en desarrollo (rectángulo azul), señalando la enzima inhibida (rectángulo blanco) y el punto de la ruta metabólica afectada (equis).

La natamicina (1955), derivada del *Streptomyces natalensis*, ha sido empleada en el tratamiento de la queratitis micótica por *Aspergillus spp., Acremonium* spp., *Fusarium spp.* y algunas especies de *Candida*[14, 15]. Los análogos sintéticos de la natamicina carecen de micosamina, por lo que no se unen a los esteroles de membrana, empleándose en la industria alimentaria para prevenir la contaminación por mohos [16].

La anfotericina B (1959) (AmB), aislada del *Streptomyces nodosus* obtenido en muestras de suelo del río Orinoco, debe su nombre a las características anfotéricas de la molécula. Con más de 50 años en el mercado (Fig. 2), sigue siendo considerada el *Gold standard* (Estándar de oro). en el tratamiento de las micosis sistémicas, sin embargo, a pesar de que los siete enlaces dobles en su estructura química le confieren mayor selectividad por el ergosterol que por el colesterol de membrana [17-20], la nefrotoxicidad es el principal efecto adverso, atribuible probablemente, a la utilización de desoxicolato y fosfato sódico como excipiente [21]. En la búsqueda de reducir los efectos adversos manteniendo el mismo espectro, en 1991 salió al mercado la primera formulación lipídica compuesta de fosfatidilcolina hidrogenada de soja: la anfotericina B liposomal (ABL), en 1994, la presentación en dispersión coloidal (ABDC), asociada a discos de sulfato de colesterol y en 1995 la anfotericina B complejo lipídico (ABCL), asociada a L-dimiristofosfatidilcolina y L-dimiristofosfatidilglicerol [22]. Con excelente respuesta terapéutica, tolerancia y menos efectos adversos, su principal limitación es el costo.

La nistatina, la anfotericina B desoxicolato y la AmB liposomal forman parte de la lista de medicamentos esenciales de la Organización Mundial de la Salud (OMS) [23].

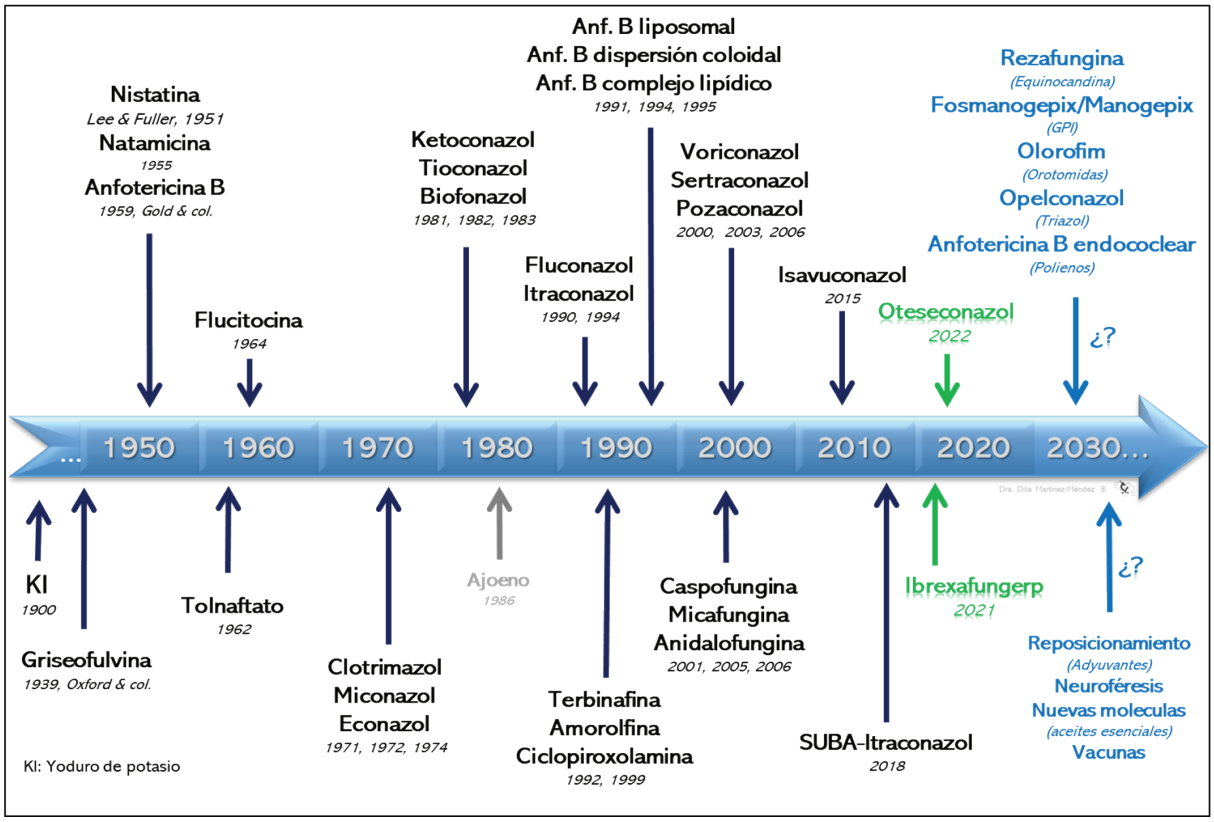

Fig. 2. Evolución histórica de los antifúngicos y las nuevas alternativas en desarrollo.

Azoles (imidazoles, triazoles, tetrazoles)

Los azoles son compuestos aromáticos heterocíclicos en los que uno o más átomos de carbono (C) son sustituidos por átomos de nitrógeno (N) que se unen mediante enlaces C-N a otros anillos aromáticos, formando cadenas con diferencias en las propiedades farmacodinámicas y farmacocinéticas [24]. Inhiben la 14-α-esterol-desmetilasa, dependiente de la citocromo P450, acumulando metil-esteroles que son tóxicos para la membrana fúngica, evitando la síntesis del ergosterol (Fig. 1) [24, 25].

Los imidazoles son: clotrimazol, miconazol, econazol, bifonazol, tioconazol, ketoconazol, sertraconazol (imidazol + grupo benzotifeno) y los triazoles: fluconazol, itraconazol, voriconazol, posaconazol, isavuconazol, SUBA-itraconazol (*Super-Bioavailability*-Itraconazol): los miembros de esta familia poseen buena absorción por vía oral (incrementada con pH ácido) y son bien tolerados, sin embargo, por su metabolismo de primer paso hepático, presentan interacción farmacológica con inhibidores o inductores de las enzimas del sistema del citocromo P450, son hepatotóxicos y pueden prolongar el intervalo QT [26-28]. En pacientes con patología renal deben monitorizarse continuamente, siendo el más seguro para estos pacientes el isavocunazol, pues por su alta solubilidad no se asocia a ciclodextrina, reduciendo la nefrotoxicidad [24].

La resistencia a los azoles está asociada a: a) la ruta de la síntesis del ergosterol por mutación del gen ERG11 que modifica el sitio diana y/o mutaciones puntuales en ERG3 e inactivación de la C5 esterol desaturasa, b) la sobreexpresión de trasportadores por modificación del CDR1/CDR2 y MDR1 con mutaciones en los factores de transcripción TAC1 y MRR1, incrementando el eflujo extracelular de la droga, c) la síntesis de biopelículas (*biofilm*) y d) las especies genéticamente resistentes a los azoles [9, 29].

Se utilizan en la profilaxis y tratamiento de infecciones fúngicas por *Aspergillus* spp, *Candida* spp, *Cryptococcus* spp, *Histoplasma* spp., *Coccidioides* spp. *Cladophialophora* spp, *Sporotrix* spp. *Fusarium* spp, *Lomentospora* spp., *Scedosporium* spp., *Rasamsonia, Schizophyllum, Scopulariopsis, Paecilomyces, Penicillium, Talaromyces* spp. *Purpureocillium* spp., *Rasamsonia* spp, *Schizophyllum* spp., *Scopulariopsis* spp., *Paecilomyces* spp *Cladophialophora* spp. Las dosis deben ajustarse según lo recomendado por las guías prácticas recientes pues son dosis y especie dependiente [17, 20, 30-32].

El fluconazol, el itraconazol y el voriconazol forman parte de la lista de medicamentos esenciales de la OMS [23].

Equinocandinas (caspofungina, micafungina, anidulofungina)

Las equinocandinas son lipopéptidos semi-sintéticos. La caspofungina (1989), derivada de *Glarea lozoyensis,* la micafungina (1990) de *Coleophoma empedri* y la anidulofungina (1974) del *Aspergillus nidulans*. Disponibles en el mercado en 2001, 2005 y en el 2006 respectivamente (Fig. 2) [33]. Inhiben la síntesis del β-1-3-D-glucano, el polisacárido estructural más importante de la pared celular, uniéndose a la subunidad FKS de la enzima β-1-3-D-glucano sintetasa inhibiendo la actividad catalítica que polimeriza la glucosa difosfato en fibras de D-glucano con enlaces β-1,3, provocando lisis por edema celular (Fig. 1) [29, 33]. Además, la exposición del ß-1,3-D-glucano induce la secreción de citocinas a través del receptor para ß-glucano dectina-1 favoreciendo la respuesta inmunitaria del hospedero para la eliminación del hongo [34]. Originalmente fueron fungicidas para las especies de *Candida* y recomendadas en primera línea para las candidemias en pacientes neutropénicos y no neutropénicos, candidemias sistémicas y en el tratamiento empírico de las cadidemias en unidad de cuidados intensivos (UCI) [17, 36]. En la actualidad se reporta cada vez con mayor frecuencia la presencia de mutaciones en las subunidades FKS1 y FKS2, por lo que su uso debe ser evaluado según la eficacia clínica a dosis terapéuticas[36]. Son fungistáticas para *Asper-*

gillus spp., poseen actividad limitada contra *Blastomyces dermatitidis, Histoplasma* spp. *Coccidioides* spp *y Paracoccidioides* spp y carecen de actividad contra *Criptococcus* spp*, Fusarium* spp y Zigomicetos, pues estos poseen D-glucano con enlaces β-1,4 y β1,6 con escaso D-glucano de enlaces β-1,3 [17]. Otra de las limitaciones en su uso es la formulación exclusiva por vía endovenosa (IV).

Las equinocandinas forman parte de la lista de medicamentos esenciales de la OMS [23].

Alilaminas (terbinafina, naftifina, butenafina)

La terbinafina, comercializada desde 1992 (Fig. 2) como una nueva familia para el tratamiento de la micosis superficial por dermatofitos y candidosis mucocutánea, ha demostrado utilidad en la terapia combinada de las micosis por mohos raros: *Lomentospora prolificans, Scedosporium* spp*, Purpureocillium* spp. y en feohifomicosis, con evidencia que sustenta el uso como monoterapia en el tratamiento de cromomicosis por *Cladophialophora carrionii* [20, 37, 38]. Inhibe la síntesis del ergosterol inactivando la escualeno epoxidasa, con la consecuente acumulación tóxica de escualeno (Fig. 1). La absorción por vía oral es independiente del pH gástrico y la presentación tópica se acumula en uñas [27]. El metabolismo hepático no inhibe el citocromo P450 por lo que tiene escasa interacción con otros medicamentos [38]. La naftifina y la butenafina son de uso tópico.

La terbinafina no se encuentra en la lista de medicamentos esenciales de la OMS [23].

Flucitosina (5-fluorocitosina)

La 5-fluorocitosina es una pirimidina fluorada sintetizada como agente antitumoral en 1957. En 1968 fue utilizada en el tratamiento de candidosis sistémica y criptococosis meníngea con buenos resultados[40] (Fig. 2). Ingresa al citoplasma a través de una permeasa en la membrana celular específica para citosina, donde es transformada a 5-fluorouracilo por acción de una citosina desaminasa para ser incorporado al ARN, convirtiéndose en un desoxinucleotido que compite con el uracilo y debido a la falta del terminal 3' no pueden agregarse otros nucleósidos, inhibiendo de esta forma, la síntesis proteica y del ADN fúngico [39-40] (Fig. 1). Las células de los mamíferos son incapaces de producir esta conversión. El mecanismo de resistencia se asocia a la inactivación de la permeasa en la membrana celular y la disminución de la acción enzimática de la citosina desaminasa [39, 40].

Se absorbe por vía oral con poca fijación en proteínas. Tiene amplia distribución en órganos, atraviesa la barrera hematoencefálica (BHE) logrando concentraciones en líquido cefalorraquídeo (LCR) de 60 a 70%[41]. El mejor efecto antimicótico se consigue a concentraciones plasmáticas de 50 a 100 mg/mL Los efectos adversos se asocian a la toxicidad de los tejidos en rápido crecimiento, como la médula ósea o las células epiteliales de la mucosa gastrointestinal. El riesgo de hipoplasia de médula ósea aumenta en tratamientos prolongados a concentraciones plasmáticas >100 mg/mL [39]. El espectro antifúngico en terapias combinadas incluye meningitis por *Cryptococcus* spp. y en casos de cromomicosis, con resultados alentadores [41-43].

La fluorocitosina se encuentra en la lista de medicamentos esenciales de la OMS [23].

Griseofulvina

Derivada del *Penicillium griseofulvum*, se describe su uso por primera vez en 1939[44] (Fig 2). Se une a la queratina de piel, pelos y uñas formando un complejo queratina-griseofulvina. Cuando los dermatofitos se unen a la queratina, la griseofulvina se fija en la tubulina fúngica inhibiendo el ensamblaje de los microtúbulos del huso mitótico evitando la división celular, así, las células sanas van reemplazando a las infectadas (Fig 1) [37, 44]. Con excelente respuesta en el manejo de las dermatofitosis por *Microsporum canis* y algunos *Trichophyton* spp. (hongos queratinofílicos y queratinolíticos) [37]. Se administra por vía oral y su absorción se incre-

menta al acompañarla con alimentos grasos. Posee metabolismo de primer paso hepático, por lo que puede generar interacción con otros fármacos [44].

La griseofulvina se encuentra en la lista de medicamentos esenciales de la OMS [23].

Yoduro de potasio

Descrito para el tratamiento de esporotricosis a principios de 1900 (Fig. 2), el yoduro de potasio es una sal compuesta por 76% de yodo y 24% de potasio, soluble en agua y fotosensible [45,46]. Sigue siendo una alternativa en el tratamiento de esporotricosis refractarias a itraconazol y terbinafina [46]. Se han reportado casos exitosos con curación total sin recidivas en el tratamiento de esporotricosis linfocutánea diseminada y basidiobolomicosis [45-49] y representa una excelente alternativa terapéutica costo/beneficio. El mecanismo de acción se relaciona con la quimiotaxis de neutrófilos que lesiona el granuloma favoreciendo la fagocitosis del *Sporothrix* spp. Recientemente, se ha descrito que inhibe la formación de biopéliculas en la forma saprófita y en la patógena de *Sporothrix schenckii species complex* [48]. Los efectos adversos más frecuentes se relacionan con el tracto digestivo y síntomas de yodismo; y con tratamientos prolongados puede desarrollarse toxicidad por potasio, hiper o hipotiroidismo [46].

El yoduro de potasio se encuentra en la lista de medicamentos esenciales de la OMS [23].

Tolnaftato (tiocarbamatos)

Derivado del tiocarbamato, es un inhibidor selectivo, reversible y no competitivo de la escualeno-2,3-epoxidasa, inhibiendo la síntesis de ergosterol [40]. Aunque comparte el mecanismo de acción con las alilaminas, no pertenece a la misma familia. Se emplea por vía tópica y tiene espectro reducido contra dermatofitos y algunas formas no inflamatorias de infección por *Malassezia* spp [27,51].

El tolnaftato no se encuentra en la lista de medicamentos esenciales de la OMS [23].

Ciclopiroxolamina (hidroxipiridona)

Es un derivado de la hidroxipiridona comercializado como antimicótico de uso tópico desde 1999 (Fig. 2) [52]. Activo frente a onicomicosis por dermatofitos, candidosis cutánea, *Pitiriasis versicolor* y dermatitis seborreica, también muestra efectividad contra algunas bacterias Gram negativas [53]. Actúa en varios aspectos del metabolismo y crecimiento celular pues quela cationes de hierro y aluminio, inhibiendo las enzimas dependientes de metales como las catalasas, peroxidasas y citocromos, con la consecuente alteración en el transporte transmembrana de electrolitos y aminoácidos [54]. La depleción de hierro también afecta la ribonucleótido reductasa, lesionando la replicación y reparación del ADN [55]. Además, inhibe la cascada del ácido araquidónico, confiriéndole actividad antiinflamatoria [53]. Debido a su mecanismo de acción está siendo estudiado como antineoplásico y en el tratamiento de la enfermedad poliquística del riñón [55, 56].

La ciclopiroxolamina no se encuentra en la lista de medicamentos esenciales de la OMS[23].

Amorolfina (morfolina)

Es un derivado de la morfolina, comercializado como antimicótico de uso tópico desde 1981 [52] (Fig. 2). Inhibe la 14-delta-reductasa y la 7-8 delta isomerasa, enzimas en la vía de la síntesis del ergosterol [57] (Fig. 1). Con buena respuesta terapéutica en las onicomicosis por dermatofitos y mohos como *Alternaria* spp*., Hendersonula* spp*., Scopulariopsis* spp. y en micosis superficiales por algunas levaduras del género *Candida* spp. y *Malassezia* spp [52].

La amorolfina no se encuentra en la lista de medicamentos esenciales de la OMS [23].

LO QUE TENEMOS DE NUEVO

Ibrexafungerp (Brexafemme®)

El ibrexafungerp es, hasta la fecha, la única molécula perteneciente a una nueva familia de antifúngicos, los triter-

penoides[58] (Fig. 2). Derivado semisintético de la enfumafungina, inhibe la enzima 1,3-β-glucanosintetasa evitando el ensamblaje del β-1-3-D-glucano de la pared celular (Fig. 1), mecanismo de acción que comparte con las equinocandinas pero a diferencia de estas, con menos inhibición del complejo enzimático citocromo P450 disminuyendo la interacción con otras drogas [59, 60]. Puede administrarse por vía oral o IV La solubilidad es pH dependiente, mejorando la biodisponibilidad en medio ácido. Estudios *in vitro* reportan actividad contra *Candida* spp. incluso las que expresan mutación en la subunidad Fskp resistentes a las equinocandinas, *Aspergillus* spp. resistentes a los azoles, *Lomentospora prolificans*, *Paelomyces variotti* y *Pneumocistis jiroveci* en pacientes inmunocomprometidos [61,62]. Sin embargo, expresan poca actividad contra *Mucor* spp y *Fusarium* spp, pues estos tienen menos β-1-3-D-glucano en su pared [62]. Ha sido aprobada por la FDA en junio de 2021 solo para el tratamiento de la vulvovaginitis severa por *Candida* spp. en tabletas de 150 mg [59] y en diciembre de 2022 se aprobó la indicación para prevenir candidosis vaginal recurrente.

Oteseconazol (tetrazol)

Perteneciente a la nueva generación de azoles: los tetrazoles, con cuatro átomos de nitrógeno que le confieren mayor especificidad por la enzima fúngica Cyp51 (lanosterol 14α-desmetilasa) que por el complejo enzimático CYP450 del humano y aunque comparte el mecanismo de acción con los triazoles (Fig. 1), tiene mayor selectividad para enzimas fúngicas y potencialmente menos efectos adversos e interacciones farmacológicas [63]. Se le describe actividad contra especies *Candida* incluyendo las resistentes a fluconazol, *Coccidioides* spp., *Cryptococcus* spp, *Histoplasma capsulatum*, *Blastomyces dermatitidis* y especies de *Trichophyton*, por lo que también se ensaya su uso en onicomicosis [59, 63, 64]. Los mecanismos de resistencia son los mismos descritos para los triazoles. En abril de 2022 la FDA aprobó su uso por vía oral en la candidosis vaginal recurrente en dosis de 600 mg el día 1, 450 mg el día 2 y luego comenzando el día 14, 150 mg una vez por semana por 11 semanas, cuando se usa como monoterapia y cuando se combina con fluconazol en régimen pulsátil, se inicia con fluconazol una vez al día los días 1, 4 y 7 luego oteseconazol una vez al día los días 14 a 20 y una vez a la semana a partir del día 28 durante 11 semanas (semanas 4 a 14) [65].

LO QUE TENDREMOS

Olorofim (orotomidas)

Es el primer miembro de una nueva familia: las orotomidas, cuya diana es la síntesis de ácidos nucleicos. El olorofim inhibe la enzima dihidroorotato deshidrogenasa evitando el paso de dihidroorotato a orotato en la vía de síntesis de la citosina (Fig. 1)[66]. En presentación oral y endovenosa, posee alta unión a proteínas y baja solubilidad en agua. Su actividad antifúngica es tiempo dependiente, llegando a ser fungicida contra algunas especies de *Aspergillus, Coccidioides* spp, *Histoplasma* spp, *Taloromyces marnefeffei, Madurella mycetomatis, Fusarium* spp. *Scedosporium* spp., *Scopulariopsis* spp., *Rasamsonia* spp. y dermatofitos [59, 64]. Carece de acción contra las especies de *Candida*, Mucorales y *Exophiala dermatitidis* [64, 66].

En 2019 y otra vez en 2020, la Administración de Drogas y Alimentos de los Estados Unidos (FDA) le otorgó la designación de terapia innovadora para el tratamiento de coccidioidomicosis del sistema nervioso central (SNC) refractaria e infecciones invasivas resistentes por *Aspergillus* spp., *Fusarium* spp., *Lomentospora prolificans, Scedosporium* spp. y *Scopulariopsis* spp., en tabletas de 30mg [59, 67]. Actualmente en fase 3 del estudio OASIS [67] (*Olorofim Aspergillus Infection Study*) en donde se evalúa la eficacia y seguridad del olorofim frente al AmBisome® en pacientes con enfermedad fúngica invasiva causada por *Aspergillus* spp. cuyos resultados se esperan entre 2024 y 2025.

Rezafungina (equinocandina)

Pertenece a la familia de las equinocandinas. Es un análogo estructural de la anidalofungina, menos hepatotóxico y con vida media de hasta 150 horas luego de la segunda y tercera dosis, facilitando su administración semanal [59]. El espectro de acción es comparable con el de otros miembros de la familia, abarcando especies de *Candida* resistentes a los azoles incluyendo *C. auris*. También es eficaz contra dermatofitos y en modelos murinos ha demostrado buena respuesta terapéutica en neumonía por *Pneumocystis jirovecii* y en aspergilosis invasiva por *A. fumigatus* [3].

En agosto de 2022, se presentó la solicitud ante la FDA y ante la Agencia Europea de Medicamentos (EMA) para la autorización del uso endovenoso de rezafungina en el tratamiento de candidiasis invasiva y la profilaxis de infecciones fúngicas invasivas en pacientes sometidos a trasplante alogénico de sangre y médula. De ser aprobada, sería el primer miembro de las equinocandinas de segunda generación en salir al mercado [59, 64].

Opelconazol (PC945) (triazol)

Es un triazol para uso inhalatorio en aspergilosis pulmonar no diseminada. Se administra en nebulizaciones de partículas lipofílicas micronizadas cuya lenta absorción garantizan la concentración efectiva localizada en pulmones, disminuyendo los efectos adversos [68]. Su uso profiláctico en pacientes con leucemia linfocítica, trasplante de células madre o trasplante de pulmón lo coloca como una promisoria vía terapéutica entre los azoles [64]. Se encuentra en estudio fase 3 para evaluar la seguridad y la tolerabilidad en la profilaxis contra la aspergilosis pulmonar en receptores de trasplantes de pulmón [69].

Fosmanogepix/Manogepix (inhibidores de la glicosil-fosfatidil-inositol (GPI))

Es el primero de una nueva familia con diana de acción contra las mananoproteínas de la pared celular. Inhibe la inositol-aciltransferasa Gwt1 en la vía de maduración de la proteína anclada al GPI que es esencial para el tráfico de mananoproteínas hacia la membrana y la pared de la célula fúngica [59] (Fig. 1). Las mananoproteínas ancladas a GPI son necesarias para la integridad de la pared celular, favorecen la adherencia y la evasión del sistema inmunitario [70]. El fosmanogepix (APX001) es un profármaco que es convertido a manogepix por las fosfatasas sistémicas[64,70]. Posee amplio espectro contra especies de *Candida* incluyendo las resistentes a los azoles, menos *Pichia kudriavzevii (a*ntes *C. krusei)*. En modelos murinos, ha demostrado eficacia contra infección diseminada por *C. albicans, Nakaseomyces glabrataa* (antes *C. glabrata*), *C. auris, C. immitis, C. neoformans, F. solani* e infección pulmonar por *A. fumigatus, A. flavus, S. prolificans, S. apiospermum, R. arrhizus* (revisado en Shaw, 2020)[70]. Con un estudio en humanos en curso, se esperan resultados en el 2026 [71].

Anfotericina B endococlear (polienos)

La novedosa formulación coclear de la AmB es una estructura en espiral multicapa compuesta de un lípido cargado negativamente (fosfatidilserina) y un catión divalente (calcio^{++}), lo que protege a la AmB de la degradación gástrica, permitiendo la administración oral con importante reducción de la toxicidad, liberándose solo cuando interactúa con las células fúngicas diana. En modelos murinos de infección diseminada por *C. albicans* y *Aspergillus* spp. mostraron similar repuesta a la AmB desoxicolato por vía intraperitoneal en la supervivencia y reducción de la carga de hongos [64, 72]. Actualmente con un estudio en curso para el uso en pacientes con VIH y meningitis criptocóccica[72].

Otras opciones terapéuticas estudiadas y/o en estudio.

- El ajoeno [(E,Z)-4,5,9-tritiadodeca-1,6,11-triene 9-oxido], es un compuesto sulfurado obtenido del ajo (*Allium sativum*) [73]. Inhibe la enzima fosfatidiletanolamina n-metil transferasa (PEMT)

evitando la transformación de fosfatidiletanolamina en fosfatidilcolina, con la consecuente lesión en la biosíntesis de la fosfatidilcolina y generación de la membrana celular (Fig. 2) [73-75]. Se ha descrito también, que interfiere en el metabolismo redox reaccionando con los grupos sulfhídricos de las proteínas de membrana, lo que afecta a los procesos de adhesión y señalización [73,75,76]. Utilizado en cromomicosis, paracoccidioidomicosis, histoplasmosis y micosis superficiales por dermatofitos [43, 74, 76, 77]. El ajoeno no ha sido comercializado para su uso como antifúngico.

- El estudio de los compuestos presentes en los aceites esenciales de las lamiáceas (Orden: *Lamiales*, Familia: *Lamiaceae*), ha reportados buenos efectos *in vitro* contra especies de levaduras formadoras de biofilms [78,79].

- El reposicionamiento de medicamentos como sertralina, tamoxifeno e inhibidores de la histona desatilasa son algunos de los fármacos que se han probado como adyuvantes en el tratamiento de las micosis con resultados controversiales [5, 80].

- La neuraféresis permite la filtración del LCR y ha sido experimentado en conejos en el tratamiento de la criptococosis meníngea con resultados alentadores lo que permite proponerlo en casos graves de meningitis criptocóccica [81, 83].

- El desarrollo de vacunas contra los principales hongos patógenos sigue siendo un desafío debido a la compleja y poco conocida respuesta inmunitaria a levaduras y hongos filamentosos [32, 83].

LO QUE QUEREMOS

Durante la pandemia por el SARS-CoV-19 se demostró que el desarrollo de las actividades científicas relacionadas con la salud y la calidad de vida pueden perfeccionarse en semanas si hay inversión económica y apoyo logístico [84]. La alerta epidemiológica mundial por el brote 2022 de la viruela del mono demostró también que eliminar la palabra "endémica" de una enfermedad permite el reporte de casos, el estudio epidemiológico mundial y la visibilidad en términos clínicos, terapéuticos y preventivos, lo que favorece el desarrollo de nuevos tratamientos y métodos diagnósticos que puedan masificarse [85]. La abrumadora realidad de la resistencia por el uso indiscriminado de los antibacterianos es, igualmente, una prueba que debe motivar al uso adecuado del escaso arsenal antifúngico.

Con estas lecciones aprendidas, vemos como las micosis van dejando de ser endémicas debido a la movilidad poblacional, la dinámica migratoria, las características del esparcimiento, las relaciones humanas y el cambio climático, entendiendo que los hongos consiguen cada vez más oportunidades de infectar a la creciente cifra de personas inmunosuprimidas que suman los pacientes con cáncer, trasplantes, enfermedades infeccionas, metabólicas, terapias con corticoesteroides y pacientes en estado crítico [70, 86].

En octubre del 2022, la OMS publicó la lista de patógenos fúngicos prioritarios, dividiéndolos en tres categorías: crítica, alta y media [4]. El documento reconoce que las micosis reciben muy poca atención y recursos y enfatiza la necesidad de entender mejor la resistencia a los antifúngicos. Además, recomienda el reporte sistemático de los casos y mantener la inversión en investigación y desarrollo [4]. En enero del 2023, Venezuela incluye a las micosis dentro de las enfermedades de denuncia obligatoria [87], siendo el primer país en América.

Históricamente las micosis habían sido consideradas de baja mortalidad y las llamadas *endémicas* eran más frecuentes en personas pobres que responden bien a los antifúngicos ya comercializados. Pareciera que la industria farmacéutica ha estado in-

teresada básicamente en continuar produciendo los antifúngicos rentables, aunque tengan importantes efectos adversos. Es probable que esto esté causando la insuficiente disponibilidad mundial de antifúngicos económicos como la griseofulvina o la 5-fluorocitocina y que haya desmotivado la investigación sobre nuevas dianas terapéuticas seguras. Cierto es también que las micosis no son enfermedades raras y afectan a mucho más de 200.000 personas al año, sin embargo, llama la atención como varios de los nuevos antifúngicos han conseguido la denominación de "medicamentos huérfanos" recibiendo el *fast track* (vía rápida) en los estudios clínicos, algunos realizados en un número reducido de personas y en países de escasos recursos económicos.

Es solo con la aparición del VIH y el estudio reciente de otras inmunodeficiencias que se va transformando el panorama, entendiendo que todas las micosis pueden comportarse como oportunistas, son cosmopolitas y cada vez más frecuentes, por lo que el éxito terapéutico depende de: a) la integración del diagnóstico eficaz y oportuno, por lo que hay que formar cada vez más profesionales especializados en las micosis y sus agentes causales; b) la correcta identificación de especie, incluyendo la susceptibilidad a los antifúngicos, para ello necesitamos masificar las técnicas diagnósticas y las herramientas moleculares; c) conocer los mecanismos de resistencia; d) disponer del tratamiento adecuado: seguro, eficaz y costo efectivo y e) realizar farmacovigilancia y reporte de casos en una red de vigilancia internacional.

La necesidad de nuevas terapias antifúngicas es cada vez más crítica, las cifras y la rápida aparición de resistencia lo demandan. Para ello, los nuevos antifúngicos deberán:

1. Tener nuevos y mejorados mecanismos de acción.
2. Con menos efectos adversos.
3. Ser de amplio espectro.
4. Ser eficaces contra las biopelículas (Biofilms).
5. Tener mejores características farmacológicas.
6. Tener buena biodisponibilidad oral.
7. A costos accesibles.

Es lo que queremos. Todo un reto.

Conflicto de intereses

Los autores declaran no tener conflicto de intereses.

Financiamiento

No se recibió financiamiento para la realización de este trabajo.

Números ORCID de los autores

- Dilia Martínez-Méndez: 0000-0003-2989-2949
- Mariolga Bravo-Acosta: 0000-0002-3569-3252
- Neomar Semprún-Hernández: 0000-0002-6635-4376

Declaración de contribución por autor

DMM realizó el diseño del artículo y figuras, revisó la literatura, realizó el análisis, escribió el primer borrador y el manuscrito final. MBA realizó el análisis, revisión crítica y participó en las correcciones del material. NSH participó en el análisis y revisión crítica del material. Todos los autores contribuyeron, leyeron y aprobaron la versión del manuscrito enviado.

REFERENCIAS

1. **Firacative C.** Invasive fungal disease in humans: are we aware of the real impact? Mem Inst Oswaldo Cruz. 2020;115 [citado, 2022, febrero 18] disponible en: *https://doi.org/10.1590/0074-02760200430.*

2. **Bongomin F, Gago S, Oladele RO, Denning DW**. Global and multi-national prevalence of fungal diseases-estimate precision. J Fungi 2017;3(4):57. *https://dx.doi.org/10.3390/jof3040057*
3. **Logan A, Wolfe A, Williamson JC.** Antifungal Resistance and the role of new therapeutic agents. Curr Infect Dis Rep 2022;24(9):105-116. *https://dx.doi.org/10.1007/s11908-022-00782-5*
4. **Organización Mundial de la Salud (OMS).** Lista de patógenos fúngicos prioritários. Octubre, 2022. [citado 2022, octubre 30] disponible en: https://www.who.int/publications/i/item/9789240060241
5. **Mota Fernandes C, Dasilva D, Haranahalli K, McCarthy JB, Mallamo J, Ojima I, Del Poeta M**. The future of antifungal drug therapy: novel compounds and targets. Antimicrob Agents Chemother 2021;65(2):e01719-20. *https://dx.doi.org/10.1128/AAC.01719-20*
6. **Perea JRA, Barberán J.** Anfotericina B forma liposómica: Un perfil farmacocinético exclusivo. Una historia inacabada. Rev Esp Quimioter 2012;25(1):17-24. Disponible en: http://seq.es/seq/0214-3429/25/1/azanza.pdf
7. **Delattin N, Cammue BP, Thevissen K.** Reactive oxygen species-inducing antifungal agents and their activity against fungal biofilms. Future Med Chem 2014;6(1):77-90. *https://dx.doi.org/10.4155/fmc.13.189*
8. **Darisipudi MN, Allam R, Rupanagudi KV.** Polyene macrolide antifungal drugs trigger interleukin-1 b secretion by activating the NLRP3 inflammasome. PLOS One 2011;6(5):1-6. *https://doi.org/10.1371/journal.pone.0019588*
9. **Forastiero A, A. C. Mesa-Arango, A. Alastruey-Izquierdo.** *6* antifungal cross-resistance is related to different azole target (Erg11p) modifications. Antimicrob Agents Chemother 2013;57(10):4769–4781. *https://doi.org/10.1128/AAC.00477-13*
10. **Mesa-Arango AC, Trevijano-Contador N, Román E, Sánchez-Fresneda R, Casas C, Herrero E, Argüelles JC, Pla J, Cuenca-Estrella M, Zaragoza O.** The production of reactive oxygen species is a universal action mechanism of amphotericin B against pathogenic yeasts and contributes to the fungicidal effect of this drug. Antimicrob Agents Chemother 2014;58(11):6627-6638. *https://dx.doi.org/10.1128/AAC.03570-14*
11. **Rivera-Toledo E, Jiménez-Delgadillo AU, Manzano-Gayosso P**. Antifúngicos poliénicos. Mecanismo de acción y aplicaciones. Rev Fac Med 2020; 63(2):7-17. *https://doi.org/10.22201/fm.24484865e.2020.63.2.02.*
12. **Semis R, Nahmias M, Lev S, Frenkel M, Segal E.** Evaluation of antifungal combinations of nystatin-intralipid against *Aspergillus terreus* using checkerboard and disk diffusion methods. J Mycol Med 2015;25(1):63-70. *https://dx.doi.org/10.1016/j.mycmed.2014.12.002*
13. **Jemel S, Guillot J, Kallel K, Botterel F, Dannaoui E.** *Galleria mellonella* for the evaluation of antifungal efficacy against medically important fungi, a narrative review. Microorganisms 2020;8(3):390. *https://dx.doi.org/10.3390/microorganisms8030390*
14. **Mellado F, Rojas T, Cumsille C.** Queratitis fúngica: revisión actual sobre diagnóstico y tratamiento. Arq Bras Oftalmol 2013;76(1):52-56. *https://doi.org/10.1590/S0004-27492013000100016*
15. **Van Leeuwen MR, Golovina EA, Dijksterhuis J.** The polyene antimycotics nystatin and filipin disrupt the plasma membrane, whereas natamycin inhibits endocytosis in germinating conidia of *Penicillium discolor*. J. Appl Microbiol 2009;106(6):1908-1918. *https://dx.doi.org/10.1111/j.1365-2672.2009.04165.x*
16. **Meena M, Prajapati P, Ravichandran C, Sehrawat R.** Natamycin: a natural preservative for food applications-a review. Food Sci Biotechnol 2021;30(12):1481-1496. *https://dx.doi.org/10.1007/s10068-021-00981-1*
17. **Hoenigl M, Salmanton-García J, Walsh TJ, Nucci M, Neoh CF, Jenks JD, Lackner M, Sprute R, Al-Hatmi AMS, Bassetti M, Carlesse F, Freiberger T, Koehler P, Lehrnbecher T, Kumar A, Prattes J, Richardson M, Revankar S, Slavin MA, Stemler**

J, Spiess B, Taj-Aldeen SJ, Warris A, Woo PCY, Young JH, Albus K, Arenz D, Arsic-Arsenijevic V, Bouchara JP, Chinniah TR, Chowdhary A, de Hoog GS, Dimopoulos G, Duarte RF, Hamal P, Meis JF, Mfinanga S, Queiroz-Telles F, Patterson TF, Rahav G, Rogers TR, Rotstein C, Wahyuningsih R, Seidel D, Cornely OA. Global guideline for the diagnosis and management of rare mould infections: an initiative of the European Confederation of Medical Mycology in cooperation with the International Society for Human and Animal Mycology and the American Society for Microbiology. Lancet Infect Dis 2021;21(8):e246-e257. *https://dx.doi.org/10.1016/S1473-3099(20)30784-2* Erratum in: Lancet Infect Dis 2021;21(4):e81. PMID: 33606997.

18. **Cornely OA, Alastruey-Izquierdo A, Arenz D, Chen SCA, Dannaoui E, Hochhegger B, Hoenigl M, Jensen HE, Lagrou K, Lewis RE, Mellinghoff SC, Mer M, Pana ZD, Seidel D, Sheppard DC, Wahba R, Akova M, Alanio A, Al-Hatmi AMS, Arikan-Akdagli S, Badali H, Ben-Ami R, Bonifaz A, Bretagne S, Castagnola E, Chayakulkeeree M, Colombo AL, Corzo-León DE, Drgona L, Groll AH, Guinea J, Heussel CP, Ibrahim AS, Kanj SS, Klimko N, Lackner M, Lamoth F, Lanternier F, Lass-Floerl C, Lee DG, Lehrnbecher T, Lmimouni BE, Mares M, Maschmeyer G, Meis JF, Meletiadis J, Morrissey CO, Nucci M, Oladele R, Pagano L, Pasqualotto A, Patel A, Racil Z, Richardson M, Roilides E, Ruhnke M, Seyedmousavi S, Sidharthan N, Singh N, Sinko J, Skiada A, Slavin M, Soman R, Spellberg B, Steinbach W, Tan BH, Ullmann AJ, Vehreschild JJ, Vehreschild MJGT, Walsh TJ, White PL, Wiederhold NP, Zaoutis T, Chakrabarti A.** Mucormycosis ECMM MSG Global Guideline Writing Group. Global guideline for the diagnosis and management of mucormycosis: an initiative of the European Confederation of Medical Mycology in cooperation with the Mycoses Study Group Education and Research Consortium. Lancet Infect Dis 2019;19(12):e405-e421. *https://dx.doi.org/10.1016/S1473-3099(19)30312-3*

19. **Morales-López SE, Garcia-Effron G.** Infections due to rare Cryptococcus species. A literature review. J Fungi 2021;7:279. *https://doi.org/10.3390/jof7040279*

20. **Chen SC, Perfect J, Colombo AL, Cornely OA, Groll AH, Seidel D, Albus K, de Almedia JN Jr, Garcia-Effron G, Gilroy N, Lass-Flörl C, Ostrosky-Zeichner L, Pagano L, Papp T, Rautemaa-Richardson R, Salmanton-García J, Spec A, Steinmann J, Arikan-Akdagli S, Arenz DE, Sprute R, Duran-Graeff L, Freiberger T, Girmenia C, Harris M, Kanj SS, Roudbary M, Lortholary O, Meletiadis J, Segal E, Tuon FF, Wiederhold N, Bicanic T, Chander J, Chen YC, Hsueh PR, Ip M, Munoz P, Spriet I, Temfack E, Thompson L, Tortorano AM, Velegraki A, Govender NP.** Global guideline for the diagnosis and management of rare yeast infections: an initiative of the ECMM in cooperation with ISHAM and ASM. Lancet Infect Dis 2021;21(12):e375-e386. *https://dx.doi.org/10.1016/S1473-3099(21)00203-6* Erratum in: Lancet Infect Dis. 2021;21(12):e363.

21. **Grudzinski W, Sagan J, Welc R, Luchowski R, Gruszecki WI.** Molecular organization, localization and orientation of antifungal antibiotic amphotericin B in a single lipid bilayer. Sci Rep 2016;32780-90. *https://doi.org/10.1038/srep32780*

22. **Hamill RJ.** Amphotericin B formulations: a comparative review of efficacy and toxicity. Drugs 2013;73(9):919-934. *https://dx.doi.org/10.1007/s40265-013-0069-4*

23. **World Health Organization.** Model List of Essential Medicines, 22nd List, 2021. World Health Organization; 2021. [citado 2022, noviembre 21] Disponible en: https://www.paho.org/en/documents/22st-who-model-list-essential-medicines-eml

24. **Nocua-Báez LC, Uribe-Jerez P, Tarazona-Guaranga L, Robles R, Cortés JA.** Azoles de antes y ahora: una revisión. Rev Chilena Infectol 2020;37(3):219-230. *https://dx.doi.org/10.4067/s0716-10182020000 300219*

25. **Zonios DI, Bennett JE.** Update on azole antifungals. Semin Respir Crit Care Med 2008;29: 198-210. *https://dx.doi.org/10.1055/s-2008-1063858*

26. Maertens JA. History of the development of azole derivatives. Clin Microbiol Infect 2004;10 (Suppl 1):1-10. *https://dx.doi.org/10.1111/j.1470-9465.2004.00841.x*

27. Martín-Aragón S, Benedí J. Antimicóticos dermatológicos. Rev Farmacia Profesional 2004;18(7):38-49. Diponible en: https://www.elsevier.es/es-revista-farmacia-profesional-3-articulo-antimicoticos-dermatologicos-13064579

28. Hamdy R, Fayed B, Hamoda AM, Rawas-Qalaji M, Haider M, Soliman SSM. Essential oil-based design and development of novel anti-Candida azoles formulation. Molecules 2020;25(6):1463. *https://dx.doi.org/10.3390/molecules25061463*

29. Pristov KE, Ghannoum MA. Resistance of Candida to azoles and echinocandins worldwide. Clin Microbiol Infect 2019;25(7):792-798. *https://dx.doi.org/10.1016/j.cmi.2019.03.028.*

30. Ullmann AJ, Aguado JM, Arikan-Akdagli S, Denning DW, Groll AH, Lagrou K, Lass-Flörl C, Lewis RE, Munoz P, Verweij PE, Warris A, Ader F, Akova M, Arendrup MC, Barnes RA, Beigelman-Aubry C, Blot S, Bouza E, Brüggemann RJM, Buchheidt D, Cadranel J, Castagnola E, Chakrabarti A, Cuenca-Estrella M, Dimopoulos G, Fortun J, Gangneux JP, Garbino J, Heinz WJ, Herbrecht R, Heussel CP, Kibbler CC, Klimko N, Kullberg BJ, Lange C, Lehrnbecher T, Löffler J, Lortholary O, Maertens J, Marchetti O, Meis JF, Pagano L, Ribaud P, Richardson M, Roilides E, Ruhnke M, Sanguinetti M, Sheppard DC, Sinkó J, Skiada A, Vehreschild MJGT, Viscoli C, Cornely OA. Diagnosis and management of *Aspergillus* diseases: executive summary of the 2017 ESCMID-ECMM-ERS guideline. Clin Microbiol Infect 2018;24 Suppl 1:e1-e38. *https://dx.doi.org/10.1016/j.cmi.2018.01.002*

31. Brito D, Fernández J, Castillo MA, Azuero S, Hernández-Valles R, Saúl-García Y, Valero N, Villalobos R, Semprún-Hernández N, Martínez-Méndez D. Fluconazole and voriconazole susceptibility in oral colonization isolates of Candida spp. in HIV patients. Invest Clin. 2019;60(4): 275 – 282. *https://dx.doi.org/10.22209/IC.v60n4a02*

32. **Martínez-Méndez D, Humbría-García L, Semprún-Hernández N, Hernández-Valles R.** Auricular chromoblastomycosis: a rare presentation case and review of published literature. Rev Soc Ven Microbiol 2017; 37(1):34-36. http://www.redalyc.org/articulo.oa?id=199452813008

33. Cortés L, Jorge A, Russi N, July A. Equinocandinas Rev Chilena Infectol 2011;28(6), 529-536. *https://dx.doi.org/10.4067/S0716-10182011000700004*

34. Brown GD, Gordon S. Immune recognition: a new receptor for beta-glucans. Nature 2001;413:36–37. *https://dx.doi.org/10.1038/35092620*

35. Pappas PG, Kauffman CA, Andes DR, Clancy CJ, Marr KA, Ostrosky-Zeichner L, Reboli AC, Schuster MG, Vazquez JA, Walsh TJ, Zaoutis TE, Sobel JD. Clinical practice guideline for the management of candidiasis: 2016 Update by the Infectious Diseases Society of America. Clin Infect Dis 2016;62(4):e1-50. *https://dx.doi.org/10.1093/cid/civ933*

36. Zuza-Alves DL, Silva-Rocha WP, Chaves GM. An update on *Candida tropicalis* based on basic and clinical approaches. Front Microbiol 2017;8:1927. *https://dx.doi.org/10.3389/fmicb.2017.01927.*

37. Mikaeili A, Kavoussi H, Hashemian AH, Shabandoost Gheshtemi M, Kavoussi R. Clinico-mycological profile of *tinea capitis* and its comparative response to griseofulvin versus terbinafine. Curr Med Mycol 2019;5(1):15-20. *https://dx.doi.org/10.18502/cmm.5.1.532.*

38. Queiroz-Telles F, Esterre P, Perez-Blanco M, Vitale RG, Salgado CG, Bonifaz A. Chromoblastomycosis: an overview of clinical manifestations, diagnosis and treatment. Med Mycol 2002;47(1):3-15 *http://dx.doi.org/10.1080/13693780802538001.*

39. Vermes A, Guchelaar HJ, Dankert J. Flucytosine: a review of its pharmacology, clinical indications, pharmacokinetics, toxicity and drug interactions. J Antimicrob Chemother 2000;46(2):171–179. *https://doi.org/10.1093/jac/46.2.171.*

40. **Bhattacharya S, Sae-Tia S, Fries BC.** Candidiasis and mechanisms of antifungal resistance. Antibiotics 2020;9(6):312. *https://dx.doi.org/10.3390/antibiotics9060312*
41. **Shiri T, Loyse A, Mwenge L, Chen T, Lakhi S, Chanda D, Mwaba P, Molloy SF, Heyderman RS, Kanyama C, Hosseinipour MC, Kouanfack C, Temfack E, Mfinanga S, Kivuyo S, Chan AK, Jarvis JN, Lortholary O, Jaffar S, Niessen LW, Harrison TS**. Addition of flucytosine to fluconazole for the treatment of Cryptococcal meningitis in Africa: a multicountry cost-effectiveness Analysis. Clin Infect Dis 2020;70(1):26-29. *https://dx.doi.org/10.1093/cid/ciz163*
42. **Limper AH, Adenis A, Le T, Harrison TS.** Fungal infections in HIV/AIDS. Lancet Infect Dis 2017;17(11):e334-e343. *https://dx.doi.org/10.1016/S1473-3099(17)30303-1*
43. **Pérez-Blanco M, Hernandez R, Zeppenfeldt G, Apitz, RJ.** Ajoene and 5-fluorouracil in the topical treatment of *Cladophialophora carrionii* chromoblastomycosis in humans: A comparative open study. Med Mycol 2003;41(6):517-520. *https://dx.doi.org/10.1080/13693780310001616519*
44. **Olson JM, Troxell T.** Griseofulvin. Treasure Island (FL): StatPearls Publishing; 2021. [citado 2021, Agosto 29]. Disponible en: https://www.ncbi.nlm.nih.gov/books/NBK537323/
45. **Estrada-Castañón R, Chávez-López G, Estrada-Chávez G, Bonifaz A.** Report of 73 cases of cutaneous sporotrichosis in Mexico. An Bras Dermatol 2018;93(6):907-909. *https://dx.doi.org/10.1590/abd1806-4841.20187726*
46. **Salero-Martínez D, Bonifaz A.** Yoduro de potasio: su administración más allá de la esporotricosis. Dermatol Rev Mex 2019;63(2):228-231. *https://dx.doi.org/10.35366/91763.*
47. **Khaitan BK, Gupta V, Asati DP, Seshadri D, Ramam M.** Successful treatment outcome with itraconazole and potassium iodide in disseminated sporotrichosis. Indian J Dermatol Venereol Leprol 2018;84(1):101-104. *https://dx.doi.org/10.4103/ijdvl.IJDVL_958_16*
48. **Brilhante RSN, Silva MLQD, Pereira VS, Oliveira JS, Maciel JM, Silva INGD, Silva LG, Melo GM, Aguiar RC, Pereira-Neto W, Pires de Camargo Z, Messias A, Costa JJ, de Souza DC, Castelo-Branco M, Gadelha MF**. Potassium iodide and miltefosine inhibit biofilms of *Sporothrix schenckii* species complex in yeast and filamentous forms. Med Mycol 2019;57:764-772. *https://dx.doi.org/10.1093/mmy/myy119.*
49. **Rajan RJ, Mohanraj P, Rose W**. Subcutaneous basidiobolomycosis resembling Fournier's Gangrene. J Trop Pediatr 2017;63(3):217-220. *https://dx.doi.org/10.1093/tropej/fmw075*
50. **Ryder NS, Frank I, Dupont MC.** Ergosterol biosynthesis inhibition by the thiocarbamate antifungal agents tolnaftate and tolciclate. Antimicrob Agents Chemother 1986;29(5):858-860. *https://dx.doi.org/10.1128/AAC.29.5.858.*
51. **Jimenez-Garcia L, Celis-Aguilar E, Díaz-Pavón G, Muñoz Estrada V, Castro-Urquizo Á, Hernández-Castillo N, Amaro-Flores E.** Efficacy of topical clotrimazole vs. topical tolnaftate in the treatment of otomycosis. A randomized controlled clinical trial. Braz J Otorhinolaryngol 2020;86(3):300-307. *https://dx.doi.org/10.1016/j.bjorl.2018.12.007.*
52. **Tabara K, Szewczyk AE, Bienias W, Wojciechowska A, Pastuszka M, Oszukowska M, Kaszuba A**. Amorolfine vs. ciclopirox - lacquers for the treatment of onychomycosis. Postepy Dermatol Alergol 2015;32(1):40-45. *https://dx.doi.org/10.5114/pdia.2014.40968*
53. **Gupta AK, Plott T.** Ciclopirox: a broad-spectrum antifungal with antibacterial and anti-inflammatory properties. Int J Dermatol 2004;43(Suppl.1):3-8. *https://dx.doi.org/10.1111/j.1461-1244.2004.02380.x*
54. **Sigle HC, Schäfer-Korting M, Korting HC, Hube B, Niewerth M.** In vitro investigations on the mode of action of the hydroxypyridone antimycotics rilopirox and piroctone on *Candida albicans*. Myco-

ses 2006;49(3):159-168. *https://dx.doi.org/10.1111/j.1439-0507.2006.01228.x*

55. **Radadiya PS, Thornton MM, Puri RV, Yerrathota S, Dinh-Phan J, Magenheimer B, Subramaniam D, Tran PV, Zhu H, Bolisetty S, Calvet JP, Wallace DP, Sharma M**. Ciclopirox olamine induces ferritinophagy and reduces cyst burden in polycystic kidney disease. JCI Insight 2021;6(8):e141299. *https://dx.doi.org/10.1172/jci.insight.141299*
56. **Yang J, Milasta S, Hu D, AlTahan AM, Interiano RB, Zhou J, Davidson J, Low J, Lin W, Bao J, Goh P, Nathwani AC, Wang R, Wang Y, Ong SS, Boyd VA, Young B, Das S, Shelat A, Wu Y, Li Z, Zheng JJ, Mishra A, Cheng Y, Qu C, Peng J, Green DR, White S, Guy RK, Chen T, Davidoff A.** Targeting histone demethylases in MYC-driven neuroblastomas with ciclopirox. Cancer Res 2017;77(17):4626–4638. *https://dx.doi.org/10.1158/0008-5472.CAN-16-0826.*
57. **Polak AM.** Preclinical data and mode of action of amorolfine. Clin Exp Dermatol 1992; 17:8-12. *https://dx.doi.org/10.1159/000247588.*
58. **Davis MR, Donnelley M, Thompson GR.** Ibrexafungerp: A novel oral glucan synthase inhibitor. Med Mycol 2020; 58 (5) :579-592. *https://dx.doi.org/10.1093/mmy/myz083.*
59. **Hoenigl M, Sprute R, Egger M, Arastehfar A, Cornely OA, Krause R, Lass-Flörl C, Prattes J, Spec A, Thompson GR 3rd, Wiederhold N, Jenks JD.** The Antifungal Pipeline: fosmanogepix, ibrexafungerp, olorofim, opelconazole, and rezafungin. Drugs 2021;81(15):1703-1729. *https://dx.doi.org/10.1007/s40265-021-01611-0*
60. **Wring S, Murphy G, Atiee G, Corr C, Hyman M, Willett M, Angulo D.** Clinical pharmacokinetics and drug-drug interaction potential for coadministered SCY-078, an oral fungicidal glucan synthase inhibitor, and tacrolimus. Clin Pharmacol Drug Dev 2019; 8:60–69. *https://dx.doi.org/10.1002/cpdd.588.*
61. **Lamoth F, Lewis R, Kontoyiannis D.** Investigational antifungal agents for invasive mycoses: a clinical perspective. Clin Infect Dis 2022;75(3):534–544. *https://doi.org/10.1093/cid/ciab1070*
62. **Gamal A, Chu S, McCormick T, Borroto-Esoda K, Angulo D, Ghannoum M.** Front Cell Infect Microbiol 2021 ; 11:642358| *https://doi.org/10.3389/fcimb.2021.642358*
63. **Wiederhold NP.** Pharmacodynamics, mechanisms of action and resistance, and spectrum of activity of new antifungal agents. J Fungi 2022;8(8):857. *https://dx.doi.org/10.3390/jof8080857*
64. **Jacobs SE, Zagaliotis P, Walsh TJ.** Novel antifungal agents in clinical trials. F1000Res. 2022;10:507. *https://dx.doi.org/10.12688/f1000research.28327.2*
65. **Vivjoa** (Oteseconazole) Package Insert: HIGHLIGHTS OF PRESCRIBING INFORMATION. VIVJOA™ (oteseconazole). Durham, NC, USA, 2022. [citado 2022, septiembre 23] Disponible en: https://www.accessdata.fda.gov/drugsatfda_docs/label/2022/215888s000lbl.pdf.
66. **Oliver JD, Sibley GEM, Beckmann N, Dobb KS, Slater MJ, McEntee L, du Pré S, Livermore J, Bromley MJ, Wiederhold NP, Hope WW, Kennedy AJ, Law D, Birch M.** F901318 represents a novel class of antifungal drug that inhibits dihydroorotate dehydrogenase. Proc Natl Acad Sci USA 2016; 113(45): 12809–12814. *https://dx.doi.org/10.1073/pnas.1608304113.*
67. **Olorofim Aspergillus Infection Study** (OASIS) [citado 2022, septiembre 15]. Disponible en: https://clinicaltrials.gov/ct2/show/study/NCT05101187
68. **Cass L, Murray A, Davis A, Woodward K, Albayaty M, Ito K, Strong P, Ayrton J, Brindley C, Prosser J, Murray J, French E, Haywood P, Wallis C, Rapeport G.** Safety and nonclinical and clinical pharmacokinetics of PC945, a novel inhaled triazole antifungal agent. Pharmacol Res Perspect 2021;9(1):e00690. *https://dx.doi.org/10.1002/prp2.690*
69. **Opelconazole.** PC945 prophylaxis or preemptive therapy against pulmonary Aspergillosis in lung transplant recipients [citada 2022, Octubre 21] Disponible en: https://clinicaltrials.gov/ct2/show/NCT0

5037851?term=opeleonazole&draw=2&rank=1

70. **Shaw KJ, Ibrahim AS.** Fosmanogepix: a review of the first-in-class broad spectrum agent for the treatment of invasive fungal infections. J Fungi 2020;6(4):239. *https://dx.doi.org/10.3390/jof6040239*
71. **Fosmanogepix** Interventional efficacy and safety phase 3 double-blind, 2-arm study to investigate iv followed by oral **fosmanogepix** (PF-07842805) compared with iv caspofungin followed by oral fluconazole in adult participants with candidemia and/or invasive candidiasis NCT05421858. [citado 2022, septiembre 16] Disponible en: https://clinicaltrials.gov/ct2/show/NCT05421858?term=fosmanogepix&draw=2&rank=1
72. **Skipper CP, Atukunda M, Stadelman A, Engen NW, Bangdiwala AS, Hullsiek KH, Abassi M, Rhein J, Nicol MR, Laker E, Williams DA, Mannino R, Matkovits T, Meya DB, Boulware DR.** Phase I EnACT trial of the safety and tolerability of a novel oral formulation of amphotericin B. Antimicrob Agents Chemother 2020;64(10):e00838-20. *https://dx.doi.org/10.1128/AAC.00838-20*
73. **Ledezma E, Apitz-Castro R.** Ajoene, el principal compuesto activo derivado del ajo (*Allium sativum*), un nuevo agente antifúngico. Rev Iberoam Micol 2006; 23(2):75-80. *https://doi.org/10.1016/S1130-1406(06)70017-1*.
74. **San Blas G, Urbina J, Marchán E, Contreras L, Sorais F, San Blas F.** Inhibition of *Paracoccidioides brasiliensis* by ajoene is associated with blockade of phosphatidylcholine biosynthesis. Microbiology 1997; 143: 1583-1586.
75. **Nakamoto M, Kunimura K, Suzuki JI, Kodera Y.** Antimicrobial properties of hydrophobic compounds in garlic: Allicin, vinyldithiin, ajoene and diallyl polysulfides. Exp Ther Med 2020;19(2):1550-1553. *https://dx.doi.org/10.3892/etm.2019.8388*
76. **Torres J, Romero H.** Actividad antifúngica in vitro del ajoeno en cinco aislamientos clínicos de *Histoplasma capsulatum* var. capsulatum. Rev Iberoam Micol 2012; 29(1):24-28. *https://dx.doi.org/10.1016/j.riam.2011.04.001*
77. **Lemus-Espinoza D, Maniscalchi MT, Ledezma E, Arrieche D.** Ultraestructura de *Microsporum canis*: un caso de *Tinea Capitis* tratado tópicamente con Ajoene. Saber. 2015; 27(3): 401-405. Disponible en: http://ve.scielo.org/scielo.php?script=sci_arttext&pid=S131501622015000300005&lng=es.
78. **Karpiński TM.** Essential oils of Lamiaceae family plants as antifungals. Biomolecules 2020;10(1):103. *https://dx.doi.org/10.3390/biom10010103.*
79. **Mutlu-Ingok A, Devecioglu D, Dikmetas DN, Karbancioglu-Guler F, Capanoglu E.** Antibacterial, antifungal, antimycotoxigenic, and antioxidant activities of essential oils: an updated review. Molecules 2020;25(20):4711. *https://dx.doi.org/10.3390/molecules25204711*
80. **Gintjee T, Donnelley M, Thompson G.** Aspiring antifungals: review of current antifungal pipeline developments. J Fungi 2020; 6:28. *https://doi.org/10.3390/jof6010028*
81. **Ngan NTT, Flower B, Day JN.** Treatment of Cryptococcal meningitis: how have we got here and where are we going? Drugs 2022;82(12):1237-1249. *https://dx.doi.org/10.1007/s40265-022-017957-5*
82. **Smilnak GJ, Charalambous LT, Cutshaw D, Premji AM, Giamberardino CD, Ballard CG, Bartuska AP, Ejikeme TU, Sheng H, Verbick LZ, Hedstrom BA, Pagadala PC, McCabe AR, Perfect JR, Lad SP.** Novel treatment of cryptococcal meningitis via neurapheresis therapy. J Infect Dis 2018;218(7):1147–1154. *https://dx.doi.org/10.1093/infdis/jiy286*
83. **Parente-Rocha JA, Bailão AM, Amaral AC, Taborda CP, Paccez JD, Borges CL, Pereira M.** antifungal resistance, metabolic routes as drug targets, and new antifungal agents: an overview about endemic dimorphic fungi. Mediators Inflamm 2017;2017:9870679. *https://dx.doi.org/10.1155/2017/9870679.*
84. **Martínez-Méndez D.** COVID-19, Angola y la respuesta inesperada. Rev Soc Ven Mi-

crobiol 2020; 40(2):151-154. Disponible en: https://pesquisa.bvsalud.org/global-literature-on-novel-coronavirus-2019-ncov/resource/pt/covidwho-1102959

85. World Health Organization. Segunda reunión del Comité de Emergencias del Reglamento Sanitario Internacional (2005) (RSI) sobre el brote de viruela símica en varios países. Julio 2022 [citado 2022, octubre 21]. Disponible en https://www.who.int/es/news/item/23-07-2022-second-meeting-of-the-international-health-regulations-(2005)-(ihr)-emergency-committee-regarding-the-multi-country-outbreak-of-monkeypox

86. Ashraf N, Kubat RC, Poplin V, Adenis AA, Denning DW, Wright L, McCotter O, Schwartz IS, Jackson BR, Chiller T, Bahr NC. Re-drawing the maps for endemic mycoses. Mycopathologia 2020;185(5):843-865. *https://dx.doi.org/10.1007/s11046-020-00431-2*

87. República Bolivariana de Venezuela. Gaceta Oficial de la República Bolivariana de Venezuela Nº 42.553. Enero de 2023 [Citado 2023, enero 22]. Disponible en: https://tugacetaoficial.com/gaceta-oficial-venezuela-42553-20-01-2023.

Índice de Autores Vol. 64, Nos. 1-4, 2023

Investigación Clínica
Vol. 64 Nº 4 / December 2023
Bilingual - Abstracts in Spanish and English

Contents

Investigación Clínica
Vol. 64 Nº 4 /Diciembre 2023
Bilingüe - Resúmenes en Español e Inglés

Contenido